DISSERTATION ZUR ERLANGUNG DES DOKTORGRADES DER NATURWISSENSCHAFTEN (DR. RER. NAT.) DER NATURWISSENSCHAFTLICHEN FAKULTÄT III – BIOLOGIE UND VORKLINISCHE MEDIZIN REGENSBURG

Role of Potassium Ion Channels (K^+ channels) on Proliferation and Development of Colonic Cancer

vorgelegt von

Melanie Spitzner aus Vacha

Regensburg, November 2007

Promotionsgesuch eingereicht am: 14.11.2007
Promotionskolloquium am: 16.01.2008

Die Arbeit wurde angeleitet von: Prof. Dr. K. Kunzelmann
PD Dr. R. Scheiber

Prüfungsausschuss:
Vorsitzender: Prof. Dr. A. Kurtz
1. Gutachter: Prof. Dr. K. Kunzelmann
2. Gutachter: Prof. Dr. S. Schneuwly
3. Prüfer: Prof. Dr. G. Längst
Ersatzperson: Prof. Dr. R. Witzgall

Zusammenfassung

Seit einigen Jahren ist bekannt, dass Kaliumionenkanäle und Chloridionenkanäle sehr wichtig für die Zellproliferation und das Überleben von Krebszellen sind. Diese Ionenkanäle weisen eine unterschiedliche Aktivität auf, wenn man normalen Zellen mit Krebszellen vergleicht.

Für *in vitro* Studien an Kaliumionenkanälen und dem mutmaßlichen Chloridionenkanal Bestrophin 1 (Best1) wurde die humane Kolonkarzinomzelllinie T_{84} benutzt. Die Expression unterschiedlicher Typen von Kaliumionenkanälen konnte durch RT-PCR gezeigt werden. Aber nur spannungsabhängige Kaliumionenkanäle (Kv Kanäle) hatten einen Einfluss auf die Zellproliferation. Messungen von Zellvolumen, intrazellulären pH und Kalziumionenkonzentration zeigten, dass Kv Kanäle den intrazellulären pH und das Kalziumsignal die Zellproliferation kontrollieren. Sie haben aber keinen Einfluss auf die Volumenregulation.

In weiteren Zellkulturexperimenten konnten zwei unterschiedliche Klone von T_{84} Zellen generiert werden: ein langsam wachsender Klon (T_{84}-slow) und ein schnell proliferierender Klon (T_{84}-fast). Die Expression des Kv Kanals Eag1 und des mutmaßlichen Chloridionenkanals Best1 war im Vergleich zu T_{84}-slow in T_{84}-fast erhöht. Die ATP induzierte Erhöhung der intrazellulären Kalziumionenkonzentration war in T_{84}-fast ebenfalls erhöht, was auf die Zunahme der Aktivität von Kv Kanälen zurückgeführt werden kann. Kv Kanäle haben die Aufgabe das Membranpotential der Zellen zu hyperpolarisieren, was zu einem erhöhtem Einstrom von Kalziumionen in die Zelle führt, welches wiederum zum Durchlaufen des Zellzyklus bei der Zellteilung notwendig ist. Die Hemmung der Expression von Eag1 oder Best1 durch RNA_i hatte eine verminderte Zellproliferation zur Folge. Des Weiteren führte eine Überexpression eines Best1-Plasmids in T_{84}-slow zu einer 30%igen Steigerung der Proliferationsrate und zu einer verbesserten Volumenregulation. Diese Experimente zeigen, dass sowohl Eag1 als auch Best1 eine wichtige Rolle bei der Proliferation von Kolonkarzinomzellen spielen.

Im zweiten Teil dieser Arbeit wurden *in vivo* Experimente im Tiermodell durchgeführt. Die molekularen und funktionellen *in vitro* Befunde aus der Zellkultur wurden zuerst in einem chemischen Mausmodell für Kolonkarzinom überprüft. Dafür wurden BL6-Mäuse mit den karzinogenen Substanzen Dimethylhydrazine (DMH) und N-methyl-N-nitrosourea (MNU) behandelt, um die Entstehung von Kolonkarzinom zu induzieren. Die so behandelten Mäuse zeigten einen verminderten elektrogenen Salztransport durch den epithelialen Natriumionenkanal ENaC und den Chloridionenkanal CFTR. Zusätzlich konnte eine erhöhte Aktivität von Kv Kanälen nachgewiesen werden. Semiquantitative PCR zeigte schon in den

ersten Wochen nach der Behandlung eine erhöhte Expression von den Kv Kanälen Kv1.3, Kv1.5, Kv3.1, Eag1, Elk1 und Erg1. Parallel dazu wurden Proteinexpressionsnachweise durch Western Blots für Eag1 durchgeführt. Es konnte eine Erhöhung von Eag1 auch auf Proteinebene nachgewiesen werden. Weiterhin konnte durch eine Kooperation mit einer Arbeitsgruppe in Basel eine genomische Amplifikation von Eag1 in 3,5% der untersuchten humanen kolorektalen Adenokarzinome mittels Fluoreszenz *in situ* Hybridisierung gezeigt werden.

Eine zweite tierexperimentelle Studie wurde in einem genetischen Mausmodell durchgeführt. BL6-Mäuse mit einer Mutation in dem Tumorsuppressorgen *APC* (APC-Min/+) entwickeln während ihres Lebens Polypen im gesamten Darmtrakt. APC-Min/+ Mäuse zeigten einen signifikanten Gewichtsverlust und eine verkürzte Lebensspanne während der Beobachtungsperiode von 21 Wochen. Durch real time PCR konnte eine erhöhte mRNA Expression des Kv Kanals Eag1, des kalziumionenaktivierten Kaliumionenkanals BK und des Natriumionenkanals ENaC nachgewiesen werden. Messungen des epithelialen Transportes durch Ussingkammertechnik zeigten eine erhöhte Natriumionenabsorption durch ENaC und verstärkte Aktivität von BK- und Eag1-Kaliumionenkanälen.

Zusammenfassend kann gesagt werden, dass die Aktivität von Kv Kanälen der Kv Ionenkanalfamilien Kv1, Eag oder BK, sowohl *in vitro* als auch *in vivo* direkt mit der Zellproliferation und Krebsentwicklung korrelieren. Diese Kanäle könnten damit als wichtiges Ziel für Diagnose und Behandlung von Kolonkarzinom dienen.

Summary

As shown in the past potassium ion channels (K^+ channels) and chloride ion channels (Cl^- channels) are important for proliferation and survival of cancer cells. These ion channels are differentially activated in cancer cells compared to normal tissue or cells.

The human colonic cancer cell line T_{84} was used for *in vitro* studies on K^+ channels and the putative Cl^- channel Bestrophin 1 (Best1). The expression of many different K^+ channel types was screened by RT-PCR. However, only voltage-gated (Kv) channels have an impact on cell proliferation. Measurements of cell volume, intracellular pH, and intracellular Ca^{2+} concentration demonstrate that Kv channels control proliferation by affecting intracellular pH and Ca^{2+} signaling, but not by cell volume regulation.

In further cell culture experiments two different clones of T_{84} cells were generated: a slow proliferating clone (T_{84}- slow) and a fast proliferating clone (T_{84}- fast). Expression of the Kv channel Eag1 and the putative Cl^- channel Best1 was enhanced in T_{84}- fast as compared to T_{84}- slow. ATP-induced enhancement of the intracellular Ca^{2+} concentration was increased in T_{84}- fast, indicating that Kv channels hyperpolarize the cell membrane and therefore enhance the driving force for Ca^{2+}, which is necessary for cell cycle progression. Down regulation of Eag1 or Best1 by RNA_i decreased cell proliferation in T_{84}-fast. Furthermore, Best1 over expression in T_{84}-slow increased the proliferation rate by 30% and improved cell volume regulation. These experiments demonstrate that Eag channels and Best1 have an important role in proliferation of colonic cancer cells.

For the second part of this study the role of Kv channels in colonic cancer was evaluated *in vivo* in an animal model. The molecular and functional expression of these ion channels found *in vitro* in T_{84} cells were examined first in a chemical mouse model. For this purpose BL6 mice were treated with the chemical carcinogens DMH and MNU to induce the development of colonic cancer and to investigate ion channel properties in early stages of carcinogenesis. In carcinogen treated mice electrogenic salt transport by the epithelial sodium channel ENaC and the chloride channel CFTR were attenuated. In addition, activity of Kv channels was enhanced. Already in the first weeks after treatment semi-quantitative PCR showed an mRNA upregulation of the Kv channels Kv1.3, Kv1.5, Kv3.1, Eag1, Elk1, and Erg1. At the same time an increased Eag1 protein expression could be demonstrated. Furthermore, in cooperation with a group in Basel a genomic amplification of Eag1 was found in 3.5% of human colorectal adenocarcinomas identified by fluorescence *in situ* hybridization analysis (FISH).

A second *in vivo* study was performed in a genetic mouse model of colonic cancer. BL6 mice with a mutation in the tumor suppressor gene *APC* (APC-Min/+) develop polyps in the whole

intestine. These APC-Min/+ mice showed a significant weight loss and a reduced lifespan during an observation period of 21 weeks. An increased mRNA expression of the Kv channel Eag1, the Ca^{2+} sensitive Kv channel BK and the sodium channel ENaC could be detected by real time PCR. Ussing chamber studies demonstrated an enhanced sodium absorption by ENaC and an enhanced activity of BK and Eag1 channels.

In summary activity of Kv channels like members of Kv1, Eag, or Ca^{2+} sensitive BK showed a direct correlation to cell proliferation and cancer development *in vitro* and *in vivo*. These channels may represent an important target for diagnosis and novel therapeutics of colonic cancer.

Table of Contents

Chapter 1

General Introduction

In the western world colorectal cancer (CRC) is the most malignant death-causing disease, besides tumors caused by smoking. Nearly 50% of the population in developed countries has colorectal tumors by the age of 70. CRC is characterized by several intermediate stages ranging from small adenomas to large metastatic carcinomas, which require decades to fully develop. Progression from normal healthy colonic epithelia to malignant colonic cancer is well described as a genetic model, where at least seven different series of genetic alterations have to occur (1-3).

But not only genetic disorders have an impact on the severity of the disease, environmental factors such as diet may also play an important role. There is a remarkable 20-fold difference in CRC-incidence worldwide between western world populations and populations in developing countries, who have a lower risk to develop colonic cancer. Dietary fat intake, with the main source being red meat, has positive effects on tumor development and enhances the risk of developing colonic cancer (4). In the next few years the number of CRC will increase even more due to a Western life style, which often includes a diet consisting of high consumption of fast food and lack of sufficient physical activity. Because there is a high likelyhood for rising numbers of colonic cancer cases and the malignancy of the disease new therapies and diagnostic methods are needed.

1.1 Ion channels and cell proliferation

Ion channels are present in the cell membrane and in intracellular membranes of every cell type, not only in excitable tissues like neuronal or muscle cells. Ion channels exist for the four ions potassium (K^+), sodium (Na^+), chloride (Cl^-), calcium (Ca^{2+}), and many more. Membrane ion channels can be activated either by ligands (ligand-gated ion channels) or changes in the membrane potential (voltage-gated ion channels), usually depolarization. The ion conducting pore of a channel is more or less selective for its specific ions. Most voltage-gated ion channels are highly selective, some ligand-activated ion channels allow more than only one

type of ion to enter the ion channel pore (5). The most important roles of ion channels are maintaining the cell membrane potential and controlling cellular parameters like Ca^{2+} signaling, ion concentration, and intracellular pH. Cells have to keep their cell volume to a certain level, even though they need to adapt to changing conditions during proliferation. As ion channels have such an important impact on proliferation and survival, it is not surprising that they might also play a crucial role in diseases (6). Disorders caused by altered or loss of individual ion channel function or alterations in the channel density are generally called channelopathies. Tumor development could also be due to changes of ion channel function, which could transform healthy epithelia to a malignant, invasive, and fast growing tissue.

1.2 The human colonic epithelium

The mammalian colonic epithelium consists of three different cell types with distinct functions. 95% of all intestinal cells are columnar epithelial cells (enterocytes) and mucus-producing goblet cells. The remaining 5% are enteroendocrine cells required for hormone production (7). One way to enhance the surface in the colon is the organization of epithelial cells in crypts (Fig. 1-1). The left part of figure 1-1 shows that the intestinal epithelium is constantly regenerated from stem cells in the colonic crypt base. The epithelial cells differentiate during migrating from the crypt to the surface along the crypt axis. The differentiated surface enterocytes undergo apoptosis and are shed to the intestinal lumen. The whole process is completed within 3-5 days (8).

The main function of the colonic epithelium is net absorption of electrolyte. Every day approximately 1.3 – 1.8 liters of electrolyte-rich fluid is absorbed (9). Beside absorptive properties the epithelium is also a secretory tissue when stimulated by secretagogoues. Therefore, colonic epithelial cells are polarized and equipped with ion channels, transporters, carriers, and pumps (Fig. 1-1) located either on the luminal or basolateral side of the membrane. These transporters are responsible for the highly efficient transport of large amounts of salt and water. Depending on their localization, cells in the colonic crypt have different transport properties. Epithelial cells in the crypt base have a high proliferative and Cl^- secretory activity due to high CFTR conductance. Surface epithelial cells are fully differentiated, have no tendency to proliferate, and show a primarily absorptive behavior due to high epithelial sodium channels (ENaC) activity when compared with basal crypt cells (10, 11). Epithelial cells build a low- resistance epithelium of about 100 $\Omega \cdot cm^2$ in the proximal colon and a two- to fourfold higher resistance epithelium in the distal colon.

1.3 Ion channels in human colonic cancer

During tumor development the proliferative zone expands and therefore ion channel and transport protein expression pattern change along the crypt axis. As shown on the right panel of figure 1-1 colonic carcinoma cells never gain the ability to absorb Na^+ (less ENaC) and increased Cl^- secretion is due to high activity of CFTR and additionally atypical Cl^- channels like Ca^{2+} activated chloride channels (CaCC) are activated (7).

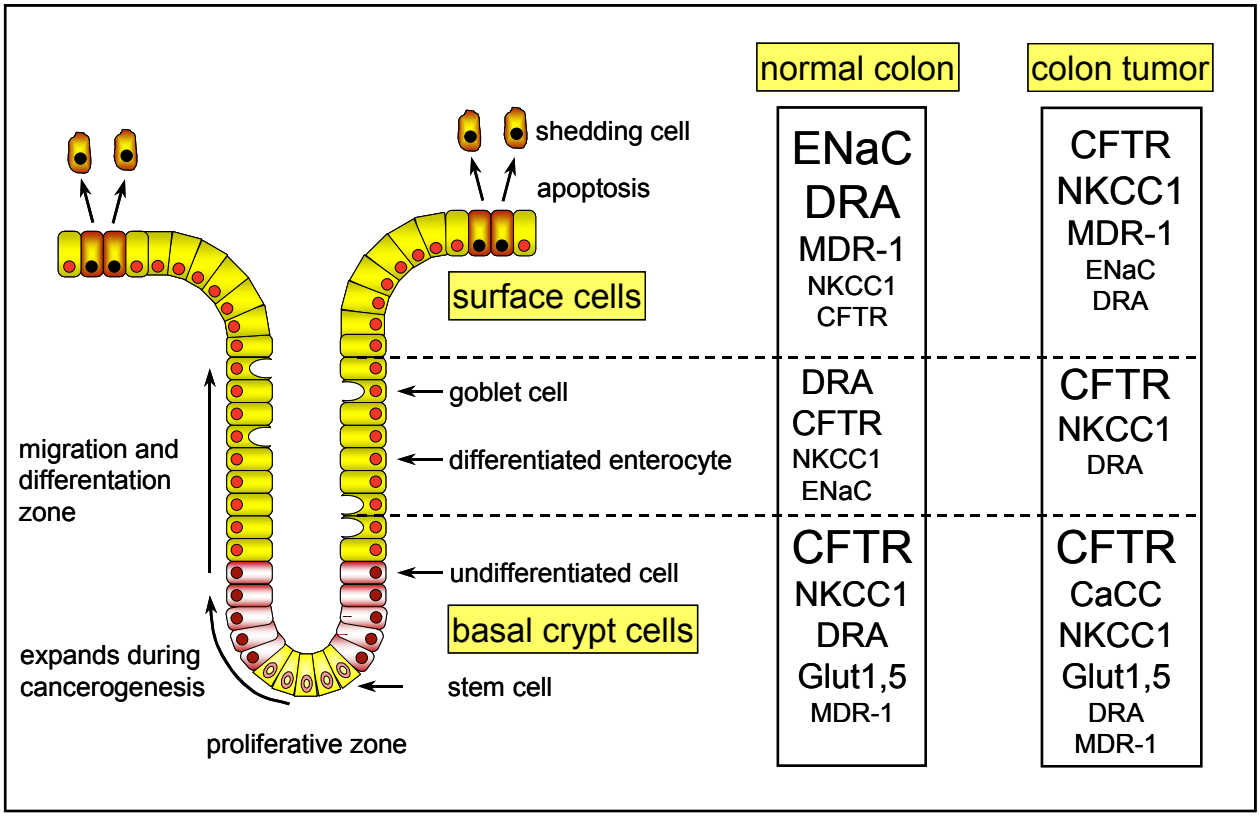

Fig. 1-1 Cellular model of colonic epithelium and the expression of ion channels and transport proteins in the crypt during tumorigenesis (adapted from 7, 12)

In crypts of colonic tumors the proliferative zone is expanded. The expression pattern of diverse ion channels and transport proteins are either up (larger letters) or down regulated (smaller letters). Due to changes in ion channel and transporter expression and therefore in their activities the colonic epithelium evolves during cancerogenesis from an absorptive to a more secretory phenotype. *ENaC* = epithelial sodium channel, *CFTR* = cystic fibrosis transmembrane conductance regulator, *DRA* = down regulated in adenoma, *NKCC1* = Na^+- $2Cl^-$- K^+ cotransporter type 1, *Glut1* = glucose transporter type 1, *MDR-1* = multi drug resistance protein 1, *CaCC* = Ca^{2+} activated chloride channels

1.4 K^+ channels and cancer

Over the last years the most intensively studied ion channels with regard to proliferation and tumor development were K^+ channels. K^+ channels are the most diverse class of ion channels expressed in the cytoplasmic membrane. They are classified in four families based on their structural relatedness and predominant functional characteristics: voltage-gated (Kv), calcium-activated (K_{Ca}), two-pore (K_{2P}), and inward rectifier (K_{ir}) potassium channels. All families are further subdivided into subfamilies (13). Increased expression of members of almost all K^+ channel families can be found in tumors and tumor cell lines (Table 1-1).

Table 1-1 Expression of K^+ channels in cancer cell lines or tumors (adapted from 14)

Examples of K^+ channels, which are upregulated in cancer cell lines or tumor tissues.

family	subfamily	members	type of tumor cell line	type of tumor
Kv channels	Kv1	Kv1.3, Kv1.5	prostate cancer cells, colonic cancer cells	neuroblastoma, breast carcinoma, small lung cell carcinoma, melanoma, lymphoma, hepatocarcinoma
	Kv3	Kv3.3, Kv3.4		colonic carcinoma
	Kv10	Eag1 Eag2	NIH 3T3, HeLa	cervix carcinoma, neuroblastoma, mammary gland carcinoma, ductal carcinoma, breast carcinoma
	Kv11	Erg1	atrial tumor cells (HL-1), breast cancer cells (SK-BR-3), colonic cancer cells	myeloid leukemia, neuroblastoma, colorectal cancer
	Kv12	Elk1, Elk2		astrocytoma
K_{Ca} channels	BK_{Ca}	BK, SK	prostate cancer cells (PC3)	glioma, pituitary GH3 lactotroph
K_{2P} channels	K_{2P}	TWIK TASK	melanoma cell line (SK-MEL-28)	glioma, neuroblastoma, medulloblastoma, leukemia, insulinoma
	K_{ATP}	K_{ATP}	liver epithelial cell lines (HepG2, HuH-7, HFL), U-373 MG, SK-N-MC	astrocytoma, neuroblastoma, insulinoma, urinary bladder carcinoma, medulloblastoma
K_{ir} channels	K_{ir}	Kir 4.1	neuroblastomaxglioma hybrid cells (NG108-15), basophilic leukemia cells (RBL-2H3)	

More than 10 years ago, Wonderlin and Strobl reviewed the potential role of ion channels for cell proliferation. Several experiments in different cell lines show that specific types of K^+ channels must be activated for progression through the different phases of the cell cycle. Treatment of mitogen-stimulated T- and B-lymphocytes with inhibitors of endogenous K^+ channels decrease proliferation and arrest the cells in early G1 phase. The main function of

K^+ channels during cell cycle is their hyperpolarizing effect on membrane voltage and therefore their impact on Ca^{2+} signaling. Ca^{2+} influx is stimulated by hyperpolarization of the membrane potential, which is required at three check points in the cell cycle (Fig. 1-2). An increased intracellular Ca^{2+} concentration is needed during progression through G1 phase and the G1/S transition (6, 15).

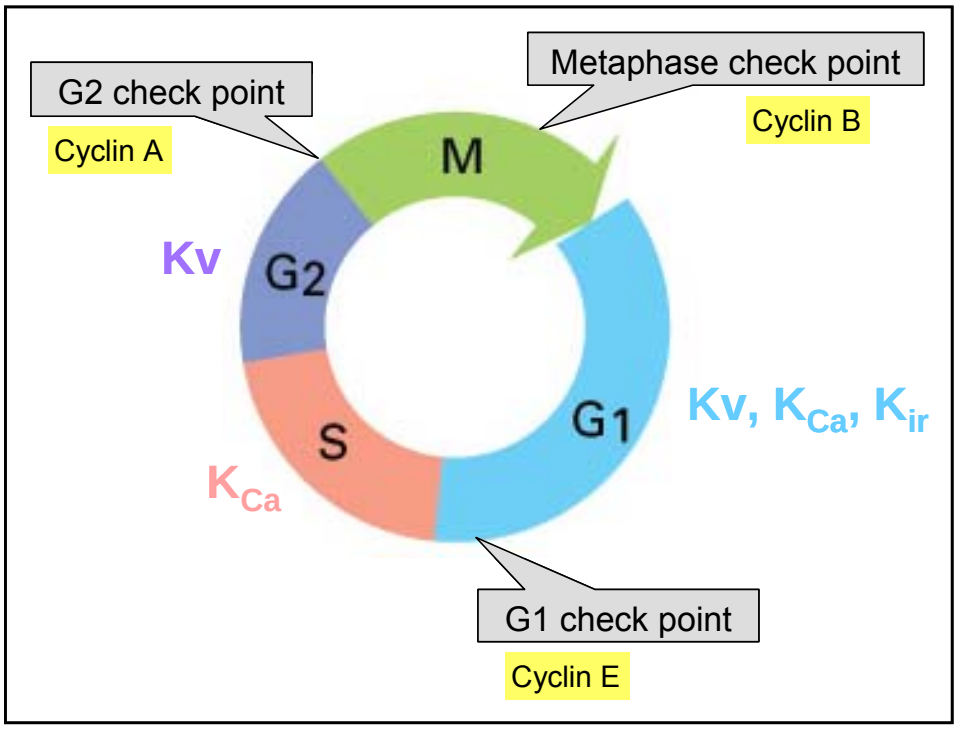

Fig. 1-2 Activity of K^+ channels during the cell cycle (15)

During cell cycle activity of K^+ channels is required to hyperpolarize the cell membrane and therefore maintain the driving force for Ca^{2+} influx into the cell. *Kv* = voltage activated K^+ channels, K_{Ca} = Ca^{2+} activated K^+ channels, K_{ir} = inwardly rectifier K^+ channels, *G1* = gap phase 1, *S* = DNA synthesis phase, *G2* = gap phase 2, *M* = mitosis

During G1/S transition and S phase cells swell and activate a regulatory volume decrease (RVD) mechanism, which allows shrinkage of the cell after mitosis. RVD requires efflux of water and solutes, which is due to simultaneous opening of K^+ and Cl^- channels. Blocking of K^+ channels leads to inhibition of RVD. Tumor cells have an optimized RVD leading to better growth conditions compared to normal cells. However, excessive and early activation of K^+ and Cl^- channels inhibit proliferation and furthermore lead to cell shrinkage and promote apoptotic cell death (6).

1.5 Eag: a cell cycle regulated K^+ channel with oncogenic properties

K^+ channels from the ether-á-go-go (Eag) type are regulated by cell cycle. These channels are further subdivided into three subfamilies: Eag, Eag-related (Erg), and Eag-like (Elk) channels. Eag channels are predominantly active in the early G1 phase (6, 16). Activation of these K^+ channels causes oscillations of the membrane potential, which may regulate cell cycle-dependent proteins, like the cyclin-dependent kinase inhibitors p27 and p21. They accumulate due to inhibition of K^+ channels and membrane depolarization (17). However, a causal relationship between the function of Eag K^+ channels and membrane voltage in specific cell cycle phases and cell cycle-dependent cellular processes like proliferation and differentiation is still unknown (18). Nevertheless it is shown that Eag channels have an oncogenic potential on cells and in severe combined immune-deficient (SCID) mice. Pardo's group demonstrated the presence of Eag mRNA transcripts in the human breast carcinoma cell line MCF-7, while this has not detected in normal human breast tissue. Eag is also expressed in several other tumor cell lines like the cervix carcinoma cells HeLa, the neuroblastoma cell line SH-SY5Y, and different mammary gland carcinoma cells. In Eag-expressing cancer cell lines Pardo et al. showed that inhibition of Eag channels by Eag-specific antisense oligomers decrease proliferation. Moreover, when Eag-transfected chinese hamster ovary cells (CHOhEag) are subcutaneously implanted into SCID mice, all of these mice developed tumors (14, 19). Both Erg mRNA and protein have been detected by many groups in tumor cell lines and in primary human cancers. Some examples are endometrial adenocarcinomas, acute myeloid and lymphoid leukemia (20-24), many colonic cancer cell lines, and primary colorectal tumors including metastatic cancers (Table 1-1). In addition Erg channels are involved in the establishment of a very invasive phenotype in colorectal cancer cells (16). With regard to their function in the cell cycle Erg channels modulate the progression through the M phase, when the cellular membrane voltage is more depolarized. Little is known about Elk channels. Elk channels are primarily expressed in the nervous system and are also found to be enhanced in tumors of the brain (25).

1.6 Genetic alterations in the development of colorectal cancer

In general tumorigenesis requires several mutational steps. Furthermore, many additional genetic alterations have been found and other routes like epigenetic pathways are also detected. For colorectal carcinogenesis two major genetic pathways are documented: microsatellite instability (MSI) and chromosomal instability (CIN) (26).

The hereditary nonpolyposis colorectal cancer (HNPCC) syndrome is a special type of CRC. It is a simple Mendelian disease where the chromosomes 2p16 or 3p21 are involved (27-30). Mutations in the human homologs of mismatch repair (MMR) genes *mutS* or *mutL* are

responsible for this hereditary disease. Approximately 65% of sporadic colonic cancers carry these two MMR gene mutations as well (3).Tumors of HNPCC patients have a high genome-wide instability of their repair system or in the microsatellites - MSI. Microsatellites are tandem-repetitive, short, simple DNA sequences consistent of 10 to 100 nucleotides. MSI can be described as an expansion in the number of tandem repeats. In MSI positive tumors other additional microsatellite mutations for the following target genes resulting cytokines, oncogenes, cell cycle controlling genes, and apoptosis have been identified:

- TGF- β (transforming growth factor-β), inhibition of cell growth
- PTEN (phosphatase and tensin homolog deleted on chromosome 10), inhibition of cell growth
- BAX, induces apoptosis
- E2F-4, control of progression through the cell cycle (26)

Figure 1-3 describes the CIN pathway of colorectal carcinogenesis. It is a multi step mutation process, where allelic losses on chromosome 5q (adenomatous polyposis coli - APC), 18q (DCC/SMAD4), and 7p (p53) occur. Mutations in the *APC* gene are very early events during the development of cancer. At the adenomatous stage *K-ras* mutations arise and as a last step to malignancy mutations of *p53* and deletions on chromosome 18q occur (31).

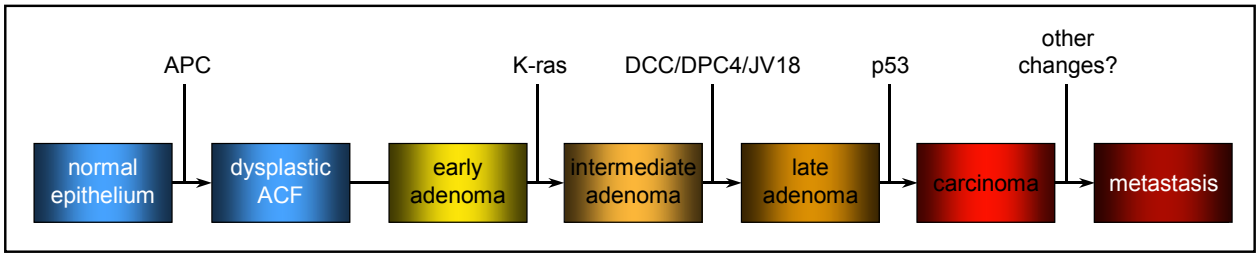

Fig. 1-3 Genetic alterations during colorectal tumorigenesis (3)

Loss of function mutations of *APC* are the initial step of the neoplastic process and cause benign adenoma. Afterwards alterations of the oncogene *K-ras* occur. These are gain of function mutations and require only one genetic event for activation. Other subsequent mutations like DCC/SMAD4 and *p53* leading to malign stages of CRC as indicated in this figure. *ACF* = aberrant crypt foci

This pathway illustrates nicely the three different gene classes important for the development of colonic cancer. Mutations in these genes lead to neoplastic transformation: oncogenes (“gain-of-function” mutations), tumor suppressor genes (“loss-of-function” mutations), and DNA repair genes. Failures during DNA replication or DNA damages are corrected by DNA repair mechanisms, which are encoded by DNA repair genes. If mutated, non-functional gene products are expressed, which then leads to diseases or formation of cancer like

HNPCC? Mutations in oncogenes generally cause unlimited cellular proliferation and inhibition of apoptosis. Over expression or aberrant expression of the normal gene product, or expression of an altered protein cause constitutive activation of oncogenes. The class of oncogenes contains members of a wide variety of genes including *p53*, the cytoplasmic second messenger *ras*, transcription factor *myc*, and growth factor *wnt*. Normally, tumor suppressor genes are responsible for inhibition of cell growth, stimulation of differentiation, and active cell death. At this time more than a dozen tumor suppressor genes have been identified. A few examples for these genes associated with cancer are *PTEN*, retinoblastoma *rb1*, Wilms' tumor *wt-1*, neurofibromatosis type 1 *nf-1*, and *APC* (32, 33).

1.7 APC and cancer

Familial adenomatous polyposis (FAP) is an autosomal dominantly inherited disease where patients develop hundreds to thousands of benign adenomatous colorectal tumors during their second and third decade of life. Out of the large number of polyps some will progress into invasive cancers and will finally metastasize. The genetic defect causing FAP are germ line mutations of the *APC* gene.

The *APC* gene is localized on chromosome 5q21-q22 and encodes a 312 kDa protein product. APC is expressed in a variety of tissues and organs during embryonic development and in adulthood. It is a multidomain protein and binds to a number of other proteins, indicating various functions in the cell. Therefore the APC protein can be detected in the cytoplasm, but it can also accumulate in the apical membrane, along the lateral margins of epithelial cells, and in the nucleus. APC is a tumor suppressor gene and its major cellular functions are:

- binding to β-catenin, which is necessary for adhesion, migration, and movement of enterocytes in the crypt
- down regulation of the Wnt signaling pathway, which results in inhibition of cell proliferation (tumor suppressor function)
- control of the cell cycle by regulation of the progression through mitosis
- control of apoptosis (12, 33-36)

The APC protein contains several distinct domains (Fig. 1-4): an oligomerization domain and an armadillo domain at the N-terminus; in the middle part three 15- and seven 20- amino acid repeats; at the C-terminus a basic domain, and binding sites for DLG (mammalian homologue of Drosophila tumor suppressor discs large), EB1 (end-binding protein 1), and PTP (protein tyrosine phosphatase) (12).

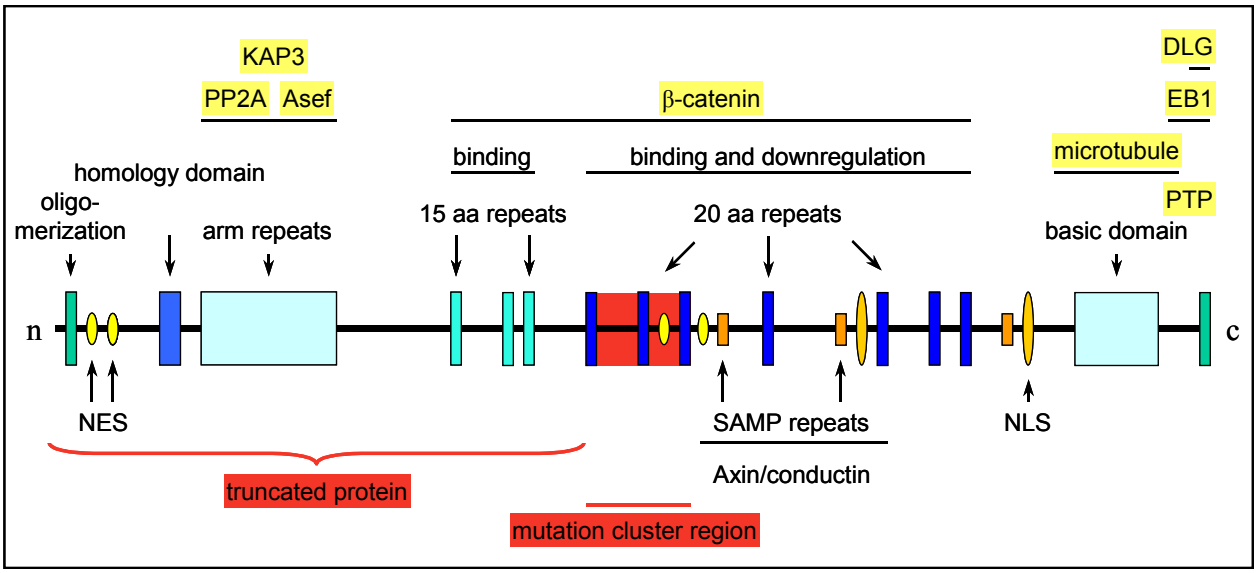

Fig. 1-4 Structure of the APC protein and its binding sites (33)

APC is a 312 kDa protein and contains multiple binding sites and domains. Arrows indicate the binding sites. APC-binding proteins are in yellow. *NES* = nuclear export signal, *Arm* = armadillo, *PP2A* = protein phosphatase 2A, *Asef* = APC-stimulated guanine nucleotide exchange factor, *aa* = amino acid, *SAMP* = serine arginine methionine proline, *NLS* = nuclear localization signal, *DLG* = Drosophila tumor suppressor discs large, *EB1* = end-binding protein 1, *PTP* = protein tyrosine phosphatase

The N-terminal oligomerization domain of the APC protein is necessary for homomerization. Binding of proteins at the armadillo repeats leads to interactions of APC with actin and the microtubule cytoskeleton, causing changes in cell morphology, motility, migration, and cell division. Proteins binding at the armadillo domain are:

- ASEF (APC-stimulated guanine nucleotide exchange factor), when activated it is involved in rearrangement of the actin network
- PP2A (protein phosphatase 2A), binds with its catalytic subunit to axin
- KAP3 (kinesin superfamily-associated protein 3), a mediator between APC and kinesin motor proteins

The three 15-amino acid repeats and seven 20-amino acid repeats in the central part of APC serve as β-catenin binding sites. Binding of APC to β-catenin down regulates the Wnt signaling pathway and lead to formation of large protein complexes with β-catenin and axin. Ubiquitin-mediated degradation of β-catenin is due to phosphorylation of axin by GSK3β (glycogen synthase kinase 3β). Another axin-binding site is the SAMP (serine arginine methionine proline) sequence. At the basic domain APC binds to microtubules and stimulates tubule growth and their elongation by tubulin polymerization. The C-terminus contains a binding region for the following proteins:

- EB1, a microtubule plus-end binding protein, associating with centromere, mitotic spindle
- DLG, binding leads to interactions with cytoskeleton proteins, may promote localization of APC to higher order protein complexes, and suppresses the G1/S progression in the cell cycle
- PTP (12, 35)

By interacting with actin, microtubules and β-catenin, APC integrates structural components of the cell, as the cytoskeleton and the spindle apparatus with one of the major signal transduction pathways, the wnt/hegdehog/notch pathway. APC thereby influences cell cycle progression, division, migration and cell shape/structural integrity, which are all processes deregulated in carcinogenesis.

Somatic mutations of the *APC* gene are concentrated in a central region of the open reading frame (mutation cluster region, Fig. 1-4) between codons 1286 and 1513. This region is located in the middle part of the protein. Germ line mutations are confined to the 5´end of the *APC* gene. Most of the mutations are C to T transitions resulting from cytosine methylation. One of these transitions changes the codon CGA to TGA, a stop codon leading to expression of a truncated protein, which is only half the size of wt protein (Fig. 1-4). Deletion of parts of the protein leads to less protein-protein interactions due to the missing binding domains in the N-terminus. Nevertheless, the truncated APC protein has still domains for β-catenin binding and an oligomerization domain leading to dimerization with a wt or a second truncated APC protein. β-catenin binding to the truncated APC protein results in accumulation of β-catenin in the cytoplasm and nucleus as observed in cancer cells and in colorectal adenomas of FAP patients. This β-catenin accumulation is an important event in cellular growth control by providing stable interactions of β-catenin with:

- cadherins
- APC
- EGF (epithelial growth factor) receptor
- TCF/LEF (T-cell factor / lymphoid enhancer factor)

In conclusion, mutations in the *APC* gene lead to inappropriate and continuous transcription of target genes. Functionally, it results in the lost of the tumor suppressor activity of APC characterized by less differentiation and apoptosis, disorganization of the cytoskeleton of epithelial cells, chromosomal instability, and influences the cell cycle regulation leading to the development of cancer (8, 12, 33, 35).

1.8 Mouse models of colorectal cancer

Mutations in the *APC* gene are correlated to carcinogenesis in the human colon. Mouse models are powerful systems for studying direct molecular interactions in diseases and to find methods for diagnosis or treatment. For colorectal cancer both exist, genetic and carcinogen induced mouse models.

DMH is a well known chemical used to induce tumors in rodents and have been the favored animal model for CRC in the last years. DMH is a procarcinogen that undergoes a series of chemical transformations in the gastrointestinal (GI) tract. After metabolization of DMH the carcinogen methyldiazonium ion is generated. This ion forms a methyl carbonium ion, which is responsible for methylations of macromolecules like DNA (37). The model has the disadvantage that tumor development is variable, depending on the mouse strain. Additionally, tumors generated by DMH have different mutations (only rarely *APC* gene mutations, and no *p53* allelic loss), compared to those appearing in human CRC (4). In order to have a mouse model available with a mutation similar to that in human CRC, the APC mouse has been developed.

The APC-Min/+ mouse (developed by Moser et al. in the 1990s) was generated by using the mutagen ethylnitrosourea (ENU). It is a genetic model for the human FAP disease. Multiple intestinal neoplasia (*Min)* mice carry a nonsense mutation in exon number 15 of the *APC* gene leading to a truncated APC protein of 95 kDa. In the homozygous form, this mutation is embryonic lethal, while heterozygotes are viable, but with a reduced lifespan. To breed these mice heterozygote males and wildtype females have to be mated. The *Min* mutation cannot be propagated through heterozygote females, because anemia and intestinal adenomas interfere with pregnancy and they would die during pregnancy. APC-Min/+ mice have a fully penetrant dominant phenotype and develop numerous intestinal and colonic polyps, and die approximately four month after birth due to severe progressive anemia, rectal prolapse, and/or intestinal obstruction (38, 39). The number of adenomas depends on the genetic background. Compared with the C57BL/6J (BL6) strain, other mouse strains seem to be less sensitive to the *Min* mutation. This is probably caused by existing alleles, which lower the tumorigenic effect of *Min*, namely *Mom-1* (modifier of *Min*) (4, 40). APC-Min/+ mice with BL6 background have more tumors than AKR, MA, and CAST back grounded mice.

1.9 Aims of the present study

In many different cancer cell lines and cancerous tumors K^+ channels are over expressed. The mechanisms, however, how these K^+ channels modulate cell proliferation remain investigated. A major goal of the present study was to investigate, which types of K^+ channels are expressed in the human colonic cancer cell line T_{84} and/or how they influence cell proliferation. Studies on intracellular Ca^{2+}, pH, and cell volume in presence and absence of K^+ channel inhibitors and RNA_i should help to clarify the contribution of K^+ channels to cell proliferation. Secondly, two mouse models of colorectal cancer were used. In one model, tumors were induced by the carcinogen DMH or its analogue MNU. In addition, we made use of the genetic APC-Min/+ model. Changes in electrolyte transport during the development of colonic cancer were investigated by Ussing chamber techniques and rectal potential difference measurements. K^+ channel mRNA expression from isolated mouse colonic crypt cells were analyzed by quantitative real time PCR and protein expression was examined by western blotting and immunocytochemistry. These experiments suggest an impact of K^+ channels in precancerous stages and developing colonic tumors.

Chapter 2

Eag1 and Bestrophin 1 are upregulated in fast growing colonic cancer cells

Abstract

Ion channels like voltage gated ether á gogo (Eag1) K^+ channels or Ca^{2+} activated Cl^- channels have been shown to support cell proliferation. Bestrophin 1 (Best1) has been proposed to form Ca^{2+} activated Cl^- channels in epithelial cells. Here we show that original T_{84} colonic carcinoma cells grow slow (T_{84}-slow) and express low amounts of Eag1 and Best1, while spontaneously transformed T_{84} cells grow fast (T_{84}-fast) and express high levels of both proteins. Both Eag1 and Best1 currents are upregulated in T_{84}-fast cells. Eag1 currents were cell cycle dependent, with an up regulation during G1/S transition, thus confirming its property as a cell cycle regulated K^+ channel in colonic cancer cells. RNAi inhibition of Eag1 and Best1 reduced proliferation of T_{84}-fast cells, while over expression of Best1 turned T_{84}-slow into fast growing cells. Eag1 and Best1 improve intracellular Ca^{2+} signaling and cell volume regulation. These results establish a novel role of bestrophins for cell proliferation.

Introduction

An increasing number of studies demonstrate proliferative effects of membrane ion channels (14). Voltage gated K^+ channels and other types of K^+ channels are expressed in numerous types of tumors, where they may serve as diagnostic and prognostic markers and potential drug targets (41-43). Eag1 channels are probably necessary for progression through the G_1 phase and G_0/G_1 transition of the cell cycle (15). A recent study demonstrates the hyperpolarizing effects of Eag1 and other Kv channels on the membrane voltage of T_{84} cells, which supports intracellular pH regulation and Ca^{2+} increase, necessary for proliferation (44).
Much less is known about the role of Ca^{2+} activated Cl^- channels for cell proliferation (6). This may be due to the ongoing controversy regarding the molecular nature of Ca^{2+} activated Cl^- channels (45). A family of putative Ca^{2+} activated Cl^- channels (CLCA) has been identified, which also controls cell-cell adhesion, apoptosis and cell cycle. However, their structure and biophysical properties are poorly understood (46, 47). Recent studies defined bestrophin proteins as bona fide Ca^{2+} activated Cl^- channels. The Cl^- currents generated upon expression of bestrophin show many of the properties found for native Ca^{2+} activated Cl^- currents (48-50). However, bestrophins have also been proposed to function as regulators of voltage gated L-type Ca^{2+} channels (51). Our own ongoing work in epithelial cells supports both concepts in that bestrophins may form part of a Cl^- channel complex or may couple intracellular Ca^{2+} signals to Cl^- channels of unknown molecular identity (52).
In the present report we demonstrate that both voltage gated Eag1 K^+ channels and bestrophin (Best1) Cl^- channels support proliferation of fast growing T_{84} colonic carcinoma cells. The fast growing T_{84} cell clone was obtained through a spontaneous transformation of slow-growing T_{84} cells. In contrast to slow growing T_{84} cells, transformed cells do not form polarized monolayers and show a remarkable up regulation of Eag1 and Best1 expression. We demonstrate that both currents are in charge of enhanced cell proliferation.

Material and Methods

Cell culture and proliferation studies

Human colorectal carcinoma epithelial T_{84} cells (American Type Culture Collection, Rockville, Human colorectal carcinoma epithelial T_{84} cells (ATCC, Rockville, MD, USA) were grown in DMEM/Ham's F-12 medium (1:1) supplemented with 10% fetal bovine serum, 2 mM glutamine, 100 units/ml penicillin and 100 µg/ml streptomycin (Invitrogen, Karlsruhe, Germany) at 5% CO_2/37ºC. Cells were seeded on fibronectin (Invitrogen)/collagen (Cellon, Luxembourg) coated glass cover slips. Typically these cells grow slowly as polarized monolayers (T_{84}-slow). Due to spontaneous transformation, a T_{84} cell line was selected which grew remarkably faster (T_{84}-fast). For proliferation assays cells were plated at a density of 2000 cells/0.35 cm^2 and incubated 2 days later with either niflumic acid (0,01–100mM) or

astemizole (0,5–5000nM). Cell proliferation was assessed by 5-bromo-2´-deoxyuridine (BrdU) incorporation using an ELISA kit (Roche, Penzberg, Germany) and cell counting. The cell number was assessed after fixation in 3.7% formaldehyde / 0.5% Triton X-100 for 30 minutes at room temperature and after staining with Mayer's hemalaun (Merck, Darmstadt, Germany) for 5 minutes. Digitized microscopic images were taken (Fluovert FS, Leitz, Germany) and nuclei were counted using imaging software (TINA 2.09g). Toxicity of the blockers was assessed using Trypan Blue (Sigma). Each experiment was performed at least in triplicate.

Cell cycle, FACS analysis, Caspase assay, RT-PCR

Cells were synchronized into early G1 by 24h serum starvation. Incubation in thymidine (2 mM), (Sigma) halted the cells at G1/S transition. 36h treatment with demecolcine (0.05 µg/ml) (Sigma) synchronized into M phase. Synchronization was verified by FACS (COULTER EPICS® XL-MCL, Beckmann, Miami, USA) using propidium iodide staining of the DNA (Sigma). Apoptosis was analyzed after 8h and 24 h incubation with the protein kinase C inhibitor staurosporine (1 µM), (Sigma) and detection of cleaved caspase-3 in western blots using rabbit anti-human caspase-3 antibody (1:1000, Cell Signaling Technology, Inc., Danvers, USA). For RT-PCR total RNA was isolated using NucleoSpin RNA II columns (Macherey-Nagel, Düren, Germany). 1 µg total RNA was reverse transcribed for 1 h at 37˚C using random primer and RT (M-MLV Reverse Transcriptase, Promega, Mannheim, Germany). For PCR the following primers were used: hEag1 (KCNH1, NM_002238): 5´-CGCATGAACTACCTGAAGACG-3´ (s), 5´-TCTGTGGATGGGGCGATGTTC-3´ (as), 560 bp. hBest1 (VMD2, NM_004183): 5´-CTGCTCTGCTACTACATCATC-3´ (s), 5´-GTGTCCACACTGAGTACGC-3´ (as), 552 bp. The conditions were: 94˚C / 2 min, 35 cycles of 94˚C / 30 sec, 58°C / 30 sec and 72˚C / 1 min. PCR products were visualized by loading on 2% agarose gels and verified by sequencing.

Down regulation of Best1 and Eag1 expression by RNAi

Three different batches (A, B, C) of duplexes of 21-nucleotide RNAi with 3'-overhanging TT were purchased from Invitrogen (Karlsruhe, Germany). The sense strands of the RNAi used to silence the Best1 gene were 5´-AAUUCCUGUCGACAAUCCA-GUUGGU-3´(A), 5´-AUCUCAUCCACA-GCCAACAGGGACA-3´(B), and 5´-UAAAUAAAGCGGAUGAUGUAG UAGC-3´(C). RNAi sequences for Eag1 are shown in (44). Fluorophore labeled RNAi and exposure to the transfection reagent lipofectamine 2000, (Invitrogen) served as controls. After 48 hrs cells were further processed in proliferation assays and for western blotting.

Detection of Eag1 and Best1 by Western blotting

T_{84} cells were homogenized in lyses buffer (mmol/l: NaCl 150, Tris 50, DTT 100, 1% NP-40, and 1% protease inhibitor cocktail) (Sigma). Equal amounts of total protein (50 µg) were separated by 7% SDS-PAGE, transferred to Hybond-P (Amersham Biosiences, Freiburg, Germany) and incubated with either rabbit anti-hKv10.1 (Eag1) (Alomone labs, Jerusalem, Israel) or rabbit anti-hVMD-2 (Best1) (52) antibodies. Proteins were visualized using goat anti-rabbit IgG conjugated to horseradish peroxidase (Acris Antibodies, Hiddenhausen, Germany) and ECL (Amersham). Signals were detected by an Fluor-STM MultiImager (Bio-Rad Laboratories, Hercules, USA).

Measurement of the intracellular Ca^{2+} concentration and cell volume

T_{84} cells were loaded with 2 µM Fura-2 AM (Molecular Probes, Eugene, USA) in Opti-MEM medium (GIBCO) with 2.5 mM probenecid (Sigma) for 1h at room temperature. Fluorescence was detected in cells perfused with ringer solution containing 2.5 mM probenecid (Sigma) at 37°C, using an inverted microscope IMT-2 (Olympus, Nürnberg, Germany) and a high-speed polychromator system (VisiChrome, Puchheim, Germany). Fura-2 was excited at 340/380 nm and emission was recorded between 470 and 550 nm using a CCD camera (CoolSnap HQ, Visitron). $[Ca^{2+}]_i$ was calculated from the 340/380 nm fluorescence ratio (after background subtraction). The formula used to calculate $[Ca^{2+}]_i$ was $[Ca^{2+}]_i = K_d \times (R-R_{min})(R_{max}-R) \times (S_{f2}/S_{b2})$ where R is the observed fluorescence ratio. The values R_{max}, R_{min} (maximum and minimum ratios) and the constant S_{f2}/S_{b2} (fluorescence of free and Ca^{2+}-bound fura-2 at 380 nm) were calculated, using 2 µmol/l ionomycin (Calbiochem), 5 µmol/l nigericin, 10µmol/l monensin (Sigma) and 5 mmol/l EGTA to equilibrate intracellular and extra cellular Ca^{2+} in intact fura-2-loaded cells. The dissociation constant for the fura-2-Ca^{2+} complex was taken as 224 nmol/l.

Cell volume was measured directly by Zeiss-Axiovert 200M/ApoTome using Axiovision software or was assessed by fluorescence measurements in calcein (2 µM; Molecular Probes, USA) loaded cells at an excitation of 500 nm and emission of 520-550 nm. The experiments were done in the presence of 2.5 mM probenecid. The control isotonic solution (290 mOsm) was prepared by adding 120 mM mannitol. The hypotonic (170 mOsm) and control isotonic solution contained 85 mM NaCl.

Patch clamping

Cell culture dishes were mounted on the stage of an inverted microscope (IM35, Zeiss, Germany), and perfused continuously (37°C) with Ringer solution. Patch-clamp experiments were performed in the fast and slow whole-cell configuration. Patch pipettes had an input resistance of 2–4 MΩ, when filled with a solution containing (mM) KCl 30, K-gluconate 95,

NaH_2PO_4 1.2, Na_2HPO_4 4.8, EGTA 1, Ca-gluconate 0.758, $MgCl_2$ 1.034, D-glucose 5, ATP 3. pH was adjusted to 7.2, the Ca^{2+} activity was 0.1 µM. The access conductance was monitored continuously and was 60–120 nS. Currents (voltage clamp) and voltages (current clamp) were recorded using an EPC7 amplifier (HEKA, Darmstadt, Germany), the LH1600 interface and PULSE software (HEKA) as well as Chart software (AD-Instruments, Spechbach, Germany). In intervals membrane voltages (V_c) were clamped in steps of 10 mV from -50 to +50 mV relative to resting potential. The membrane conductance G_m was calculated from the measured current (I) and V_c values according to Ohm's law.

Materials and statistical analysis

All compounds used were of highest available grade of purity. Astemizole, niflumic acid (NFA), DIDS, tetrapentylammonium (TPeA), carbachol, and ATP were all from SIGMA (Taufkirchen, Germany). Student's t-test (for paired or unpaired samples as appropriate) and analysis of variance (ANOVA) was used for statistical analysis. $P<0.05$ was accepted as significant.

Results

Fast growing colonic carcinoma cells (T_{84}-fast) express Eag1 and Best1

T_{84} cells typically grow in slowly expanding patches (T_{84}-slow), which form tight and polarized monolayers after 10 to 14 days, even when grown on impermeable supports (Fig. 2-1A, B). Apoptotic cells are regularly observed in the supernatant. At passage number 73, the cell line spontaneously changed its growth pattern, i.e. the cells grew remarkably faster (T_{84}-fast) as singe single cells, non-polarized and above each other (Fig. 2-1A, B). No apoptotic cells were found in the supernatant. We examined apoptosis by analyzing uncleaved and cleaved caspase 3 by Western blotting and found small amounts of cleaved caspase 3 in T_{84}-slow, but not in T_{84}-fast cells after treatment with the PKC inhibitor staurosporin (1 µM) (Fig. 2-1C).

RT-PCR analysis of the voltage gated K^+ channel Eag1 and the putative Ca^{2+} activated Cl^- channel Best1 suggested a higher number of transcripts for Eag1 and Best1 in T_{84}-fast cells (Fig. 2-1D). Increased expression of Eag1 and Best1 was confirmed by Western blotting, which demonstrated much higher levels of Eag1 protein and Best1 protein in T_{84}-fast cells (Fig. 2-1E). The membrane conductance properties were analyzed in T_{84}-slow and T_{84}-fast cells in whole cell patch clamp experiments and membrane voltages (Vm) were measured in the current clamp mode. T_{84}-slow cells (n = 8) were more hyperpolarized (-51.7 $\pm$ 5.6 mV) and had a lower baseline conductance (3.8 $\pm$ 0.7 nS) than T_{84}-fast cells (-36.6 $\pm$ 2.9 mV and 23.8 $\pm$ 2.9 nS, n = 8). The increased baseline conductance and depolarized Vm of T_{84}-fast cells was due to a higher activity of Cl^- channels, since replacement of extra cellular Cl^- by

gluconate (5Cl) shifted the I/V curve to more positive clamp voltages. This was not observed for T_{84}-slow cells (Fig. 2-1F).

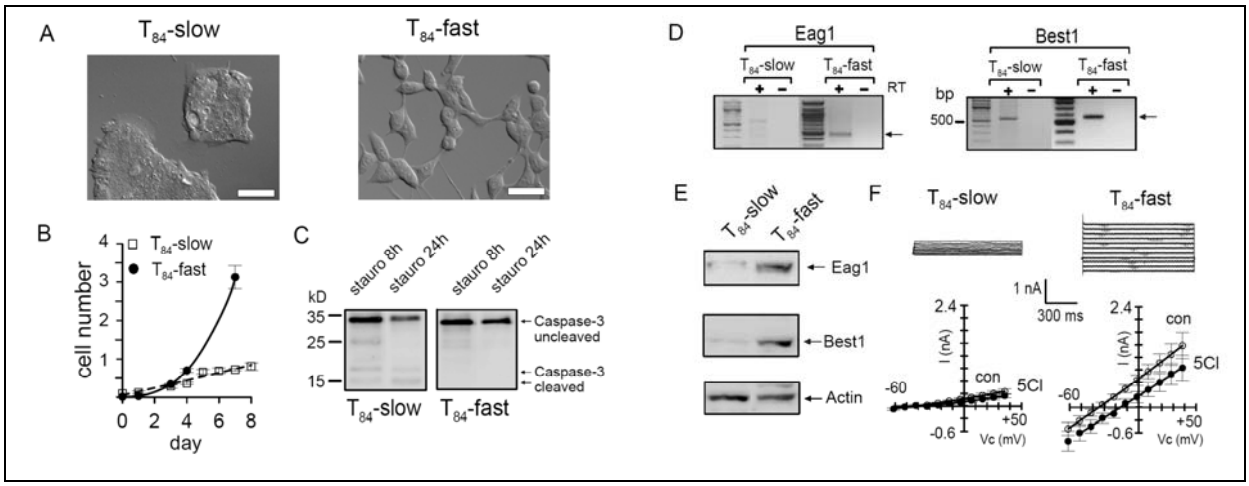

Fig. 2-1 Slow and fast growing T_{84} cells

A) Typical growth patterns of T_{84}-slow cells as obtained from ATCC, and spontaneously transformed T_{84}-fast cells. Bars indicate 50 µm. B) Proliferation curves for T_{84}-slow and T_{84}-fast cells, as obtained by cell counting (n = 4). C) Western blot for uncleaved and cleaved caspase-3 in T_{84}-slow and T_{84}-fast cells after 8 and 24 h incubation with 1 µM staurosporine (stauro). D) RT-PCR analysis of mRNA expression for Eag1 (560 bp) and Best1 (552 bp) in slow and fast growing T_{84} cells. +/- RT indicates presence or absence of reverse transcriptase. For PCR conditions c.f. Methods. E) Western blot analysis of the expression of Eag1 and Best1 in slow and fast growing T_{84} cells. Actin indicates equal loading of the gel. F) Whole cell currents measured in slow and fast growing T_{84} cells under control conditions (upper panels). Corresponding current/voltage relationships (n = 8 for both cell types; lower panels). Replacement of extracellular Cl- by gluconate (5Cl) shifted the i/v curve to more depolarized clamp voltages only in fast growing T_{84} cells, indicating the presence of a baseline Cl- conductance. RT-PCR and Western blots were performed at least in triplicates.

Eag1 controls proliferation of fast but not of slow growing T_{84} cells

Eag1 has been demonstrated to support proliferation of several different cell types (44, 53). We therefore examined if high expression levels of Eag1 correlate with increased proliferation of T_{84}-fast cells. To that end T_{84}-slow and T_{84}-fast cells were treated with three different batches (A-C) of siRNA for Eag1. Incubation of the cells with either fluorescence labeled scrambled oligos or lipid (transfection reagent) and non-treated cells served as controls. Measurement of BrdU incorporation clearly indicates inhibition of proliferation of T_{84}-fast cells after treatment with siRNA for Eag1 (Fig. 2-2A). siRNA treatment of T_{84}-slow cells did not affect cell proliferation, suggesting a proliferative function of Eag1 only in T_{84}-fast

cells. Notably, Eag1 expression was significantly upregulated by re-addition of 10% FCS in serum starved cells (data not shown). Using the inhibitor astemizole (5 µM), we examined the contribution of Eag1 to whole cell currents measured in T_{84}-slow and T_{84}-fast cells. Astemizole inhibited whole cell currents in both cell types, however, the effect was more pronounced in T_{84}-fast cells and thus astemizole-sensitive whole cell currents were significantly larger in T_{84}-fast cells (Fig. 2-2B,C).

A previous report supplied evidence that hyperpolarizing Eag1 currents assist in the increase of intracellular Ca^{2+} ($[Ca^{2+}]_i$), when cells are stimulated with secretagogues (ATP, carbachol) or mitogens, and may thereby support proliferation (44). We compared increase in $[Ca^{2+}]_i$ in Fura-2 loaded T_{84}-slow and T_{84}-fast cells upon stimulation with ATP (100 µM). ATP binds to purinergic $P2Y_2$ receptors and thereby induces a peak and plateau $[Ca^{2+}]_i$ increase in both cell lines (Fig. 2-2D). However, the peak $[Ca^{2+}]_i$ increase was doubled in T_{84}-fast when compared with T_{84}-slow cells, which may indicate a role of Eag1 for Ca^{2+} signaling in T_{84}-fast cells (Fig. 2-2D,E).

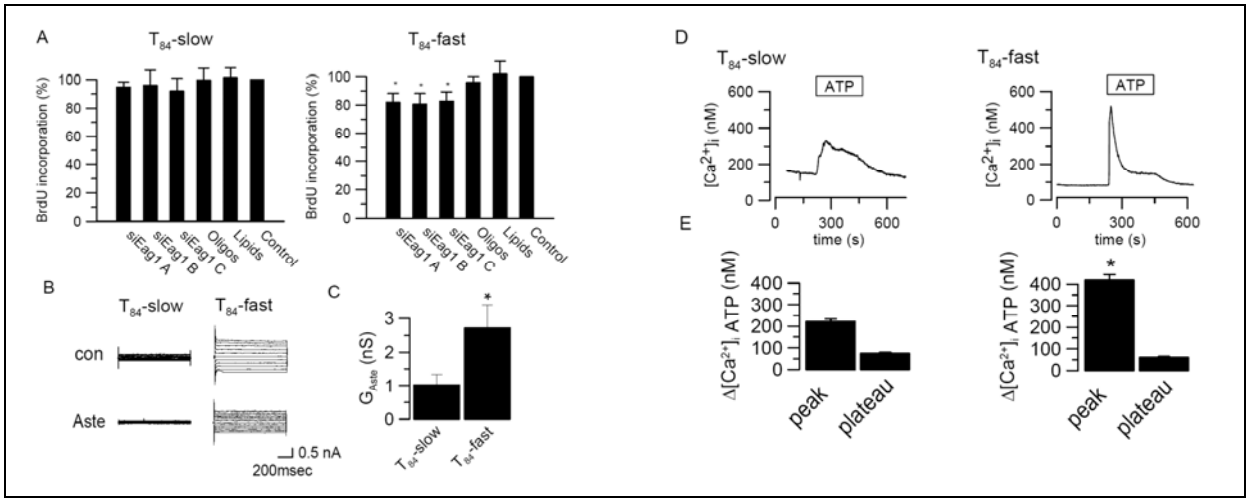

Fig. 2-2 Eag1 supports proliferation of fast growing T_{84} cells

A) Proliferation of slow and fast growing T_{84} cells as measured by BrdU incorporation. Cells were treated with three different batches (A-C) of siRNA for Eag1. Incubation of the cells with fluorescence labeled scrambled oligos (Oligos) or transfection reagent only (Lipid) and non-treated cells (Control) served as controls. Assays were performed at least in triplicates. * indicate significant inhibition of proliferation by RNAi in T_{84}-fast cells (ANOVA). B) Whole cell currents in T_{84}-slow and T_{84}-fast cells and effect of the Eag1 inhibitor astemizole (Aste; 5 µM). C) Summary of the calculated astemizole sensitive whole cell conductances (GAste) in T_{84}-slow (n = 8) and T_{84}-fast (n = 9) cells. GAste was significant in both cell lines and was enhanced in T_{84}-fast cells (unpaired t-test). D) Increase of the intracellular Ca^{2+} concentration ($[Ca^{2+}]$i) by stimulation with ATP (100 µM) in T_{84}-slow and T_{84}-fast cells. E) Summary of the ATP induced peak and plateau increase

in $[Ca^{2+}]i$ in slow (n = 59) and fast (n = 69) growing T_{84} cells. * indicates significant difference in peak $[Ca^{2+}]i$ increase in T_{84}-fast cells.

Eag1 activity in T_{84}-fast cells is cell cycle dependent

In other cell types Eag1-activity varies during the cell cycle (53). Therefore we examined cell cycle dependence of Eag1 in T_{84}-fast cells. Cells were synchronized in early G1 (eG1), G1/S or M phase (c.f. methods), and synchronization was verified by FACS analysis (Fig. 2-3A).

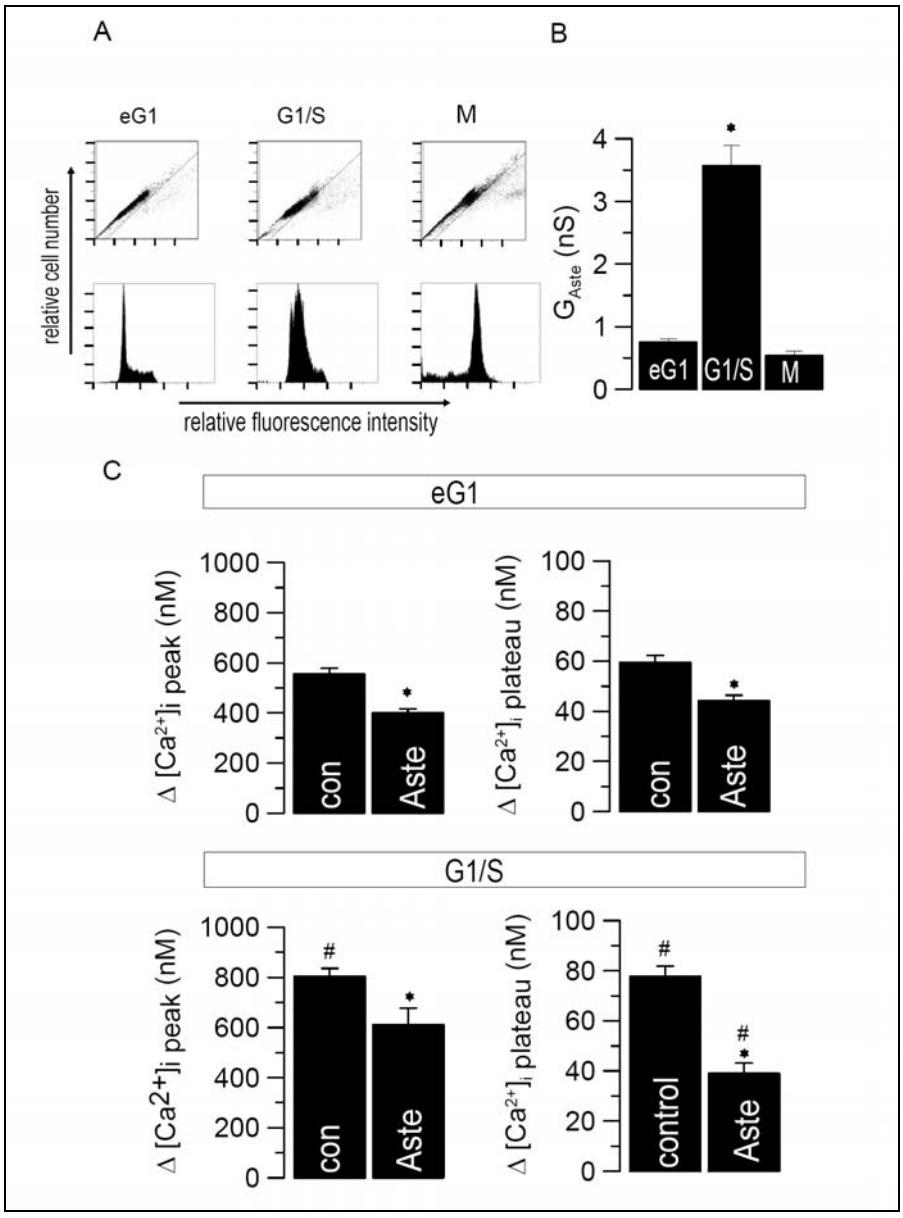

Fig. 2-3 Eag1 operates as a cell cycle regulated channel in fast growing T_{84} cells

A) FACS analysis of fast growing T_{84} cells synchronized in early G1 (eG1), G1/S transition and M phase (c.f. Methods). Experiments were performed at least in triplicates. B) Astemizole sensitive whole cell conductances (GAste) measured in T_{84}-fast cells synchronized in eG1 (n = 14), G1/S (n = 9) and M (n = 9) phase. GAste was significant

during all cell cycle phases but was enhanced during G1/S (ANOVA). C) Upper panel: Summary of the peak and plateau $[Ca^{2+}]i$ increase induced by CCH in T_{84}-fast cells, synchronized into eG1 and effects of 0.5 µM astemizole (Aste, n = 73). Lower panel: Summary of the peak and plateau $[Ca^{2+}]i$ increase induced by CCH in T_{84}-fast cells, synchronized into G1/S and effects of 0.5 µM astemizole (Aste, n = 64). The effect of astemizole was significant in all series (paired t-test) and was enhanced for plateau $[Ca^{2+}]i$ increase in G1/S when compared to eG1 (unpaired t-test).

We found that astemizole sensitive whole cell currents were augmented in cells synchronized in G1/S, when compared to eG1 or M phase (Fig. 2-3B). T_{84} cells also express other voltage gated K^+ channels such as Kv1.5 or Kv3.4, which are blocked by the inhibitor TPeA (44). However, in contrast to Eag1, TPeA sensitive whole cell currents were not cell cycle dependent (data not shown). We further compared the increase in $[Ca^{2+}]_i$ in T_{84}-fast cells synchronized in eG1 and G1/S phase. Both peak and plateau $[Ca^{2+}]_i$ increase were significantly enhanced in G1/S-cells. Moreover, the Eag1-blocker astemizole inhibited peak and plateau $[Ca^{2+}]_i$ increase in both cell cycle phases, but the effect of astemizole on plateau $[Ca^{2+}]_i$ was augmented in the G1/S phase (Fig. 2-3C). These results supply evidence for cell cycle regulated Eag1-currents in T_{84}-fast cells and cell cycle dependent effects of Eag1 on Ca^{2+} signaling.

Best1 controls proliferation of fast but not of slow growing T_{84} cells

Because T_{84}-fast cells show much higher expression of Best1 when compared with T_{84}-slow cells (Fig. 2-4A), we examined the effect of this putative Ca^{2+} activated Cl^- channel on cell proliferation. T_{84}-slow and T_{84}-fast cells were treated with three different batches (A-C) of siRNA for Best1, which reduced Best1 levels in T_{84}-fast cells. Expression levels in T_{84}-slow cells were already very low (Fig. 2-4A,B). Incubation of the cells with either fluorescence labeled scrambled oligos or transfection reagent (lipid) and non-treated cells served as controls. Measurement of BrdU incorporation clearly indicates inhibition of proliferation of T_{84}-fast cells after treatment with siRNA for Best1 (Fig. 2-4C). No effects of siRNA were seen in T_{84}-slow cells, suggesting a proliferative function of Best1 only in T_{84}-fast cells.

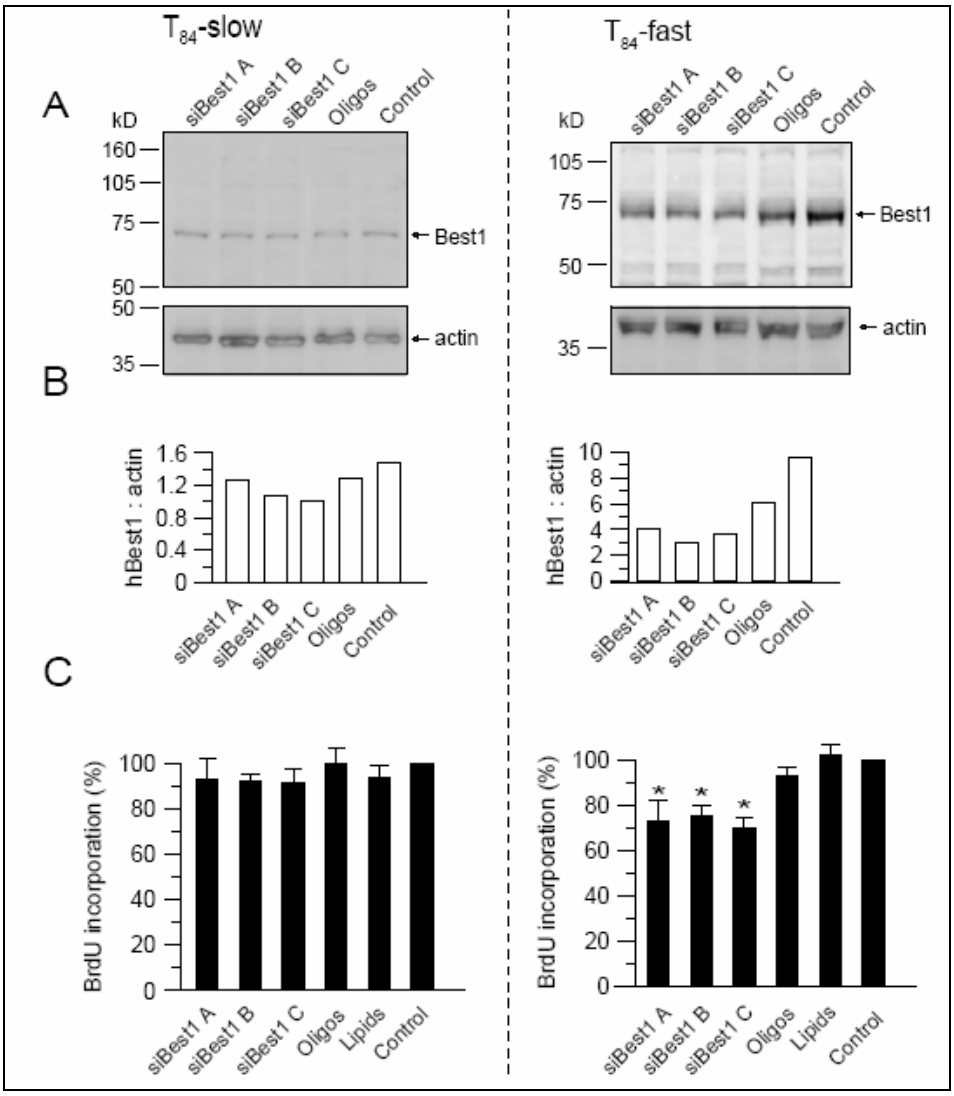

Fig. 2-4 Best1 supports proliferation of fast growing T_{84} cells

A) Western blot analysis of Best1 in T_{84}-slow and T_{84}-fast cells treated with three different batches (A-C) of siRNA for Best1. Incubation of the cells with fluorescence labeled scrambled oligos (Oligos) or non-treated cells (Control) served as controls. Actin indicates equal loading of the gels. B) Densitometric analysis of Best1 expression and ratio between Best1 and actin expression. C) Proliferation of slow and fast growing T_{84} cells as measured by BrdU incorporation. Assays were performed at least in triplicates. * indicate significant inhibition of proliferation by RNAi in T_{84}-fast cells (ANOVA).

In whole cell patch clamp experiments, the high baseline conductance found in T_{84}-fast cells could be partially inhibited by the blockers of Ca^{2+} activated Cl^- channels, NFA and DIDS (both 100 µM). Both inhibitors had no effect in T_{84}-slow cells (Fig. 2-5A). Stimulation with ATP (100 µM) to increase intracellular Ca^{2+} (Fig. 2-2D), activated a whole cell current in T_{84}-slow but not in T_{84}-fast cells (Fig. 2-5B). In T_{84}-slow cells, ATP activated primarily a K^+ conductance, as indicated by the hyperpolarizing effect of ATP on the membrane voltage

(Fig. 2-5C). Little effects of ATP were seen in T_{84}-fast cells. Correspondingly, replacement of extra cellular Cl^- by impermeable gluconate (5Cl) showed no effects in T_{84}-slow cells, but reduced the baseline conductance in T_{84}-fast cells (Fig. 2-5D). Taken together, these results suggest active Best1 Cl^- channels in non-stimulated T_{84}-fast cells, which cause enhanced proliferation.

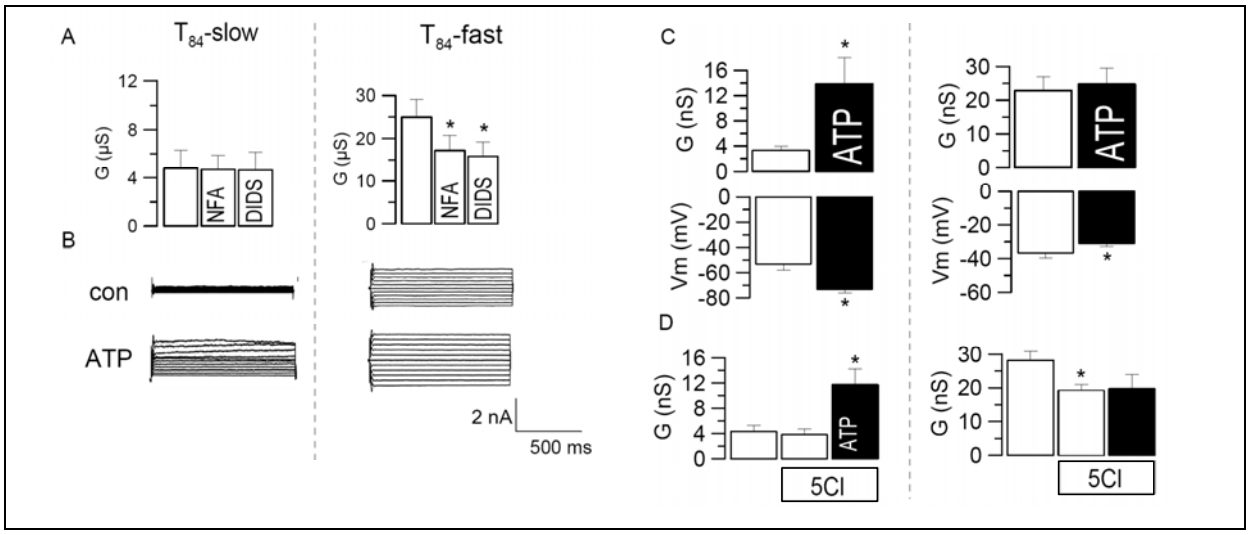

Fig. 2-5 T_{84}-fast but not T_{84}-slow cells have a Cl- conductance.

A) Summaries for the baseline whole cell conductances (G) and effects of the inhibitors of Ca^{2+}-activated Cl- channels, niflumic acid (NFA; 10 µM) and DIDS (100 µM) in slow and fast growing T_{84} cells (n = 8 – 11). * indicate significant effects of NFA and DIDS (paired t-test). B) Whole cell currents measured in T_{84}-slow and T_{84}-fast cells. Stimulation of the cells with ATP (100 µM) activated a whole cell conductance only in T_{84}-slow but not in T_{84}-fast cells. C) Summaries for the whole cell conductances (upper panels) and membrane voltages (lower panels) measured in T_{84}-slow (n = 13) and T_{84}-fast (n = 14) cells, and effects of ATP (100 µM). * indicate significant effects on whole cell conductance and membrane voltages (paired t-test). D) Summaries for the whole cell conductances measured in T_{84}-slow (n = 9) and T_{84}-fast (n = 8) cells, and effect of replacement of extracellular Cl- by gluconate (5Cl) and ATP (100 µM). * indicate significant activation of conductance by ATP in T_{84}-slow cells and significant inhibition by 5Cl (paired t-test).

Increased proliferation and Cl- conductance in Best1-transfected T_{84}-slow cells

To further demonstrate that Best1 contributes to proliferation of T_{84} cells, we expressed human Best1 in T_{84}-slow cells. As shown in Fig. 2-6A, transfection of 100 ng of exogenous Best1 increased Best1 expression in T_{84}-slow cells almost to the level found in T_{84}-slow cells. No change was seen in mock-transfected cells. Notably, over expression of Best1 changed the growth pattern of T_{84}-slow cells towards that found for T_{84}-fast cells (Fig. 2-6B). Moreover, after expression of Best1, a DIDS-sensitive whole cell current appeared in T_{84}-slow cells,

which was not found in mock-transfected or parental cells (Fig. 2-6C). Measurement of the BrdU-incorporation indicated a significant increase in proliferation of Best1-transfected T_{84}-slow cells, which was not observed for mock-transfected cells (Fig. 2-6D). In summary, both Eag1 K^+ channels and Best1 Cl^- channels are upregulated in spontaneously transformed T_{84} cells, where they augment proliferation.

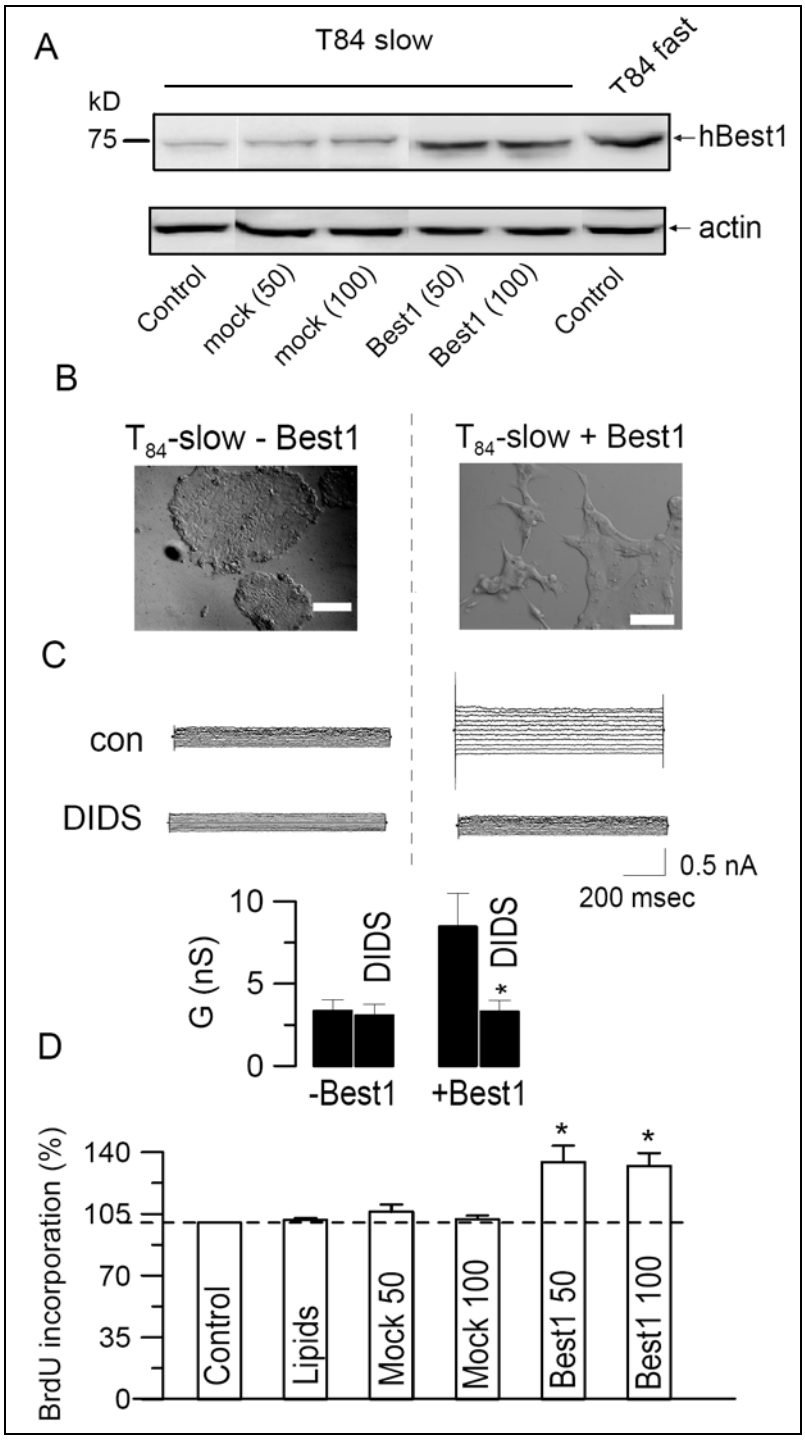

Fig. 2-6 Expression of Best1 in T_{84}-slow cells enhances Cl- currents and proliferation

A) Western blot analysis of human Best1 expression in T_{84}-slow cells after transfection of 50 or 100 ng of Best1 cDNA, or mock (50 and 100 ng) transfection, and comparison with the level of Best1 expression in T_{84}-fast cells and non-transfected T_{84}-slow cells. Actin indicates equal loading of the gel. B) Growth pattern of mock transfected (- Best1) and Best1 transfected (+Best1) T_{84}-slow cells. Bars indicate 50 µm. C) Upper panel: Whole cell currents measured in mock-transfected and Best1-transfected T_{84}-slow cells and effect of DIDS (100 µM). Lower panel: Summaries of the whole cell conductances and effects of DIDS on mock transfected (n = 7) and Best1 transfected (n = 7) T_{84}-fast cells. * indicates significant inhibition of whole cell conductance by DIDS (paired t-test). D) Proliferation of mock transfected (50 and 100 ng) and Best1 transfected (50 and 100 ng) cells. Non-transfected cells (Control) and cells exposed the transfection reagent only (Lipids) served as controls. * indicate significant increase in proliferation (ANOVA).

Eag1 and Best1 support intracellular Ca^{2+} signaling and volume regulation, respectively

Eag1 K^+ channels (and to some degree Best1) have a clear impact on intracellular Ca^{2+} signaling. This was demonstrated by stimulation with ATP (100 µM), which increased intracellular peak (ER- Ca^{2+} release) and plateau (Ca^{2+} - influx through SOC) in T_{84}-fast cells. Treatment with siRNA for Eag1 significantly reduced peak and plateau Ca^{2+} increase (Fig. 2-7A). Volume measurements indicate stronger cell swelling and potent regulatory volume decrease (RVD) in T_{84}-fast, when compared to T_{84}-slow cells, as identified by direct volume measurements and indirect measurements of calcein fluorescence (Fig. 2-7B-E). T_{84}-fast cells treated with siRNA-Best1 show reduced RVD (Fig. 2-7B). As both intracellular Ca^{2+} and cell volume control is essential for the mitotic cell cycle, these results may provide a mechanism for the proliferative role of Eag1 and Best1.

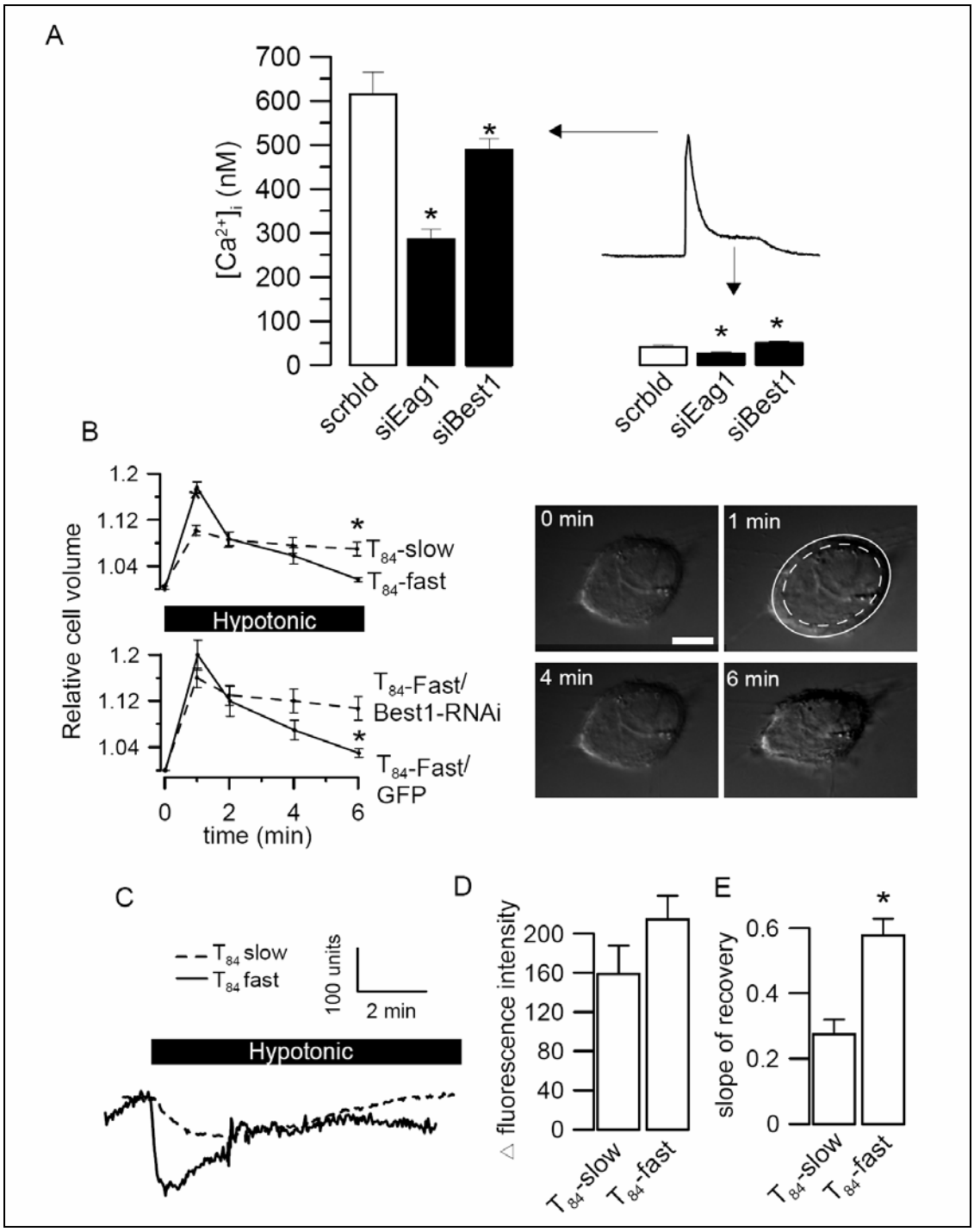

Fig. 2-7 Eag1 and Best1 support intracellular Ca^{2+} signaling and volume regulation

A) Summary of intracellular peak (left) and plateau (right) Ca^{2+} increase in T_{84}-fast cells, upon stimulation with ATP (100 µM). Cells were treated with scrambled siRNA or siEag1 and siBest1, respectively (n = 24 – 57). B) Hypotonic (170 mosmol) cell swelling assessed by volume measurement in T_{84}-slow and T_{84}-fast cells (upper trace) and T_{84}-fast cells treated with siRNA-Best1 or control transfection (GFP) (n = 5 each time point). C) Change in calcein fluorescence due to hypotonic cell swelling. D,E) Summaries for maximal change in fluorescence intensity and slope of recovery (from swelling) of T_{84}-slow and T_{84}-fast cells (n = 12). * indicate significant difference (paired t-test).

Discussion

Transformation of colonic epithelial cells increases proliferation and ion conductances

T_{84} colonic carcinoma cells are well established (7, 54). They grow slowly in patches and form tight and polarized monolayers, when cultured on permeable supports. T_{84} cells were used for numerous electrophysiological studies and resemble a model for electrolyte transport in the colonic epithelium (54). They show many aspects of native epithelial cells such as a relatively hyperpolarized membrane voltage and Cl^- secretion by cAMP-dependent cystic fibrosis transmembrane conductance regulator (CFTR) channels. When stimulated by secretagogues, which increase the intracellular Ca^{2+} concentration such as ATP or carbachol, predominantly K^+ channels are activated, hyperpolarizing the membrane voltage. This is comparable to colonic crypt cells, which also activate Ca^{2+} activated K^+ channels upon stimulation of basolateral muscarinic M3 and apical purinergic $P2Y_2$ receptors (7, 55). In contrast, T_{84} cells that had undergone spontaneous transformation were remarkably different. They proliferated much faster, showed typical features of malignancy and had different membrane conductances.

A change in membrane ion conductance has also been reported for spontaneously transformed Madin-Darby canine kidney (MDCK) cells. These fast growing MDCK-F cells express Ca^{2+} activated K^+ channels that largely enhance cell migration (56). The fast growing T_{84} cells described in the present study, showed a strong increase in the expression of the Best1 Cl^- channel, along with Eag1 potassium channels. Notably, the Cl^- channels were already active in non-stimulated cells, i.e. without purinergic stimulation. Additional increase of intracellular Ca^{2+} by ATP or carbachol did not further increase Cl^- conductance. A similar result was obtained when Best1 was over expressed in T_{84}-slow cells, and has also been observed when Best1 was expressed in Hek293 cells (45). It suggests that additional components may be required for Ca^{2+} -regulation of Best1 currents, which may not be present in cancer cells. The presence of these DIDS-sensitive Cl^- currents along with astemizole inhibited Eag1 K^+ currents clearly augmented cell proliferation

Ion channels induce malignancy and metastatic cell growth

Clonal selection of fast proliferating T_{84} cells (T_{84}SF) has previously been reported (57). These cells demonstrate invasive and metastatic cell growth, when transferred into nude mice. Basal tyrosine phosphorylation and expression of src kinase were enhanced in these T_{84}SF cells (57). Along this line, the src-inhibitor PP2 reduced cell growth, invasion and cell adhesion of T_{84}SF cells (58). In Jurkat T lymphocytes, src kinase controls voltage-dependent Kv1.3 K^+ channels, which also affect cell proliferation (59). Src kinase may also be up

regulated in fast growing T_{84} cells and may be responsible for changes in membrane conductance. It will be interesting to examine in subsequent studies the impact of Eag1 and Best1 on cell migration and tissue invasion, since we previously found that genomic amplification of Eag1 in human colorectal carcinoma is an independent marker of adverse prognosis (60).

How do ion channels determine malignancy?

K^+ and Cl^- channels are essential for cell migration and metastasis of cancer (61). It has been shown that enhanced intracellular Ca^{2+} activates Kv channels during intestinal wound healing (62). Cell migration and formation of tumor metastasis is due to fluctuations in the activity of membrane transporters and ion channels, since they cause localized cell swelling and shrinkage (61). These changes in cell volume appear to be a prerequisite for cell migration and malignant invasion. There are only a few studies investigating the role of Cl^- channels in cell migration. Cl^- channels are probably necessary for cell movement, since K^+ transport needs to be accompanied by a counterion (56). Notably, bestrophin has been shown to operate as a volume sensitive Cl^- channel (63).

A novel function of bestrophin for cell proliferation?

Cl^- currents induced by expression of bestrophins share many of the properties attributed to Ca^{2+} activated Cl^- channels, such as an anion selectivity of $I^- > Cl^-$ and inhibition by NFA and DIDS (48-50, 52). There is, however, an ongoing controversy whether bestrophins are actually channel forming proteins or rather regulators of ion channels. Moreover, other proteins have also been proposed as molecular candidates for the Ca^{2+} activated Cl^- channel (reviewed in (45). The present results would support the role of Best1 as a Cl^- channel. As known from previous studies, Ca^{2+} and volume regulated Cl^- channels support cell proliferation (6). Thus bestrophins may provide the molecular basis for an understanding of the role of these channels in cell proliferation.

Chapter 3

Voltage gated K^+ channels support proliferation of colonic carcinoma cells

Abstract

Plasma membrane potassium (K^+) channels are required for cell proliferation. Evidence is growing that K^+ channels play a central role in the development and growth of human cancer. Here we examine the contribution and the mechanism by which K^+ channels control proliferation of T_{84} human colonic carcinoma cells. Numerous K^+ channels are expressed in T_{84} cells, but only voltage gated K^+ (Kv) channels influenced proliferation. A number Kv channel inhibitors reduced DNA- synthesis and cell number, without exerting apoptotic or toxic effects. Expression of several Kv channels such as Eag1, Kv 3.4 and Kv 1.5 was detected in patch clamp experiments and in fluorescence based assays, using a voltage sensitive dye. The contribution of Eag1 channels to proliferation was confirmed by siRNA, which abolished Eag1 activity and inhibited cell growth. Inhibition of Kv channels did not interfere with the ability of T_{84} cells to regulate their cell volume, but restricted intracellular pH regulation. In addition, inhibitors of Kv channels as well as siRNA for Eag1 attenuated intracellular Ca^{2+} signaling. The data suggest that Kv channels control proliferation of colonic cancer cells by affecting intracellular pH and Ca^{2+} signaling.

Introduction

Apart from their specific epithelial transport function, membrane ion channels are essential for maintaining cellular homeostasis and signaling. Thus they contribute to the control of essential parameters such as cell volume, intracellular pH and intracellular Ca^{2+} concentration. K^+ selective ion channels form the largest ion channel protein family, which may be subdivided into voltage gated, Ca^{2+} dependent, 2-pore domain, and inward rectifier K^+ channels. It has recently been suggested that in addition to the physiological parameters controlled by K^+ channels, they also affect mitotic cell cycling, proliferation and development of cancer. A role of K^+ channels for proliferation and tumor cell growth has been demonstrated for a number of carcinoma, like those of prostate, colon, lung, breast and others (14). K^+ channels of different subfamilies have been correlated with tumor proliferation, including Ca^{2+} activated K^+ channels, Shaker-type voltage-gated K^+ channels, the ether-á-go-go (Eag1) family of voltage gated K^+ channels and the 2P-domain K^+ channels (14, 15, 41, 64). It is not known currently, why different types of K^+ channels induce proliferation in the different cancer models. Most of the previous studies describe expression of a particular type of K^+ channel in a cancer cell line and correlate expression and functional activity of the channel with proliferation. However, mammalian cells always express a whole array of various types of K^+ channels, and it is not clear to what degree these individual K^+ channels contribute to proliferation, or if there is a specific association between particular K^+ channel subtypes and proliferation. Moreover the mechanisms by which these K^+ channels facilitate cell proliferation remain obscure.

Colonic carcinomas belong to the most frequent cancers in human. A previous study found a correlation between the activity of voltage gated K^+ channels and proliferation and metastasis of a colonic cancer cell line and native colonic cancers, respectively (16, 65). Interestingly Ca^{2+} influx into colonic cancer cells was affected by voltage gated K^+ channels in one study (65). Identification of K^+ channels which are relevant for the growth of colonic carcinomas may provide novel therapeutic targets (66, 67). Moreover, K^+ channels abnormally expressed in colonic cancer cells could be potentially useful as markers for malign transformation. In the present study, we therefore screened T_{84} colonic carcinoma cells for expression of a broad spectrum of K^+ channels. We then tried to identify the K^+ channels that have an impact on proliferation of these cells. Using a variety of K^+ channel blockers and siRNA, we found that voltage gated K^+ channels take part in controlling cell proliferation, while other K^+ channel subtypes do not. A further aim of this study was to uncover how these channels affect proliferation. The data suggest that voltage gated K^+ channels control basic cellular properties like intracellular Ca^{2+}, elicited by agonist stimulation of the cells, and regulation of the intracellular pH. Both effects are likely to be due to the hyperpolarizing effect of Kv channels on the membrane voltage.

Material and Methods

Cell culture and proliferation studies

Human colorectal carcinoma epithelial T_{84} cells (American Type Culture Collection, Rockville, MD, USA), were grown in DMEM/Ham's F-12 medium (1:1), supplemented with 10% fetal bovine serum (FBS), 2 mM glutamine, 100 units/ml penicillin and 100 µg/ml streptomycin (Pen/Strep) (GIBCO, Germany) in a 5% CO_2 atmosphere at 37ºC. Cells were seeded on bovine plasma fibronectin (Invitrogen, Germany) and bovine dermal collagen (Cellon, Luxembourg) coated plastic dishes or glass cover slips. For proliferation assays, T_{84} cells were plated at a density of 2000 cells/0.35 cm^2 on coated 96 well plates (Sarstedt, Nürnberg, Germany). After 2 days, cells were incubated with inhibitors of potassium channels dissolved in serum reduced Opti-MEM 1 medium (GIBCO, Germany). After additional 2 days, cell proliferation was assessed by 5-bromo-2´-deoxyuridine (BrdU) incorporation and cell counting. BrdU incorporation was determined using an immunoassay cell proliferation ELISA kit (Roche, Germany), according to the manufacturer's protocol. For cell counting, cells were fixed with 3.7% formaldehyde and 0.5% Triton X-100 in ringer solution (mmol/l: NaCl 145; KH_2PO_4 0,4; K_2HPO_4 1,6; Glucose 5; $MgCl_2$ 1; Ca^{2+}-Gluconat 1,3, pH 7.4) for 30 min and stained with Mayers Hemalaun (Merck, Darmstadt, Germany). Digital images were obtained and nuclei were counted using imaging software. Toxicity of the blockers was assessed by counting non-stained dead cells in the supernatants (Trypan Blue). Each experiment was performed in triplicate.

Expression of potassium channels in T_{84} cells and real time PCR analysis

Total RNA was isolated from T_{84} cells using NucleoSpin RNA II columns (Macherey-Nagel, Germany). 1 µg total RNA was reverse transcribed for 1 h at 37˚C using random primer and RT (M-MLV Reverse Transcriptase, Promega, Germany). RT-PCR was used to detect expression of the mRNAs for potassium channels. The oligonucleotide primers were designed for the mRNA of each gene product (name, gene, accession number: sense and antisense primer, size of PCR product): Kv1.3, KCNA3, NM_002232: 5´-GCCATCCTCTACTACTATCAG-3´, 5´-CCACAATGTCGATCAGGTTC-3´, 532 bp; Kv1.5, KCNA5, NM_002234: 5´-CTACTTCGACCCCCTGAG-3´, 5´-GCTCGAAGGTGAACCAGATG-3´, 555 bp; KvLQT, KCNQ1, NM_000218: 5´-CCACGGGGACTCTCTTCTG-3´, 5´- GGCACCTTGTCCCCATAG-3´, 504 bp; Kv3.3 / Kv3.4, KCNC3/KCNC4, NM_004977: 5´- GACGTGCTGGGCTTCCTG-3´, 5´-GCTTCTGCTTGGCCATGG-3´, 442 bp; Kv4.1 , KCND1, NM_004979: 5´-GGAAGAATACGCTGGACCG-3´, 5´- GCGGCATGGGATGGTCTC-3´, 472 bp; Kv5.1, KCNF1, NM_002236: 5´- GAGTCGTCGTGCCCGGC-3´, 5´- GTCTCTGGATGGCTCTGCTC-3´, 530bp; Kv9.3 , KCNS3, NM_002252: 5´- GTGCAGCCTGATCTTCCTC-3´, 5´-

GTGTCAAACTTCTCCAGCTC-3´, 540 bp; Eag1, KCNH1, NM 002238: 5´-GCATGAACTACCTGAAGACG-3´, 5´- CTTCTCAATGTCTGTGGATGG-3´, 488 bp; Erg1, KCNH2, NM 000238: 5´- CAATGCCAACGAGGAGGTG -3´, 5´- GGAGAGACGTTGCCGAAG -3, 468 bp; Elk1, KCNH8, NM_144633: 5´- GCCCGAACTGAAGTCATGC-3´, 5´-CAAAATAAGCCAGTCCCAGC-3´, 522 bp; Kir6.1, KCNJ8, NM_004982: 5´-GTTTGGAGTCCACTGTGTGTG-3´, 5´- CAGAATAACTATGACCTCCAAG-3´, 548 bp; TWIK1, KCNK1, NM_002245: 5´- GCTTCGGCTTCCTGGTGC-3´, 5´-GACAAACCCAAGGAGCACG-3´, 505 bp; TASK2 , KCNK5, NM_009740: 5´-GGCCATCACAGGGAACCAG-3´, 5´- GCCAGGCCAGCCCCAAG-3´, 496 bp; TWIK2, KCNK6, NM_004823: 5´- GATCTTTGCCCACCTCGAG-3´, 5´-GATGCTGGGAAACAAAGGAG-3´, 520 bp; BK_{Ca} channel ß-subunit, KCNMA1, NM_002247: 5´- GTGGATGAAAAAGAGGAGGC-3´, 5´- CAAATGGATGAACCCGGCTG -3´, 528 bp; BK_{Ca} channel ß-subunit, KCNMB3, NM_014407: 5´- CGACCTGCACTGCCATCC-3´, 5´-GGGCACCACCTAGCAGAG-3´, 398 bp; BK_{Ca} channel ß-subunit, KCNMB4, NM_014505: 5´-CCAGGTCTACGTGAACAAC-3´, 5´- CTGTTGCCACTGAGGGATG-3´, 520 bp; SK4 , KCNN4, NM_002250: 5´- GATTTAGGGGCGCCGCTGAC-3´, 5´-CTTGCCCCACATGGTGCCC-3´, 520 bp. The PCR reactions were performed at 94˚C for 2 min, 35 cycles at 94˚C for 30 s, annealing temperature 60°C for 30 s and 72˚C for 1 min. PCR products were visualized by loading on agarose gels and were verified by sequencing.

Real time PCR was performed in a Light Cycler (Roche, Germany), using the Quanti Tect SYBR Green PCR Kit (Quiagen, Germany). Each reaction contained 2 µl Master Mix (including Taq polymerase, dNTPs, SYBR Green buffer), 1 pM of each primer (Eag1: 5´-GGAGTTCCAGACGGTGCAC-3´, 5´- CCTCATCATCTTGGATCACC-3´, 116 bp; β-actin , ACTB, NM 001101: 5´- CAACGGCTCCGGCATGTG-3´, 5´- CTTGCTCTGGGCCTCGTC-3´, 151 bp), 2.5 mM $MgCl_2$ and 2 µl cDNA. After 10 min at 94°C for activation of Taq polymerase, cDNA was amplified by 15 s at 94°C, 10 s at 60°C, and 20 s at 72°C, for 50 cycles. The amplification was followed by a melting curve analysis to control of the PCR products. As negative controls, water instead of cDNA was run with every PCR experiment. To verify accuracy of the amplification, PCR products were further analyzed on ethidium bromide stained 2% agarose gels. Analysis of the data was performed using Light Cycler software 3.5.3. Standard curves for Eag1 channel mRNA and β-actin mRNA were produced by using cDNA of 16HBE cells at different dilutions. The ratio of the amount of Eag1 to β-actin mRNA was calculated for each sample.

Downregulation of Eag1 expression by small interfering RNA

Duplexes of 21-nucleotide siRNA with 3'-overhanging TT were designed according to Ahn et al 2003 (68) and synthesized by IBA (Göttingen, Germany). The sense strand of the siRNA used to silence the Eag1 gene was 5´- GACACGAUUGAA AAAGUGCTT-3´, corresponding to positions 268-286 of the Eag1 mRNA, relative to the start codon. The sense strand of the siRNA used to silence the potassium channel SK4 gene was 5´- GCGCUU GCUGGAGCAGGAGTT-3´, corresponding to positions 48-66 of the SK4 mRNA relative to the start codon. A control siRNA oligonucleotide, Lmo2, designed to silence the LIM domain only 2 T-cell oncogene (Mus musculus), has no target gene in T_{84} cells and was used as a negative control for transfection. It had the sequence 5´- GCC AUC GAC CAG UAC UGG CTT-3´ (positions 133-151 relative to the start codon) of the Lmo2 gene. Transfection of T_{84} cells was carried out in Opti-MEM 1, one day after seeding using Oligofectamine (Invitrogen, Karlsruhe, Germany). After a 48 h rest, T_{84} cells were used for proliferation assays, patch clamp, real time PCR and western blot.

Detection of Eag1 protein by Western blot

Lysates of T_{84} cells were resolved by 7% SDS-PAGE, transferred to Hybond-P (Amersham Biosiences, Germany) and incubated with mouse anti-Kv10.1 (Eag1) antibodies (alomone labs, Jerusalem, Israel). Proteins were visualized using a goat anti-mouse IgG conjugated to horseradish peroxidase (Acris Antibodies, Germany) and ECL Advance Detection Kit (Amersham Biosiences, Germany).

Measurement of the intracellular Ca^{2+} concentration, pH, cell volume and membrane potential

T_{84} cells were loaded with 2 µM Fura-2 AM (Molecular Probes, USA) in Opti-MEM 1 medium with 2.5 mM probenecid (Sigma, Germany) for 1 h at room temperature. For fluorescence measurements of the intracellular Ca^{2+} concentration $[Ca^{2+}]_i$, cells were perfused with ringer solution containing 2.5 mM probenecide (Sigma, Deisenhofen, Germany) at 37°C. Fluorescence was measured continuously using an inverted microscope IMT-2 (Olympus, Nürnberg, Germany) and a high speed polychromator system (VisiChrome, Visitron Systems, Germany). Fura-2 was excited at 340/380 nm and emission were recorded between 470 and 550 nm using a CCD camera (CoolSnap HQ, Visitron Systems, Puchheim, Germany). $[Ca^{2+}]_i$ was calculated from the ratio of 340/380 nm fluorescence values (after subtraction of background fluorescence). The formula used for calculation of $[Ca^{2+}]_i$ was $[Ca^{2+}]_i = K_d \times (R-R_{min})(R_{max}-R) \times (S_{f2}/S_{b2})$ where R is the observed fluorescence ratio. The values R_{max}, R_{min} (maximum and minimum ratios) and the constant S_{f2}/S_{b2} (fluorescence of free and Ca^{2+}-bound fura-2 at 380 nm) were calculated using 2 µmol/l ionomycin (free acid,

Calbiochem, Merck Biosciences, Bad Soden, Germany), 5 µmol/l nigericin (Sigma, Germany), 10µmol/l monensin (Sigma, Deisenhofen, Germany) and 5 mmol/l EGTA to equilibrate intracellular and extracellular Ca^{2+} in intact fura-2-loaded cells. The dissociation constant for the fura-2-Ca^{2+} complex was taken as 224 nmol/l.

For assessment of intracellular pH, cells were incubated in standard bath solution (mM: 145 NaCl, 0.4 KH_2PO_4, 1.6 K_2HPO_4, 5 glucose, 1 $MgCl_2$, 1.3 Ca-gluconate, pH 7.4) containing 8 µM BCECF-AM and 0.05% Pluronic for 30 - 60 min at room temperature (RT). For cell volume measurements M1 cells were loaded with 2.5 µM calcein-AM and 0.025% Pluronic in standard bath solution for 30 – 60 min at RT. Excitation wavelengths of 488/440 and 500 nm were used for BCECF and calcein loaded cells, respectively. Emission wavelengths were >520 nm for BCECF fluorescence and 520-550 nm for calcein fluorescence. We screened for the effect of K^+ channel blockers on the membrane voltage, using the voltage sensitive dye FMP (69). Cells were incubated with FMP (FLIPR Membrane Potenial Assay Kit, Molecular Devices, Ismaning, Germany) in ringer solution at room temperature. FMP was exited with 485 nm and emission was detected between 515 and 560 nm. All experiments were controlled and analyzed using the software package Meta-Fluor (Universal imaging, USA). All optical filters and dichroic mirrors were from AHF (Tübingen, Germany).

Patch clamp

Cell culture dishes were mounted on the stage of an inverted microscope (IM35, Zeiss) and kept at 37 °C. The bath was perfused continuously with Ringer solution at about 10 ml/min. Patch-clamp experiments were performed in the fast whole-cell configuration. Patch pipettes had an input resistance of 2–4 MΩ, when filled with a solution containing (mM) KCl 30, K-gluconate 95, NaH_2PO_4 1.2, Na_2HPO_4 4.8, EGTA 1, Ca-gluconate 0.758, $MgCl_2$ 1.034, D-glucose 5, ATP 3. pH was adjusted to 7.2, the Ca^{2+} activity was 0.1 µM. The access resistance was measured continuously during the recordings and was 8.3 – 14.2 MΩ. Currents (voltage clamp) and voltages (current clamp) were recorded using a patch-clamp amplifier (EPC 7, List Medical Electronics, Germany), the LH1600 interface and PULSE (HEKA, Germany) and Chart (AD-Instruments, Germany) software. In regular intervals, membrane voltages (V_m) were clamped in steps of 10 mV from -50 to +50 mV relative to resting potentials. The membrane conductance G_m was calculated from the measured current (I) and V_m values, according to Ohm's law.

Materials and statistical analysis

All compounds used were of highest available grade of purity. 4-AP, TPeA, astemizole, calciseptine, EIPA, carbachol, quinidine, and terfenadine were all from Sigma (Deisenhofen,

Germany). BDS-I, charybdotoxin, and iberiotoxin were from Alamone labs (Jerusalem, Israel). Clotrimazole was from Calbiochem (Merck Biosciences, Bad Soden, Germany). Scyllatoxin was from Latoxan (Valence, France). TRAM-34 was a generous gift by Dr. H. Wulff (Department of Medical Pharmacology and Toxicology, University of California Davis, San Francisco, USA). 293B, AVE0118 and AVE1231 were gifts from Aventis Pharma (Frankfurt, Germany). All other chemicals were obtained from Merck (Darmstadt, Germany). The acetomethyl ester (2´,7´)-bis(carboxyethyl)-5(6)-carboxyfluorescein (BCECF-AM), calcein (calcein-AM), Fura2-AM and Pluronic were all from Molecular Probes (U.S.A.). Student's t-test (for paired or unpaired samples as appropriate) and analysis of variance (ANOVA) was used for statistical analysis. $P<0.05$ was accepted as significant.

Results

Expression of cancer related K^+ channels in T_{84} colonic carcinoma cells

We broadly screened T_{84} cells for expression of K^+ channels, based on previous reports indicating a role of K^+ channels for proliferation of cancer cells (database SAGEmap of the Cancer Genome Anatomy Project, http://cgap.nci.nih.gov, (70) and recent publications).

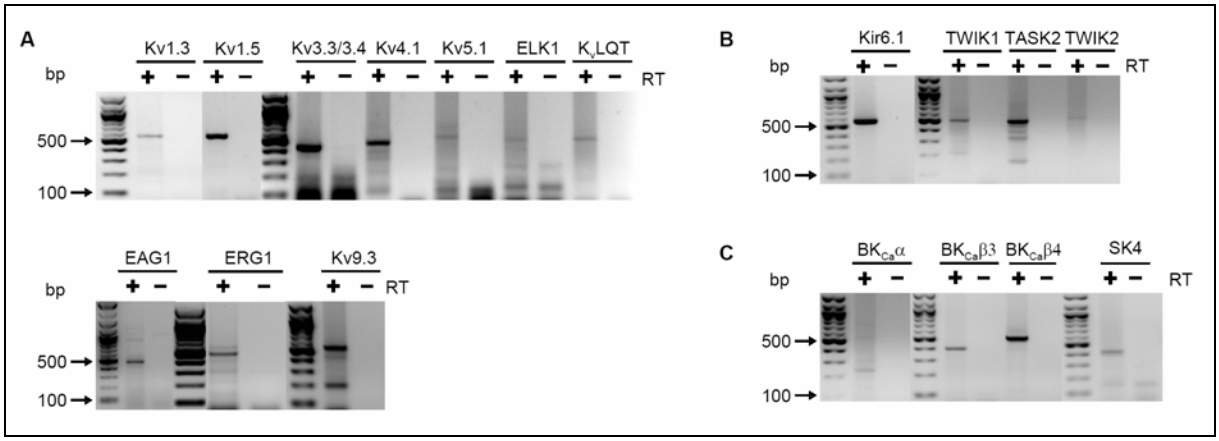

Fig. 3-1 Expression of K^+ channels in T_{84} cells

Expression of A) voltage gated (Kv3.3/3.4, Kv4.1, Kv5.1, Elk1, KvLQT1, Eag1, Kv9.3), B) inward rectifier (Kir6.1), two pore domain (TWIK1, TASK2, TWIK2), and C) large ($BK_{Ca}\beta3$, $BK_{Ca}\beta4$) and small (SK4) conductance Ca^{2+}- activated K^+ channels, after reverse transcription (RT).

RT-PCR detected transcripts of a number of voltage-gated (Kv) K^+ channels (Fig. 3-1A). Moreover, the ATP sensitive K^+ channels Kir6.1 and the two-pore (2P)-domain K^+ channels TWIK1, TWIK2 and TASK2 are expressed in T_{84} cells (Fig. 3-1B). Although, transcripts of the α-subunit of the large conductance Ca^{2+} sensitive (BK) channel could not be detected, the

two β-subunits β3 and β4 are expressed in these cells, along with intermediate conductance Ca^{2+} activated SK4 K^+ channels (Fig. 3-1C). Taken together, several K^+ channels are expressed in T_{84} colonic carcinoma cells, which may potentials support cell proliferation.

Inhibition of T_{84} cell proliferation by blockage of Kv channels

In order to identify K^+ channels which affect cell proliferation, we used a variety of inhibitors (Table 3-1, Fig.3-2 and 3-3). Cell proliferation was assessed independently, by quantifying DNA replication (BrdU incorporation) and by cell counting. Potential toxicity of the K^+ channel blockers was assessed by Trypan blue staining. At the concentrations used in this study, the channel inhibitors caused no toxic effects on T_{84} cells.

Concentration dependent inhibition of cell proliferation was found for the non-selective Kv channel blockers TPeA and quinidine (71, 72), for the toxin inhibitor BDS-1, which blocks Kv3.4 channels (73), and for the Eag1 blocker terfenadine (74) (Fig. 3-2A-D). Other Kv inhibitors such as 4-AP (5 µM - 2mM), AVE0118 or AVE1231 (0.5 nM - 50 µM) and the K_vLQT blocker 293B (1 nM - 10µM) also inhibited cell proliferation, albeit at higher concentrations (Table 2-1). Inhibitors of Ca^{2+} activated K^+ channels, such as charybdotoxin, clotrimazole, iberiotoxin, scyllatoxin and TRAM-34 did not affect proliferation (Table 2-1). Thus, Ca^{2+} activated K^+ channels do not seem to support proliferation. Surprisingly, activation of SK4 channels by riluzole (75) enhanced proliferation (Fig. 3-2E). These experiments suggest that only endogenous Kv channel activity supports proliferation of T_{84} colonic carcinoma cells, however, when up-regulated other K^+ channels such as intermediate conductance SK4 channels may also enhance proliferation. Endogenous Kv channels not only support proliferation of T_{84} cells, but also that of other colonic cell lines, like HT_{29}. Proliferation of HT_{29} cells was inhibited between 60 – 80% (n = 4) by 4-AP and astemizole. Moreover, Kv channels have been identified recently in human and murine colonic cancers (76).

Table 3-1 Inhibition of T_{84} cell proliferation by K^+ channel blocker.

Asterisks indicate significant difference when compared to control (ANOVA). Experiments were carried out in triplicates and numbers of different experiments are given in parentheses.

inhibitor	blocked channels	concentration	BrdU incorporation (% of control)	cell number (% of control)
293B	K_vLQT	10µM	79.0 ± 4.9 (3)*	88.0 ± 1.3 (3)*
		1µM	79.3 ± 1.4 (3)*	90.8 ± 0.5 (3)*
		0.1µM	80.7 ± 2.5 (3)*	97.1 ± 0.9 (3)
		0.01µM	82.2 ± 5.1 (3)	99.7 ± 1.4 (3)
		0.001µM	84.6 ± 5.9 (3)	99.3 ± 1.3 (3)
4-AP	K_v channels	2mM	72.2 ± 8.1 (3)*	73.8 ± 3.4 (5)*
		1mM	84.4 ± 5.9 (4)	80.5 ± 3.5 (5)*
		0.5mM	89.6 ± 0.2 (3)	83.2 ± 3.9 (5)*
		0.05mM	88.1 ± 4.0 (4)	87.2 ± 3.5 (5)
		0.005mM	92.8 ± 3.2 (5)	92.6 ± 2.1 (5)
astemizole	Eag1, Elk, Erg	5µM	83.5 ± 5.1 (7)*	81.5 ± 2.1 (8)*
		0.5µM	84.3 ± 3.0 (6)*	85.1 ± 2.7 (7)*
		0.05µM	90.3 ± 2.8 (7)	88.5 ± 1.0 (9)*
		0.005µM	91.3 ± 3.1 (7)	91.4 ± 1.1 (9)*
		0.5nM	94.1 ± 3.1 (6)	96.5 ± 1.0 (8)
AVE 0118	K_v1.5, 4.3, 2.1, 3.1	50µM	67.6 ± 8.1 (5)*	60.0 ± 4.3 (5)*
		5µM	76.1 ± 7.4 (4)	80.7 ± 2.4 (4)*
		0.5µM	86.5 ± 4.2 (4)	82.4 ± 1.2 (5)*
		0.05µM	89.1 ± 7.2 (4)	87.1 ± 2.3 (5)*
		0.005µM	94.8 ± 7.3 (4)	93.4 ± 2.4 (6)
AVE 1231	K_v1.5, 4.3, 2.1, 3.1	50µM	59.7 ± 7.8 (3)*	61.6 ± 3.1 (3)*
		5µM	89.9 ± 2.3 (4)	80.8 ± 1.6 (3)*
		0.5µM	92.7 ± 1.0 (3)	85.2 ± 2.0 (3)*
		0.05µM	95.0 ± 1.2 (4)	86.9 ± 0.2 (3)*
		0.005µM	100.4 ± 0.6 (4)	95.0 ± 1.8 (3)
charybdotoxin	BK_{Ca}, SK4, K_v1.3	100nM	79.7 ± 4.5 (3)*	89.2 ± 3.1 (3)
		10nM	87.8 ± 3.6 (3)	92.3 ± 2.3 (3)
		1nM	89.2 ± 3.8 (3)	92.3 ± 1.7 (3)
		0.1nM	91.5 ± 4.2 (3)	95.9 ± 1.5 (3)
		0.01nM	91.4 ± 2.3 (3)	97.3 ± 6.1 (3)
clotrimazole	SK4	1µM	84.9 ± 7.7 (3)	79.1 ± 6.4 (3)
		0.1µM	92.6 ± 6.4 (3)	80.5 ± 6.0 (3)
		0.01µM	99.0 ± 6.9 (3)	86.0 ± 7.6 (3)
		0.001µM	94.8 ± 10.1 (3)	88.9 ± 4.8 (3)
		10nM	93.0 ± 4.2 (3)	76.4 ± 11.2 (3)
iberiotoxin	BK_{Ca}	1nM	93.5 ± 4.3 (4)	85.3 ± 9.8 (3)
		0.1nM	96.0 ± 5.0 (4)	86.3 ± 9.8 (3)
		0.01nM	94.2 ± 1.4 (4)	94.1 ± 4.8 (3)
		0.001nM	96.7 ± 8.2 (4)	97.8 ± 4.5 (3)
scyllatoxin	SK-family	10nM	89.8 ± 8.6 (3)	110.7 ± 13.1 (3)
		1nM	99.6 ± 7.7 (3)	108.8 ± 12.9 (3)
		0.1nM	97.2 ± 5.6 (3)	103.5 ± 1.3 (3)
		0.01nM	96.1 ± 2.6 (3)	105.8 ± 4.2 (3)
		0.001nM	102.8 ± 4.6 (3)	117.6 ± 10.4 (3)
TRAM-34	SK4	100nM	89.7 ± 3.8 (3)	94.0± 3.4 (3)
		10nM	94.5 ± 3.0 (3)	93.2± 6.1 (3)
		1nM	90.5 ± 3.1 (3)	95.8± 3.8 (3)
		0.1nM	94.7 ± 1.4 (3)	93.0± 0.5 (3)

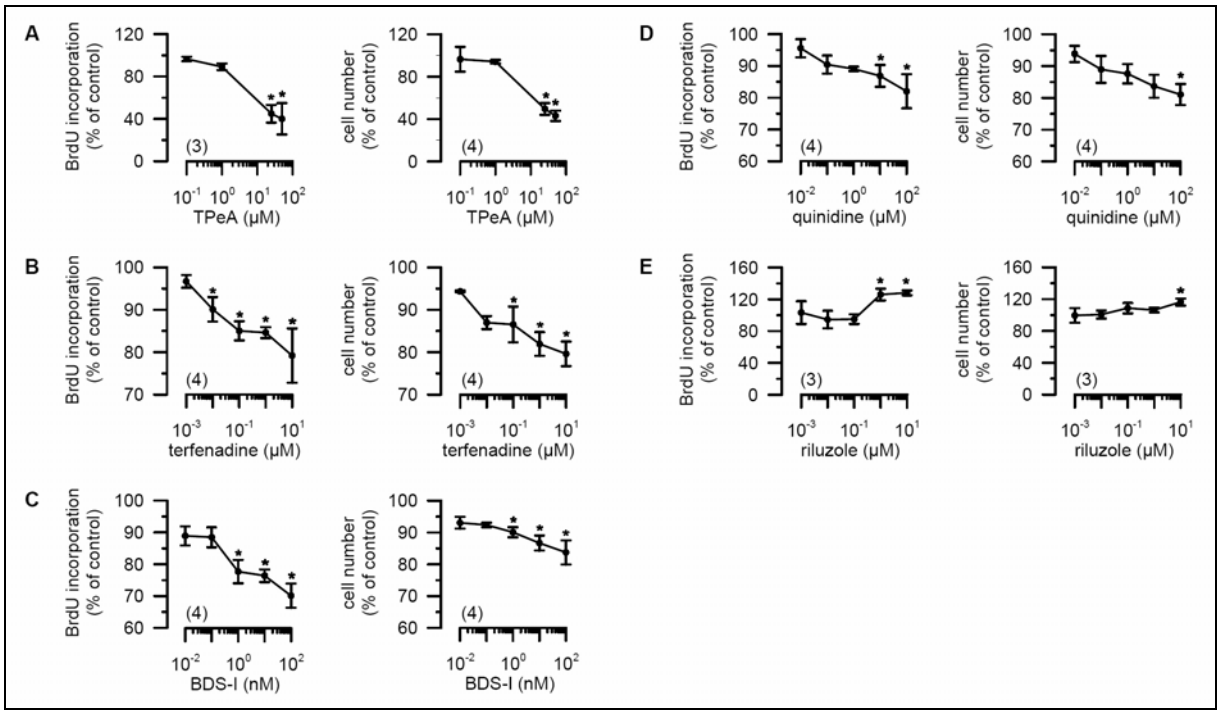

Fig. 3-2 Inhibition of proliferation of T_{84} cells by Kv channel blockers

Cell proliferation of T_{84} cells was assessed by BrdU incorporation and cell counting. The K^+ channel blockers A) TPeA, B) terfenadine, C) BDS-I, and D) quinidine caused dose dependent inhibition of proliferation. E) Additional activation of SK4 channels by riluzole further enhanced proliferation. Asterisks indicate significant differences when compared to control (ANOVA). Experiments were carried out in triplicates. (number of experiments).

Kv channels are active in colonic carcinoma cells

We screened for the effects of K^+ channel blockers in a fluorescence based assay, using the voltage sensitive dye FMP. After loading of the cells with FMP, the Kv channel blocker 4-AP (50 μM) enhanced fluorescence intensity, due to depolarization of the membrane voltage. The effects of individual blockers were analyzed as fraction of the effect of $BaCl_2$ (5 mM), which induced maximal depolarization. The largest changes were observed for the Kv channel blockers 4-AP (50 μM), quinidine (10 μM), terfenadine (10 μM) and astemizole (5 μM). This demonstrates a contribution of Kv channels to the overall K^+ conductance in T_{84} cells (Fig. 3-3A, right panel). K^+ channel blockers were also applied in whole cell patch clamp experiments. The blockers were used at lower concentration range, in order to achieve best specificity. As shown in Fig. 3-3B, C, K^+ channel blockers had small but significant effects on whole cell conductance and membrane voltage (V_m). Blockers were typically applied in the presence of Ringer solution; however, similar effects were also observed when blockers were examined in the presence of culture medium (Opti-MEM), i.e. under proliferation assay conditions (data not shown). Taken together Kv channels contribute only about 10 - 15% to

the total membrane conductance, which is sufficient to support proliferation of T_{84} cells. Similar has been observed in previous studies (6).

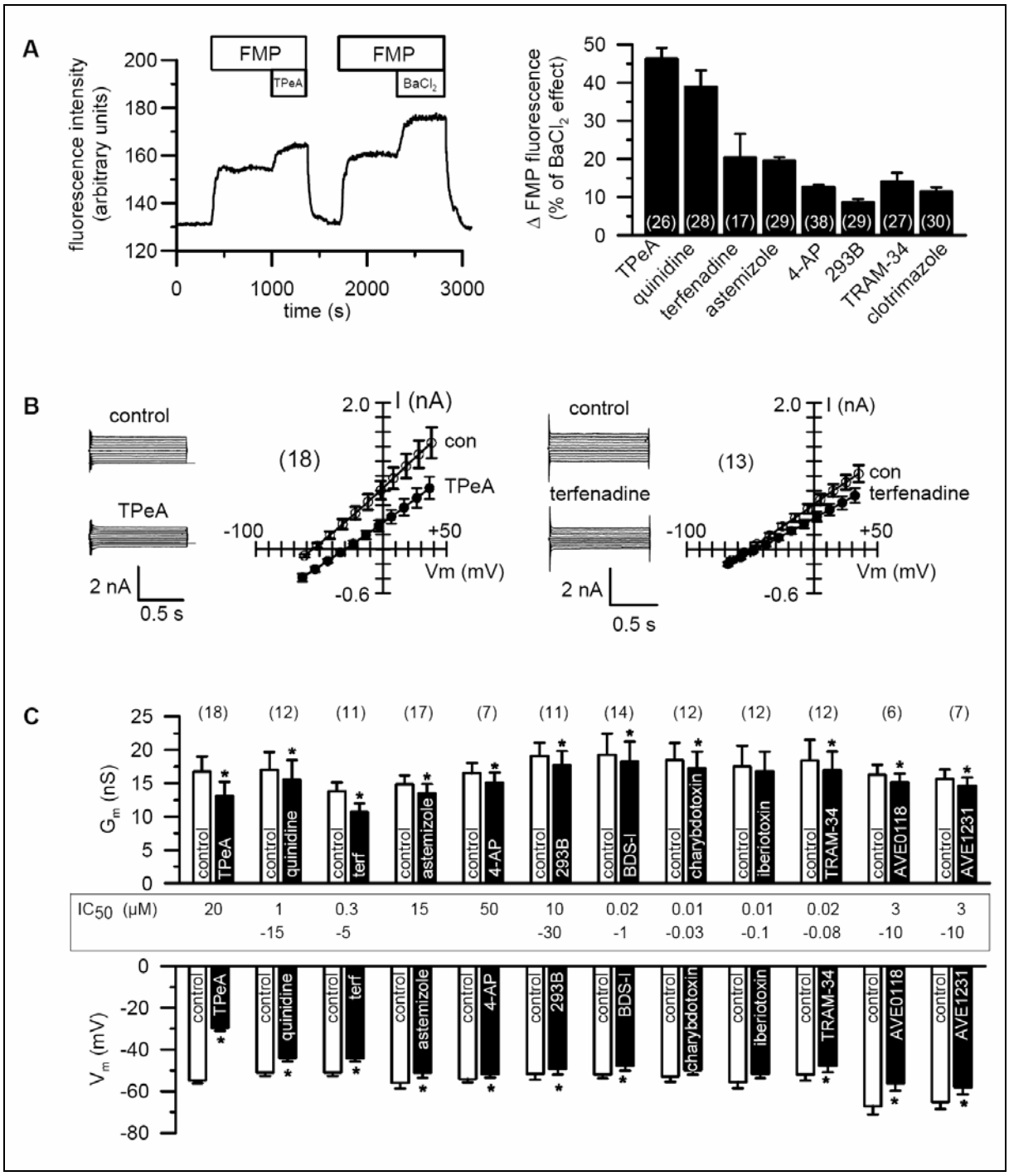

Fig. 3-3 Effects of Kv channel blockers on membrane voltage whole cell conductance

A) Uptake of the voltage sensitive fluorescence dye FMP. Loading of T_{84} cells with FMP induced fluorescence. 4-AP (50 μM) further increased fluorescence intensity due to depolarization of V_m. $BaCl_2$ (5 mM) completely inhibited K^+ channels, thereby inducing maximal depolarization and further fluorescence increase. The right panel shows the

summary of the effects of the K^+ channel blockers TPeA (50 µM), quinidine (10 µM), terfenadine (10 µM), astemizole (5 µM), 4-AP (50 µM), 293B (10 µM), TRAM-34 (100 nM) and clotrimazole (100 nM) on FMP fluorescence, relative to the effects of $BaCl_2$. B) Effect of TPeA and terfenadine on whole cell currents obtained in T_{84} cells and summary i/v curves in the absence or presence of the inhibitor. C) Summary of the effects of the K^+ channel blockers on whole cell conductance and membrane voltage, at concentrations as indicated above. Concentrations for the other inhibitors were: BDS-I (10 nM), charybdotoxin (100 nM), iberiotoxin (10 nM), AVE0118 (10 µM) and AVE1231 (10 µM). IC_{50} values were determined experimentally or were obtained from literature. Asterisks indicate significant differences when compared to control (paired Student´s *t*-test). (number of experiments).

Down regulation of Eag1 inhibits proliferation

Proliferation of T_{84} cells may be supported by a number of different Kv channels. Although patch clamping and expression studies suggested a dominant role of Eag channels, we used siRNA-Eag1 to specifically down regulate expression of Eag1 protein. Quantitative analysis of gene expression using real time PCR, indicated a significant loss of Eag1 transcripts after treatment with siRNA-Eag1 and reduced Eag1 expression was verified by Western blotting (Fig. 3-4A).

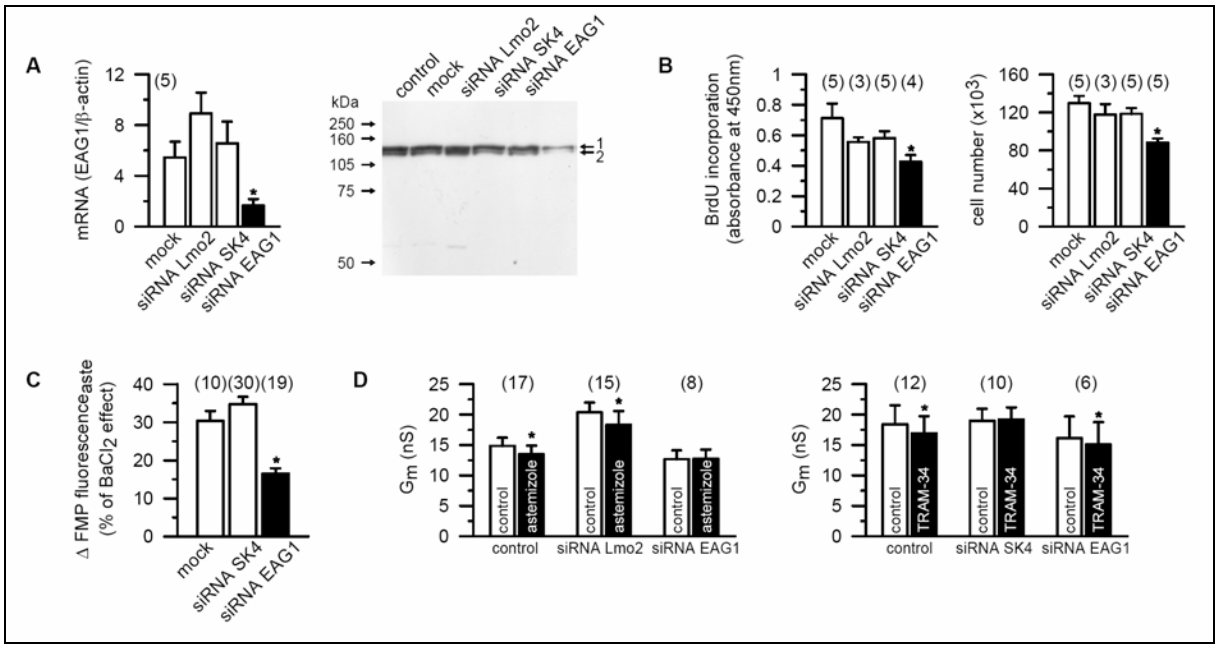

Fig. 3-4 Down regulation of Eag1 inhibits cell proliferation and astemizole sensitive currents

A) Suppression of Eag1- mRNA and protein in T_{84} cells by siRNA-Eag1 but not by unrelated siRNA (Lmo2; SK4), or in mock transfected cells. B) Inhibition of cell proliferation by siRNA Eag1, but not by unrelated control siRNA. C) Reduced astemizole

sensitive FMP fluorescence (ΔFMP) in siRNA Eag1 transfected cells, but not in control cells. D). siRNA Eag1 abolished astemizole sensitive G_m (left panel). In contrast, siRNA SK4 abolished TRAM-34 sensitive G_m (right panel), which, however, did not affect proliferation of T_{84} cells (shown in B). Asterisks indicate significant difference when compared to control (ANOVA, Student's *t*-test). Proliferation assays were carried out in triplicates. (number of experiments).

We found that down regulation of Eag1 expression inhibited proliferation, while mock transfection, unrelated siRNA (for Lmo2 oncogene) or siRNA- inhibition of the Ca^{2+} activated K^+ channel SK4 did not reduce cell proliferation (Fig. 3-4B). In the FMP fluorescence assay we found a reduced effect of astemizole (5 µM) on membrane voltage, i.e. FMP uptake (ΔFMP) (Fig. 3-4C). Along this line suppression of astemizole sensitive Eag1 conductance was detected in whole cell patch clamp experiments. In contrast TRAM-34 sensitive SK4 conductance was eliminated by siRNA-SK4, which had no impact on proliferation of T_{84} cells (Fig. 3-4D). Taken together, endogenous Eag1 currents control proliferation of T_{84} colonic carcinoma cells, while endogenous SK4 currents are not relevant for cell growth.

Kv channels control regulation of intracellular pH and Ca^{2+} signaling, but not cell volume

Kv channels contribute to the negative membrane voltage, which may be crucial for volume and pH regulation, as well as proper Ca^{2+} signaling particularly during cell cycling (6, 15, 77, 78). We therefore asked if Kv channels enhance proliferation by affecting cell volume or pH regulation, or by supporting intracellular Ca^{2+} signaling. T_{84} cells were swollen by removing 120 mmol/l mannitol (Hypo), or were shrunken by adding 120 mmol/l mannitol (Hyper) to an isotonic Ringer solution. Swelling and shrinkage was assessed by changes in calcein fluorescence (Fig. 3-5A). Repetitive exposure to hypotonic bath solution produced identical changes in cell volume (n = 41, data not shown). Cell swelling was not different in the presence or absence of Kv channel blockers (Fig. 3-5B,C). We further examined if pH recovery from an acid (NH_4Cl; 20 mM) load and thus regulation (recovery) of intracellular pH is affected by inhibitors of Kv channels. To that end cells were acid loaded using a NH_4Cl pulse. The slope for initially recovery from cellular acidification was determined in the absence or presence of Kv channel blockers. Repetitive acidification under control condition showed similar recovery of the intracellular pH (n = 62, data not shown). Recordings of the intracellular pH and the summary for the recovery rates demonstrate impaired pH regulation in T_{84} cells when exposed to the Kv channel blockers 4-AP or astemizole (Fig. 3-5D,E). These results indicate that Kv channels are important for pH regulation in colonic carcinoma cells. pH recovery is primarily due to the function of the Na^+/H^+ exchanger NHE (6, 79). In

fact, blockage of NHE by 5-(N-Ethyl-N-Isopropyl) amiloride (EIPA) inhibited proliferation of T_{84} cells (Fig. 3-5F).

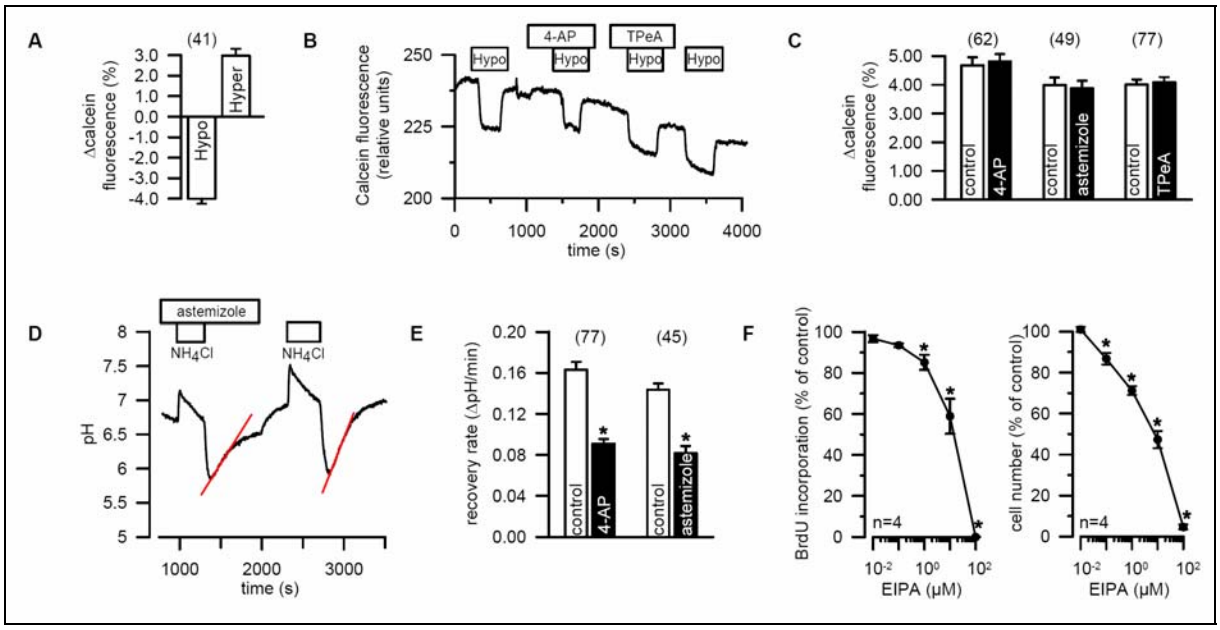

Fig. 3-5 Kv channels affect pH regulation but not cell swelling

A) T_{84} cells were swollen (removal of 120 mmol/l mannitol; Hypo) or shrunken (adding 120 mmol/l mannitol; Hyper), as assessed by changes in calcein fluorescence. Repetitive exposure to hypotonic bath solution produced identical changes in cell volume (n = 41, data not shown). B) Kv channel inhibitors 4-AP or TPeA did not affect cell swelling. C) Summary of the effects of 4-AP, astemizole and TPeA on cell swelling, as measured by calcein fluorescence. D) Original recording of intracellular pH and effect of astemizole on pH recovery from acid (NH_4Cl) load. E) Summary of the effects of 4-AP and astemizole on pH recovery after acid load. F) Effect of the NHE1- inhibitor EIPA on cell proliferation. Asterisks indicate significant difference when compared to control (Student's *t*-test). (number of experiments).

We further examined potential effects of Kv channels on intracellular Ca^{2+} signaling. As shown in Fig. 3-6, baseline intracellular Ca^{2+} in resting cells was not affected by Kv channel inhibitors. We stimulated T_{84} cells with the muscarinic secretagogue carbachol (CCH, 100 μM). This induced a release of Ca^{2+} from intracellular stores (transient peak response) and a subsequent influx through store operated Ca^{2+} channels (Ca^{2+} plateau) (original traces in Fig. 3-6).

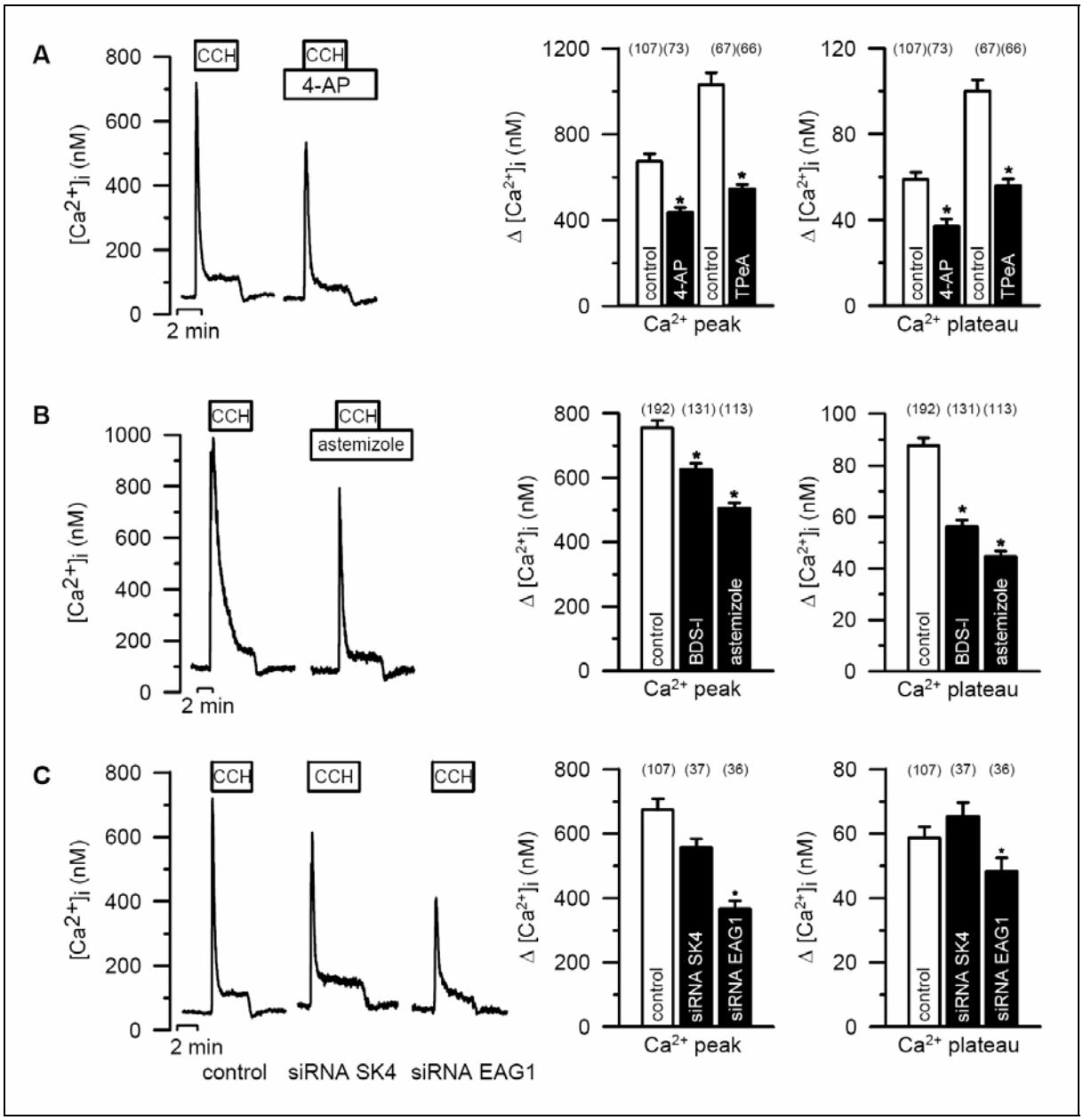

Fig. 3-6 Kv channels affect carbachol induced Ca^{2+} signaling

A) Original recordings of $[Ca^{2+}]_i$ in fura-2 loaded T_{84} cells and effects of carbachol (CCH; 100 µM) and 4-AP on transient (store release; peak) and persistent (influx; plateau) Ca^{2+} increase. Right panel: Summary of the effects of 4-AP (50 µM) and TPeA (5 µM) on Ca^{2+} peak and plateau. B) Original recordings of the effects of carbachol and astemizole. Right panel: Summary of the effects of BDS-I (10 nM) and astemizole (0.5 µM) on Ca^{2+} peak and plateau. C) Original recordings of the effects of carbachol on control cells and cells treated with siRNA Eag1 or siRNA SK4. Right panel: Summary of the effects of siRNA Eag1 or siRNA SK4 on Ca^{2+} peak and plateau. Asterisks indicate significant difference when compared to control (ANOVA, Student's *t*-test). (number of experiments).

Both Ca^{2+} peak and plateau were significantly reduced in the presence of the non-selective Kv blockers 4-AP (50 µM) and TPeA (5 µM) (Fig. 3-6A). Similar effects on $[Ca^{2+}]_i$ were observed with the Eag1 inhibitor astemizole (0.5 µM) and the $K_V3.4$ blocker BDS-I (10 nM) (Fig. 3-6). Moreover, inhibition of Eag1 expression by siRNA also attenuated Ca^{2+} signaling, while siRNA - suppression of SK4 had no effects on the carbachol induced Ca^{2+} signaling (Fig. 3-6B,C). The contribution of K^+ channels to Ca^{2+} signaling was further confirmed by the nonselective K^+ channel inhibitor Ba^{2+}, which also attenuated Ca^{2+} signaling T_{84} cells (data not shown). Taken together, Kv channels affect intracellular Ca^{2+} signaling probably by their hyperpolarizing effects which provides a driving force for Ca^{2+} release and influx through store operated Ca^{2+} channels (SOCs) (80, 81).

Although upregulation of voltage gated Ca^{2+} channels (VOCC) in T_{84} cells has been reported previously (82), they are probably of limited importance for proliferation since we did observe any impact of the VOCC inhibitor calciseptine had no effect on proliferation (Fig. 3-7A). Moreover, agonist (carbachol) induced Ca^{2+} signaling was not affect by calciseptine in either T_{84} or HT_{29} cells (Fig. 3-7B,C).

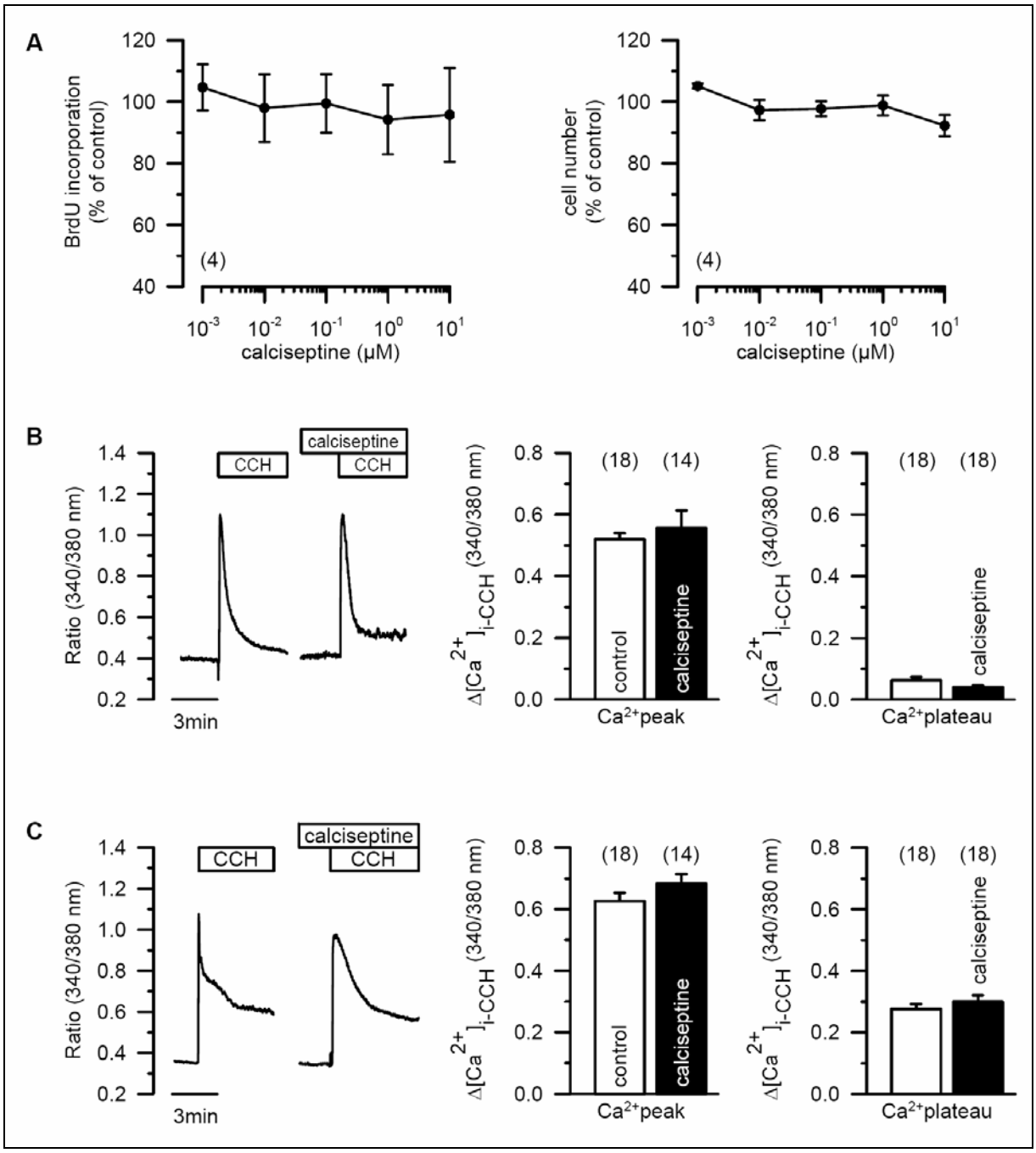

Fig. 3-7 Voltage gated Ca^{2+} channels do not affect proliferation or Ca^{2+} signaling in colonic cancer cells

A) Cell proliferation of T_{84} cells was not affected by the inhibitor of L-type Ca^{2+} channels, calciseptine. carbachol (CCH, 100 µM) induced Ca^{2+} increase in T_{84} (B) or HT_{29} (C) cells was not affected by calciseptine. (number of experiments).

Discussion

K^+ channels and cancer

Several types of K^+ channels have been detected in human cancers (6). Ca^{2+} activated K^+ channels were found in prostate cancer (83), uterine cancer (84), human gliomas (85), gastric cancer (86), pituitary adenomas (87) and colorectal cancer (16, 83, 88). In other tumors proliferation is supported by ATP sensitive Kir channels or two-pore (2P)-domain channels (89-91). Nevertheless, in the majority of cancer cells, Kv channels were correlated to proliferation (19, 41, 64, 65, 92-94). Other data from human biopsies and carcinogen treated mice suggest high levels of Eag1 protein in colonic cancers, which is not observed in the native colon (76). Also in the present study we found a role of Kv channels for proliferation of cultured colonic carcinoma cells. Thus, the results obtained in T_{84} cells may be representative for the changes that occur in the native colon during carcinogenesis.

Kv but not other K^+ channels control proliferation in T_{84} cells

Kv channels operate at rather depolarized membrane voltages (V_m), which are typically not found in terminally differentiated epithelial cells (41, 64). The depolarized V_m of carcinoma cells provides the basis for activation of Kv channels (95). When studied under proliferative conditions, serum containing culture medium depolarizes V_m (96). *In vivo,* cells are exposed to 20 – 30 g/l protein present in the interstitial fluid, which may depolarize V_m and allow for activation of Kv channels in carcinoma cells *in situ* (97). Remarkably the contribution of Kv channels to the overall conductance in T_{84} cells was only 10 – 15%. However, this is in line with previous reports, which indicate that pro-proliferative K^+ currents are often of smaller amplitude, while large K^+ currents are detected during apoptosis (6, 98).

Because of the limited specificity of most K^+ channel inhibitors (99), we also used siRNA to identify the K^+ channels in charge of cell proliferation. Only Kv channels appear to affect cell proliferation, although other K^+ channels are expressed and functional in T_{84} colonic carcinoma cells, such as SK4 channels. Obviously Eag1 and other Kv channels operate well in proliferating T_{84} cells, while SK4 channels only support proliferation after additional activation by riluzole. Surprisingly, even the K^+ ionophore valinomycin increased proliferation of T_{84} cells when applied at very low (100 fM) concentrations (unpublished data from the author's laboratory). We suggest that the oncogenic potential of Kv channels is linked to the K^+ channel function. This has been demonstrated recently for TASK3 channels (100). In principle, any type of K^+ channel may be able to support proliferation, depending on additional cell specific properties that determine K^+ channel activity.

How do Kv channels control cell proliferation?

The present study was performed to determine the mechanism by which K^+ channels affect cell growth. Progression through the cell cycle is dependent on K^+ channels and blocking of these channels causes inhibition of proliferation (15). This clearly suggests a cell cycle specific function of K^+ channels. Apart from this specific role, Kv channels may also have homeostatic functions in T_{84} cells. The present data demonstrate an impact of Kv channels on intracellular Ca^{2+} signaling and pH regulation. The importance of pH_i for cell proliferation and cancer development is well established (77). pH_i is varying during the cell cycle and need to be tightly controlled, probably by the Na^+/H^+ exchanger NHE1 (79). The experiments with the NHE – blocker EIPA presented here, clearly show the importance of NHE for cell proliferation. Na^+/H^+ exchange requires low intracellular Na^+ concentrations, and V_m need to stay hyperpolarized, Both is facilitated by the Na^+/K^+ - ATPase in parallel with K^+ channels. Kv channels may provide a K^+ recycling pathway and hyperpolarize the membrane voltage, and may thus contribute indirectly to pH regulation.

Equally important is the control of intracellular Ca^{2+} in proliferating cells, especially during the mitotic cell cycle (79). We found that agonist induced Ca^{2+} release and influx of Ca^{2+} through SOCs, dependents on the function of Kv channels. Thus Ca^{2+} dependent activation of ion currents was reduced significantly by 3.2 ± 0.5 nA (100 µM 4-AP, n = 4) and 2.8 ± 0.4 nA (5 µM astemizole, n = 5). It has been demonstrated by others (81) that depolarization of the membrane voltage reduces Ca^{2+} signaling. Since inhibitors of Kv channels depolarize V_m, this may explain why Ca^{2+} signaling is affected. Furthermore, a previous study demonstrated that activation of store operated Ca^{2+} Channels (SOCs) in T_{84} cells induces proliferation (80). Moreover, capacitative Ca^{2+} influx through SOCs is reduced at acidic pH (101). Since Kv channels also affect intracellular pH, this may provide an independent mechanism, by which Kv channels affect intracellular Ca^{2+} signaling. Voltage gated Ca^{2+} channels (VOCC) are probably not related to the effects of Kv channel inhibitors, although L-type Ca^{2+} channels are expressed in T_{84} colonic carcinoma cells (82). This is further substantiated by the fact that the L-type Ca^{2+} channel inhibitor calciseptine did not reduce proliferation or Ca^{2+} signaling (Fig. 3-7). Taken together hyperpolarization of V_m by Kv channels may be necessary to maintain pH regulation and Ca^{2+} signaling, which allows progression through the G_1 phase of the cell cycle (15, 78).

Chapter 4

Expression of voltage gated potassium channels in human and mouse colonic carcinoma

Abstract

Purpose: Voltage gated Kv potassium channels like ether-á-go-go (Eag) channels have been recognized for their oncogenic potential in breast cancer and other malignant tumors.

Experimental design: We examine the molecular and functional expression of Kv channels in human colonic cancers and colon of mice treated with the chemical carcinogens DMH and MNU. The data were compared with results from control mice and animals with chemically induced DSS colitis.

Results: Electrogenic salt transport by amiloride sensitive Na^+ channels and cAMP activated CFTR Cl^- channels were attenuated during tumor development and colitis, while Ca^{2+} dependent transport remained unchanged. Kv channels, in particular Eag1 were enhanced during carcinogenesis. Multiplex RT-PCR showed increased mRNA expression for Kv1.3, Kv1.5, Kv3.1 and members of the Eag channel family after DMH and MNU treatment. Eag1 protein was detected in the malignant mouse colon and human colonic cancers. Genomic amplification of Eag1 was found in 3.4% of all human colorectal adenocarcinoma and was an independent marker of adverse prognosis.

Conclusions: The study predicts an oncogenic role of Kv and Eag channels for the development of colonic cancer. These channels may represent an important target for a novel pharmacotherapy of colonic cancer.

Introduction

Membrane ion channels are essential for cell proliferation and have a role in the development of cancer. A substantial body of evidence exists that voltage gated potassium (Kv) channels have an oncogenic function (102-105). Moreover, during carcinogenesis changes in expression or activity of ion channels may affect electrolyte transport properties in epithelia, similar to the changes observed during inflammation (102). K^+ channels are involved in the development of cancer of prostate, colon, lung and breast (102, 106). K^+ channels were identified in different cancer tissues, such as Ca^{2+}- activated and voltage-gated K^+ channels (Kv channel), the ether-à-go-go (Eag) family and 2P-domain K^+ channels (102). However, Kv channels seem to play a central role in tumor cells, particularly in those of epithelial origin (102-104). Cell cycle regulated Eag1 channels, normally only expressed in excitable tissues and oocytes are also found in cancer cells (105, 107, 108). Activation of these channels induces hyperpolarization of the plasma membrane, which may be essential for cell proliferation (103). Hyperpolarization of the membrane voltage facilitates Ca^{2+} signaling, and is necessary for regulation of intracellular pH and cell volume. All of these parameters, Ca^{2+}, pH and volume clearly affect cell proliferation (102, 103, 109).

Most studies on the oncogenic role of ion channels have been performed in cell lines, leaving open their relevance for tumor development *in vivo*. We therefore designed the present study to examine the role of ion channels for tumor development *in vivo* in carcinogen treated mice. DMH and MNU were used as carcinogenic agents. Dimethylhydrazine (DMH) is organotropic for the rodent colon. It is metabolized to methylazoxymethanol and methyldiazonium and causes methylation of nucleotides (110). Rectal application of N-methyl-N-nitrosourea (MNU) causes direct alkylation of DNA and also induces colonic tumors (111, 112). During the development of colonic cancer, alterations in colonic electrolyte transport have been reported in previous studies (113, 114). Electrolyte transport appears to be affected in the pre-malignant colon, which may contribute to the irregularities in defecation, often observed in patients with human colonic cancer. We found that electrolyte transport was affected in colitis and during carcinogenesis. However, over-expression of cell cycle regulated Eag1 K^+ channels was only found in the pre-malignant mouse colon and in human colonic cancers.

Material and Methods

Patients, tumor material for FISH analysis, biological samples

386 surgically resected colorectal adenocarcinomas were selected from the files of the Institutes of pathology of the University of Basel and from the Triemli Hospital, Zürich, Switzerland. Tissue micro array was constructed as previously described (115). Specimens were kept anonymous, and experiments were conducted according to the guidelines of the ethical committee of the University of Basel. pTNM stage was determined according to the

International Union Against Cancer (116). Colon biopsies were obtained from patients hospitalized at the children's hospital of the University of Freiburg/Germany and the department of internal medicine of the University of Regensburg, according to the guidelines of the local ethical committee.

DMH, MNU, and DSS treatment

Animal studies were conducted according to the guidelines of the National Institute of Health guidelines for the care and use of animals in research and the German laws on protection of animals. C57BL/6NCrl mice were obtained from Charles River (Sulzfeld, Germany). DMH or control saline were dissolved in 0.9% saline and injected s.c. into the groin at a dose of 40 mg/kg once a week for 5 wks. Proximal and distal colons were removed for RNA and protein isolation, histology and functional measurements. For MNU treatment, mice were anaesthetized by intraperitoneal injection of Ketamin/Xylazin (120 mg/8 mg/kg * bodyweight). MNU (2.6 mg/0.4 ml 0.9% NaCl solution) was given intrarectally two times a week for 2 weeks and once a week for additional 4 weeks. For RPD measurements a catheter (PE 10 tubing) containing ringer solution was inserted 2 cm into the rectum, and perfused continuously at a rate of 1 ml/h. The catheter was attached via an agar bridge to an AgCl-electrode. A subcutaneous needle positioned in the abdomen and connected via an agar bridge served as the reference electrode. For DSS treatment of BALB/cOlaHsd mice, 3 % DSS was added to drinking water for 7 -10 days.

Histology

Mice were sacrificed under CO_2 inhalation; the colon was removed and stripped mechanically from submucosal tissues. Tissues were fixed for 20 min with 4% paraformaldehyde, 0.1% glutaraldehyde, 15% picric acid in PBS (pH 7.4) followed by a 12 h incubation in 4% paraformaldehyde, 15% picric acid in PBS (pH 7.4) at 4°C. Tissues were washed in PBS and incubated in 10%, 20% and 30% sucrose solutions, dehydrated and embedded in paraffin. Paraffin-embedded tissues were cut at with a rotary microtome (Leica Mikrotom RM 2165, Wetzlar, Germany). Sections were de-waxed and re-hydrated and stained with hematoxylin and eosin. Some tissues were chock frozen in iso-pentan, sectioned at 5 µm, fixed with 4% paraformaldehyde in PBS (pH 7.4) and stained with hematoxylin.

Ussing chamber experiments

Stripped colon was put into ice cold bath solution (mM: NaCl 145, KH_2PO_4 0.4, K_2HPO_4 1.6, d-glucose 6, $MgCl_2$ 1, Ca-gluconate 1.3, pH 7.4) containing amiloride (20 µM) and indomethacin (10 µM). Tissues were mounted into an Ussing chamber with a circular

aperture of 0.785 mm^2. Luminal and basolateral sides of the epithelium were perfused continuously at a rate of 5 ml/min. Bath solutions were heated to 37 °C, using a water jacket. Experiments were carried out under open circuit conditions. Data were collected continuously using PowerLab (AD-Instruments, Australia). Values for transepithelial voltages (V_{te}) were referred to the serosal side of the epithelium. Transepithelial resistance (R_{te}) was determined by applying short (1 s) current pulses (ΔI = 0.5 µA). R_{te} and equivalent short circuit currents (I_{SC}) were calculated according to Ohm's law ($R_{te} = \Delta V_{te}/\Delta I$, $I_{SC} = V_{te}/R_{te}$).

Crypt cell isolation and expression analysis of ion channels in colonic epithelial cells

Colonic crypts were isolated from an inverted colon in Ca^{2+} free buffer solution. Total RNA was prepared from isolated crypts (NucleoSpin, Macherey-Nagel, Düren, Germany). After reverse transcription, semi- quantitative multiplex RT-PCR was performed. The following primers (accession number) were used: mKv1.3 (NM_00_{84}18): 5´-GTACTTTGACCCACTCCGC -3´ (s), 5´-GCAAGCAAAGAACCGCACC-3´ (as); mKv1.5 (NM_145983): 5´-GCTACTTCGATCCCTTGAG -3´ (s), 5´-GCTCAAAAGTGAACCAGATC-3 (as); mKv3.1 (NM_00_{84}21): 5´-CCAGACGTACCGCTCGAC 3´ (s), 5´-CGAACAGCGCCCAGATGC-3´ (as); mEag1 (NM_010600): 5´-GGATTCTGCAAGCTGTCTG-3´ (s), 5´-GTAGAAGGTCAGGATCAAG-3´ (as); hEag1 (NM 172362, NM 002238): 5´-CGCATGAACTACCTGAAGACG-3´ (s), 5´-TCTGTGGATGGGGCGATGTTC-3 (as); mErg1 (NM_172057): 5´-CCTCGACACCATCATCCGC-3´ (s), 5´-GTCCGCACAGATGATTCCC-3´ (as); mElk1 (NM_001031811): 5´-GGTTTCCCCATAGTCTACTG-3´ (s), 5´-CAAAATGAGCCAGTCCCAGC-3´ (as); mENaCα (NM_011324): 5´-CCTTGACCTAGACCTTGACG-3´ (s), 5´- CGAATTGAGGTTGATGTTGAG-3´ (as); mENaCβ (NM_000336): 5´-CAATAACACCAACACCCACG-3´ (s), 5´- GAGAAGATGTTGGTGGCCTG-3´ (as); mENaCγ (NM_011326): 5´-GCACCGACCATTAAGGACC-3´ (s), 5´-GCCTTTCCCTTCTCGTTCTC-3´ (as); mCFTR (NM_021050): 5´-GAATCCCCAGCTTATCCACG-3´ (s), 5´- CTTCACCATCATCTTCCCTAG -3´ (as). PCR reactions were performed at 94°C for 2 min, 28-38 cycles at 94°C for 30 s, annealing temperature 56°C for 30 s and 72°C for 1 min using GoTaq DNA Polymerase (Promega, Mannheim, Germany). Expression of mRNA of each gene product was normalized against β-actin expression.

Detection of Eag1 protein

Isolated crypt cells from distal and proximal colon were lysed and total protein (50 µg) was resolved by 7% SDS-PAGE, transferred by semi- dry blotting to Hybond-P (Amersham, Freiburg, Germany) and incubated with rabbit anti-Kv10.1 (Eag1) (Alomone labs, Israel) and

rabbit anti- actin antibodies (Sigma, Taufkirchen, Germany). Proteins were visualized using a goat anti-rabbit IgG conjugated to horseradish peroxidase (Acris Antibodies, Hiddenhausen, Germany) and ECL Advance Detection Kit (Amersham). Signals were detected by Fluor-S^{TM} MultiImager system (Bio-Rad Laboratories, Hercules, USA) and analyzed with Multi-Analyst software (Bio-Rad). Expression of EAG1protein was normalized against actin protein expression.

FISH analysis

The bacterial artificial chromosome (BAC) RP11-75i2, containing parts of the Eag1gene sequence at 1q32.2-3 was obtained from the German Resource Centre for Genome Research (RZPD; Berlin, Germany). 1 µg of purified plasmid DNA was labelled using a modified Bio Nick kit (Invitrogen, Carlsbad, CA). Nick translation was performed at 16°C for 90 min. The labeled FISH probe was purified by precipitation and re-dissolved in 50 µl H_20. Paraffin removal (3x 5min in Xylene followed by 2x 2min ethanol 95% and air-drying) and enzymatic tissue pretreatment (Vysis pretreatment solution, 80°C, 15 min) of tissue sections mounted on glass slides was performed in a VP2000 Processor device (Vysis, Downers Grove, IL). A premixed hybridization cocktail containing 0.5 µl centromere 1 probe (CEP 1 SpectrumOrange labeled; Vysis), 1.5 µl Eag1 probe, 1 µl Cot DNA (Invitrogen), and 7 µl hybridization buffer (Vysis) was added to each slide with denatured target DNA. Probes were allowed to hybridize overnight at 37°C in a humidified chamber. After washing steps, Eag1 probe was detected using the Dig detection kit (Roche Diagnostics). Amplification was defined as a signal ratio of Eag1 probe / centromere 1 of at least 2 and at least 4 gene signals.

Materials and statistical analysis

All used compounds were of highest available grade of purity. DMH, MNU, amiloride, 4-AP, astemizole, carbachol, and IBMX were from Sigma-Aldrich (TaufKirchen, Germany). DSS was from ICN (Eschwege, Germany). Forskolin and 293B were gifts from Aventis Pharma (Frankfurt, Germany). Student's t-test (for paired or unpaired samples as appropriate) and analysis of variance (ANOVA) were used for statistical analysis. $P < 0.05$ was accepted as significant. Survival curves were plotted according to Kaplan-Meier. A log rank test was applied to examine the relationship between alterations clinicopathological data or Eag1 amplification status and overall survival. Patients were censored at the time of their last clinical control. Cox proportional hazard model with stepwise selection of the covariates was used to determine the parameters with greatest influence on the risk of recurrence and progression.

Results

Histopathology

From week 12 on, DMH treated animals showed a significantly reduced weight increase. MNU treated mice also demonstrated a reduced body weight and a growth delay compared to untreated mice. Frequently the animals developed diarrhea upon treatment with carcinogens. 6 to 8 weeks after DMH treatment, local mucosal infiltration of leucocytes indicated inflammatory processes in distal colon (Fig. 4-1A,B). After 10 and 12 weeks changes of mucosal architecture such as tortuous crypts and crypt loss were observed in distal colon (Fig. 4-1C). No obvious histological changes were found in the proximal colon. Rectal MNU application 4 times in 2 weeks induced hyperplastic crypts in distal colon, indicated by an increase of crypt heights and decreased number of globlet cells along the cryptal wall. Moreover nuclear to cytoplasmic ratio was increased (Fig. 4-1D).

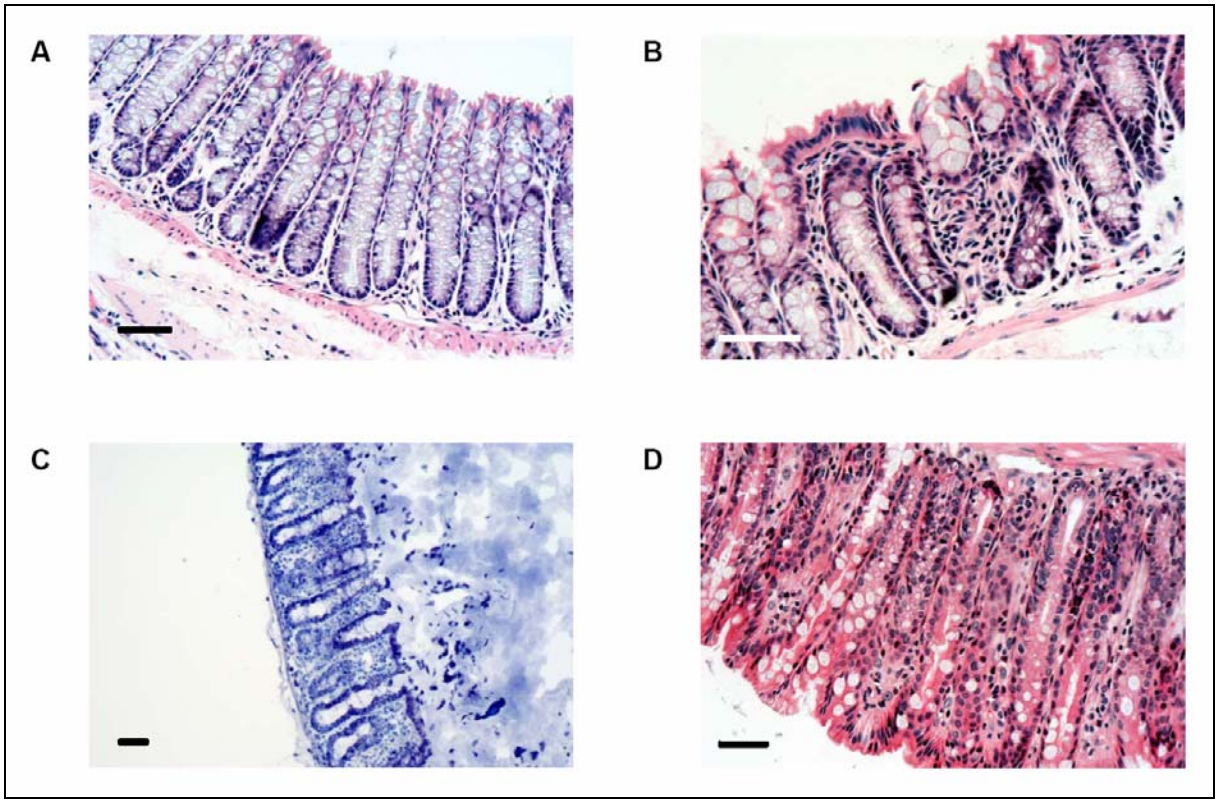

Fig. 4-1 Effects of DMH, MNU, and DSS treatment on colonic architecture

A) Hematoxylin and eosin staining of control distal colon. B) Infiltration by inflammatory cells of distal colonic mucosa after DMH treatment. C) Loss of crypts in distal colonic mucosa of DMH treated mice. D) Hyperplastic crypts in distal colon after MNU treatment. Bars = 50 µm.

Cellular redistribution and nuclear accumulation of ß-catenin was not clearly correlated with carcinogen treatment and was therefore not used as an independent marker for carcinogenesis (data not shown). Mucosal infiltration by inflammatory cells was observed in the proximal colon. After 8 treatments (week 6), extension of the Lamina submucosea and M. submucosea, and dysplasia of distal colonic mucosa were observed. Administration of DSS caused severe changes of the tissue architecture, ulceration, and inflammatory cell infiltration, areas of complete epithelial denudation as well as submucosal edema in distal and proximal colon. Thus, inflammation and carcinogenesis induced by chemicals is clearly demonstrated by histological changes.

DMH, MNU and DSS treatment inhibits Na^+ absorption and Cl- secretion

In essence, electrogenic ion transport in the colon is due to Na^+ absorption by amiloride sensitive Na^+ channels (ENaC) and cAMP- or Ca^{2+}- induced Cl^- and K^+ secretion. The amount of electrogenic Na^+ absorption is determined by inhibition with amiloride and calculation of the amiloride sensitive short circuit current $I_{sc\ Amil}$ (Fig. 4-2A). DMH treatment reduced $I_{SC\ Amil}$ in distal colon 6 and 8 weeks after the first DMH injection, which recovered at week 10 and 12 (Fig. 4-2A,B). Similar effects on amiloride sensitive Na^+ absorption were seen in MNU treated mice. Rectal potential difference (PD) measurements *in vivo* after 2 and 6 weeks of MNU treatment showed a reduced rectal PD, due to attenuated amiloride sensitive transport (Fig. 4-2C). Ussing chamber experiments and I_{SC} measurements confirmed reduced Na^+ absorption in distal colon of MNU treated mice (19.6 $\pm$ 4.3 µA/cm^2; n = 11), when compared to control mice (57.8 $\pm$ 9.6 µA/cm^2; n = 13) (Fig. 4-2D). Also in the inflamed colon, during treatment with DSS amiloride sensitive rectal PD was significantly reduced from -7.2 $\pm$ 0.58 mV (n = 7) to -4.9 $\pm$ 0.73 mV (n = 10).

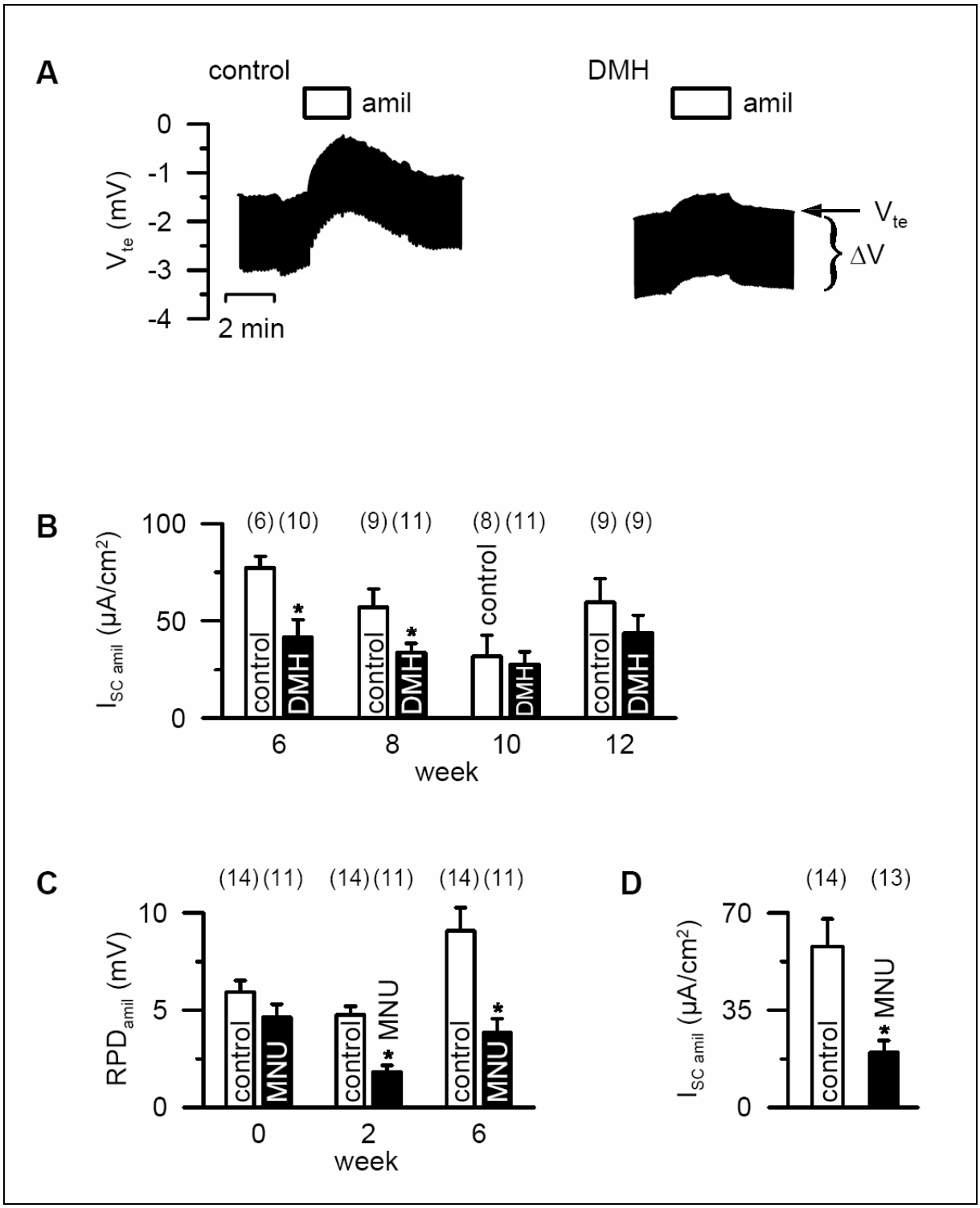

Fig. 4-2 Change of amiloride sensitive transport by carcinogens

A) Ussing chamber recordings of the transepithelial voltage. Amiloride (20 µM), a specific inhibitor of epithelial Na^+ channels reduced V_{te} and increased ΔV_{te} due to inhibition of Na^+ absorption. The effect of amiloride on V_{te} was reduced after 6 weeks of DMH treatment. B) Amiloride (20 µM) sensitive I_{SC} ($I_{SC\ Amil}$) was reduced in Ussing chamber experiments 6 and 8 weeks after initial DMH injection. C) Rectal potential difference (RPD) measurements showed reduced effects of amiloride (RPD_{Amil}), 2 and 6 weeks after rectal

application of MNU. D) Ussing chamber experiments confirmed reduced $I_{SC\ Amil}$ in distal colon, 6 weeks after rectal application of MNU. Asterisks indicate significant differences compared to control (Student´s *t*-test). (number of mice).

Increase in intracellular cAMP by IBMX (100 µM) and forskolin (2 µM) induced Cl^- secretion ($I_{SC\ cAMP}$) in proximal and distal colon, by activation of the cystic fibrosis transmembrane conductance regulator (CFTR). DMH caused a reduced $I_{SC\ cAMP}$ response in both proximal and distal colon at week 6 and 8. In contrast, later stages (week 12) $I_{SC\ cAMP}$ was significantly elevated in proximal colon (Fig. 4-3A,B). It is well known that basolateral cAMP- dependent activation of the cotransporter NKCC1, and 293B sensitive KCNQ1 K^+ channels ($I_{SC\ 293B}$) facilitate CFTR dependent Cl^- secretion. Accordingly DMH treatment inhibited $I_{SC\ 293B}$ in cAMP stimulated proximal colon at week 6 and increased $I_{SC\ 293B}$ at week 12 (Fig. 4-3C).

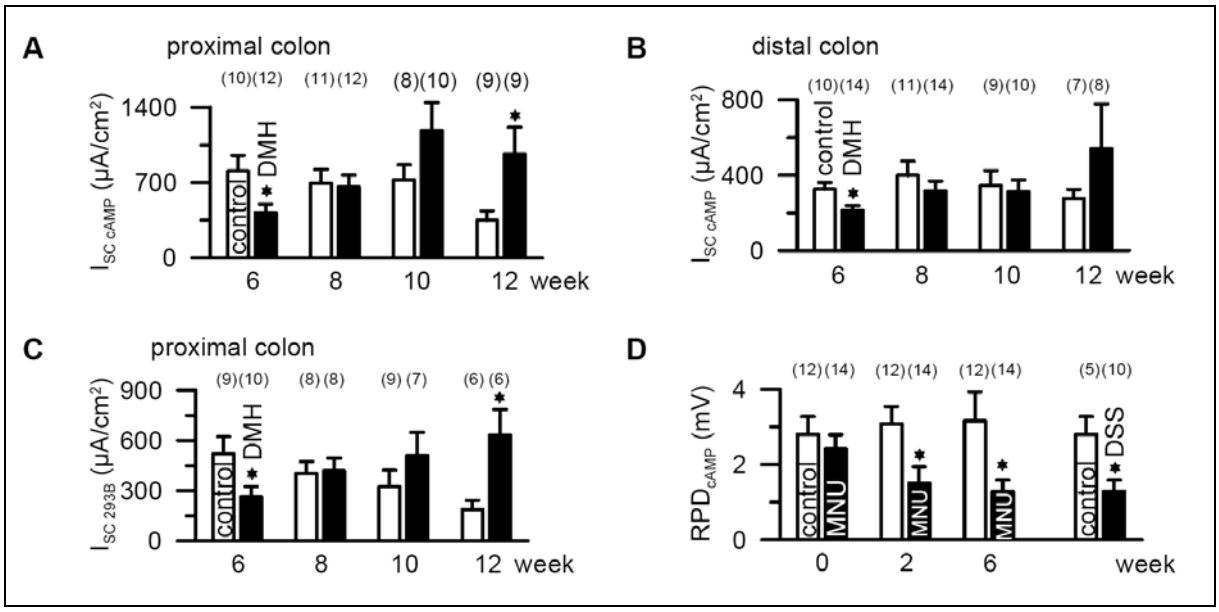

Fig. 4-3 Treatment with DMH, MNU and DSS reduced CFTR dependent Cl- secretion

A) IBMX and forskolin increased intracellular cAMP and activated CFTR dependent Cl^- secretion. In proximal colon, cAMP induced I_{SC} ($I_{SC\ cAMP}$) was reduced 6 weeks after DMH injection, but was and elevated after 12 weeks. B) Summary of the effects of DMH on $I_{SC\ cAMP}$ in distal colon. C) The 293B sensitive I_{SC} ($I_{SC\ 293B}$) was reduced 6 weeks after DMH injection and was elevated after 12 weeks. D) Increase in rectal PD by IBMX and forskolin (RPD_{cAMP}) was reduced in MNU and DSS treated mice, respectively. Asterisks indicate significant differences compared to control (Student´s *t*-test). (number of mice).

Similar to DMH in the early phase, MNU and DSS also reduced cAMP dependent Cl^- secretion in RPD measurements (Fig. 4-3D). This was further confirmed in Ussing chamber recordings. Here, cAMP activated transport was significantly attenuated by 62.3 ± 5.3 µA/cm^2

(n = 14) in MNU treated animals and by 174.3 ± 18.2 μA/cm^2 (n = 7) in DSS treated mice. In contrast, Ca^{2+} activated Cl^- secretion, stimulated by carbachol (CCH, 100 μM) and blockage by niflumic acid (NFA, 100 μM) remained unchanged (data not shown). Hence electrogenic Na^+ absorption via ENaC and cAMP dependent Cl^- secretion by CFTR are changed during inflammation and carcinogenesis, while Ca^{2+} activated Cl^- secretion remains unaffected. Since both ENaC and CFTR are the major determinants for net fluid transport in the colon, these changes are likely to affect digestive functions of the colon.

Carcinogens induce voltage gated K^+ channels

A major goal of the present study was to identify potential oncogenic ion channels during inflammation and carcinogenesis of the colonic epithelium. It is well established that proliferation of cancer cells and metastasis require the activity of plasma membrane K^+ channels (102, 103). We investigated the function of Kv channels in the pre-malignant colon using the non-selective Kv channel inhibitor, 4-aminopyridine (4-AP, 100 μM) and the inhibitor of the Eag channel family, astemizole (5 μM). Application of both 4-AP and astemizole had only minor effects on I_{SC} in control animals, but inhibited I_{SC} significantly in proximal and distal colon of DMH treated mice (Fig. 4-4A,B). These results suggest that DMH treatment induced activation of Kv and Eag related K^+ channels in both distal and proximal colon. Similar results were obtained in distal colon of MNU treated mice, where I_{sc} was significantly reduced by 4.3 ± 0.54 μA/cm^2 (n = 14). The inflamed (DSS) colon did not exhibit Kv channel activity in Ussing chamber recordings and showed only small RPD changes upon application of 4-AP (data not shown). In summary, Kv channels and cell cycle regulated Eag channels were clearly detected in the pre-malignant colon, but were absent in the inflamed colon.

Expression of ion channel mRNA in crypt cells of DMH, MNU and DSS treated mice

Since we detected changes in electrolyte transport as well as enhanced Kv channel activity in the pre-malignant colon, we investigated molecular expression of the underlying ion channels. Total RNA was prepared from freshly isolated crypt cells of proximal and distal colon of DMH, MNU and DSS (each n = 6) treated animals and control mice. Changes in ion channel expression relative to the control group were calculated. We found a small but significant increase in the mRNA expression for α, β and γ subunits of ENaC in DMH treated animals. No changes in expression of CFTR could be detected (Table 4-1). Thus changes in Na^+ absorption and Cl^- secretion due to the DMH treatment are not explained by changes in transcript expression of the respective ion channels but are due to other secondary changes (c.f. discussion). Enhanced 4-AP sensitive K^+ currents detected in carcinogen treated animals may also be caused by enhanced expression of Kv channels. In fact, mRNAs

encoding the channels Kv3.1, Kv1.3 and Kv1.5 were clearly up regulated in both distal and proximal colonic crypt cells of DMH and MNU treated animals. Moreover, corresponding to the enhanced astemizole sensitive currents (Fig. 4-4A, B), we detected enhanced mRNA expression of ether-á-go-go subtypes Eag1, Erg1 and Elk1 in the pre-malignant proximal and distal colon of DMH and MNU treated mice, but not in the inflamed (DSS) colon (Table 4-1).

Table 4-1 Changes in ion channel mRNA expression in crypt cells of proximal and distal colon of DMH, MNU and DSS treated mice

Expression of mRNA was normalized against β-actin expression and changes relative to the control group were calculated. Asterisk indicates significant difference to control (Student´s *t*-test). n.c. = no change. Number of mice is given in parentheses

gene	DMH week 6	DMH week 8	DMH week 10	DMH week 12	MNU week 6	DSS
proximal colon						
ENaCα	n.c. (5/6)	n.c. (4/6)	n.c. (6/6)	-0.57 ± 0.06 (4/5)*	n.c. (6/6)	n.c. (4/6)
ENaCβ	-0.45 ± 0.08 (5/5)*	n.c. (6/6)	n.c. (6/5)	2.65 ± 0.97 (5/6)*	n.c. (5/6)	n.c. (4/6)
ENaCγ	n.c. (6/5)	n.c. (6/4)	n.c. (6/5)	9.75 ± 4.27 (5/5)*	n.c. (6/6)	2.21 ± 0.62 (4/6)*
CFTR	n.c. (5/6)	-0.77 ± 0.07 (4/5)*	n.c. (6/5)	n.c. (6/6)	n.c. (6/6)	n.c. (4/6)
Kv1.3	n.c. (5/6)	13.59 ± 4.27 (4/6)*	n.c. (6/6)	n.c. (5/6)	n.c. (6/6)	n.c. (4/6)
Kv1.5	n.c. (6/6)	n.c. (6/6)	n.c. (6/6)	n.c. (5/5)	3.13 ± 0.85 (5/6)*	n.c. (4/6)
Kv3.1	n.c. (3/3)	6.19 ± 1.64 (3/3)*	1.36 ± 0.43 (6/6)*	4.03 ± 1.31 (4/5)*	1.41 ± 0.60 (6/6)*	n.c. (4/6)
Eag1	n.c. (5/6)	n.c. (5/4)	2.04 ± 0.59 (4/4)*	8.15 ± 2.06 (4/5)*	n.c. (6/6)	n.c. (4/6)
Erg1	1.96 ± 0.80 (6/6)*	6.44 ± 2.17 (3/3)*	8.64 ± 1.47 (3/3)*	30.38 ± 2.81 (3/3)*	n.c. (6/6)	n.c. (4/6)
Elk1	n.c. (6/6)	1.09 ± 0.37 (5/5)*	2.83 ± 1.42 (5/3)*	2.25 ± 0.76 (4/5)*	-0.73 ± 0.14 (5/6)*	n.c. (3/6)
distal colon						
ENaCα	n.c. (6/6)	n.c. (5/5)	n.c. (6/6)	-0.54 ± 0.08 (5/4)*	n.c. (6/6)	-0.79 ± 0.08 (4/5)*
ENaCβ	-0.55 ± 0.09 (5/6)*	n.c. (5/5)	n.c. (6/6)	2.54 ± 0.56 (5/6)*	n.c. (6/5)	n.c. (4/6)
ENaCγ	n.c. (6/5)	n.c. (5/5)	n.c. (6/6)	5.60 ± 2.22 (5/5)*	n.c. (6/5)	1.14 ± 0.47 (4/4)*
CFTR	n.c. (5/6)	0.61 ± 0.11 (5/6)*	n.c. (6/6)	n.c. (6/6)	n.c. (6/6)	n.c. (4/6)
Kv1.3	n.c. (6/6)	n.c. (6/6)	n.c. (6/6)	n.c. (5/6)	15.32 ± 7.48 (5/4)*	4.13 ± 1.57 (4/5)*
Kv1.5	7.52 ± 1.86 (6/6)*	n.c. (6/6)	n.c. (6/6)	n.c. (5/5)	n.c. (6/6)	n.c. (4/6)
Kv3.1	n.c. (3/3)	1.80 ± 0.65 (3/3)*	0.93 ± 0.29 (3/3)*	1.06 ± 0.17 (3/3)*	n.c. (6/5)	n.c. (4/6)
Eag1	n.c. (6/6)	n.c. (5/5)	n.c. (6/5)	2.65 ± 0.83 (4/4)*	n.c. (6/6)	n.c. (3/6)
Erg1	4.44 ± 0.37 (3/3)*	n.c. (5/5)	1.41 ± 0.22 (3/3)*	2.78 ± 2.12 (3/2)*	2.78 ± 1.14 (6/6)*	n.c. (4/6)
Elk1	n.c. (6/6)	n.c. (6/6)	n.c. (6/6)	n.c. (6/6)	n.c. (5/5)	n.c. (4/6)

DMH and MNU treatment increased expression of Eag1 protein

Cell cycle dependent regulation of Eag1 is well established, and so far expression of the channel was only found in cancer cells but not in normal epithelial tissues (108). Because DMH treatment induced an astemizole sensitive I_{SC} and increased Eag1 mRNA expression in proximal and distal colon, we also examined protein expression in isolated crypt cells. In the control group, Western blot analysis showed no uniform Eag1 expression in crypt cells (Fig. 4-4C). In contrast in crypt cells of DMH treated mice, Eag1 protein was well detected in proximal and distal colon (Fig. 4-4C). The carcinogen MNU enhanced Eag1 expression in the proximal colon, while no changes were observed in the inflamed colon (DSS), as indicated by densitometric analysis relative to actin staining (Fig. 4-4D).

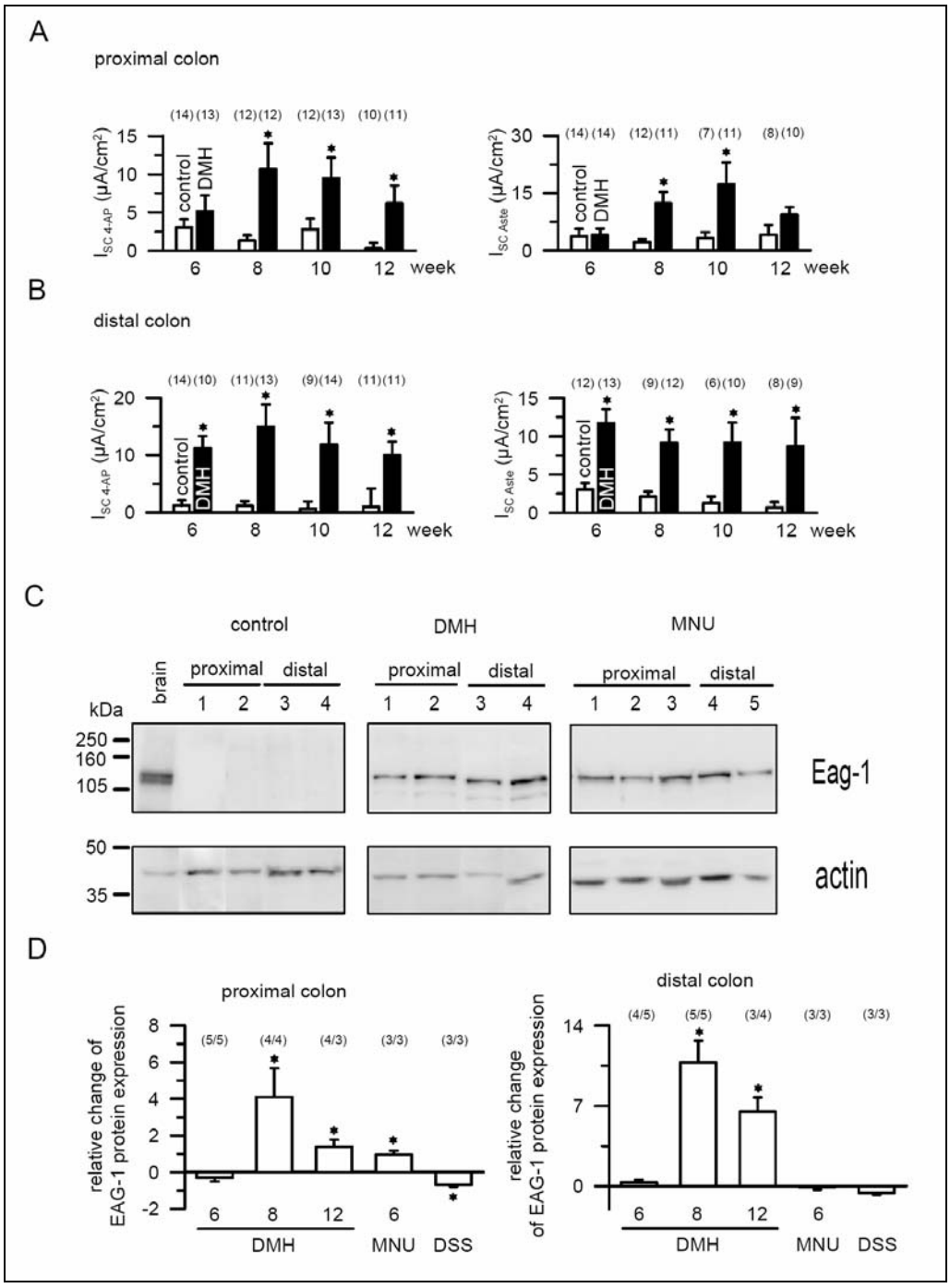

Fig. 4-4 Treatment with carcinogens enhanced expression of voltage-gated K^+ channels

In proximal (A) and distal (B) colon, application of 4-AP and astemizole indicated enhanced activity of voltage-gated K^+ channels after treatment with carcinogens. C) Western blot analysis of Eag1 (111 kDa) and ß-actin (42 kDa) expression in brain (positive control) and crypt cells of proximal and distal colon of control, DMH and MNU treated mice. D) Summary of the changes in Eag1 expression (normalized against ß-actin) in crypt cells of DMH, MNU and DSS treated mice. Asterisks indicate significant differences compared to control (Student´s *t*-test). (number of mice).

Eag1 protein expression in human carcinomas and diverticulitis

Eag1 expression was analysed by RT-PCR in biopsies of two colorectal carcinomas and the Eag1 transcript variants 1 and 2 were found in the centre of the carcinoma as well as in the macroscopically unaffected periphery. However, no expression of Eag1 mRNA was found in the colon of a healthy volunteer (Fig. 4-5A).

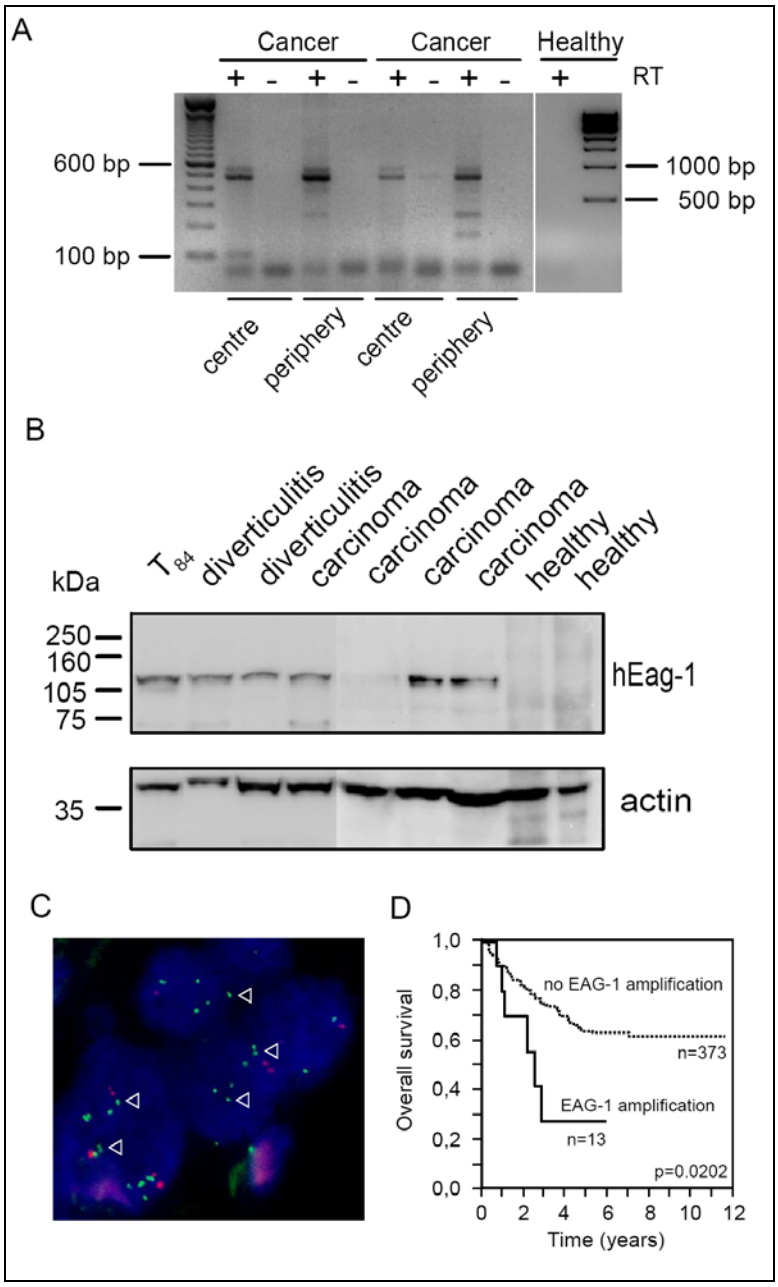

Fig. 4-5 Eag1 is expressed in colonic crypt cells of patients with cancer and diverticulitis

A) RT-PCR showed mRNA expression of the two variants of Eag1 (variant 1, 560 bp, variant 2, 479 bp) in the centre and peripheral tissue of the cancer in two patients. In a colonic biopsy of a healthy volunteer, no Eag1 transcripts were detected. B) Total protein

was isolated from T_{84} colonic cancer cells and from crypt cells derived from patients with different diagnosis. Colonic biopsies of healthy patients served as controls. C) Fluorescence in situ hybridization of a colorectal adenocarcinoma with Eag1 amplification. Tumor cell nuclei contain numerous green Eag1 signals, but only few reference signals in red (centromer 1; x1000). Nuclei counterstained with DAPI (blue). D) Impact of Eag1 gene amplification on overall survival in surgically resected colorectal adenocarcinoma.

Expression of Eag1 protein was analysed in isolated crypt cells from patients, diagnosed with sigma diverticulitis, ulcerative colitis, colorectal adenocarcinoma, coecum carcinoma and colonic neoplasm (Fig. 4-5C). Samples were also obtained from patients with unrelated diseases, such as cystic fibrosis. No expression of Eag1 was detected in these samples. The variability of the tissue sample quality was assessed by simultaneous detection of ß-actin expression. In summary, expression of Eag1 was detected in most carcinomas and in some patients diagnosed with diverticulitis, while the healthy colon does not seem to express cell cycle regulated K^+ channels (Fig. 4-5B).

The Eag1 gene is amplified in tumor specimens and is associated with adverse outcome

pTNM stage, histological grade, and UICC stage were strongly associated with overall survival ($p<0.0001$ each; data not shown). FISH analysis showed amplification of the Eag1 gene in 13 (3.4%) of the 386 tumor specimens (Table 4-2). A representative case with Eag1 amplification is shown in figure 4-5C. Univariate survival analysis revealed that Eag1 amplification was significantly associated with adverse outcome ($p=0.0202$; Fig. 4-5D). If entered in a multivariate model (Cox proportional hazard), amplification of Eag1 emerged as an independent prognostic marker ($p=0.0126$, RR=3.55) together with UICC stage ($p<0.0001$, RR 15.56) and histological grade ($p=0.0167$, RR 1.77, n=386). Thus expression of Eag1 is associated with reduced overall survival in patients with colonic carcinoma.

Table 4-2 Clinicopathologic characteristics of colorectal adenocarcinomas (n=386)

sex	male	200 (48.1%)
	female	186 (51.8%)
age	years (range)	71.6±1.1 (36-96)
localisation	right colon	164 (43.4%)
	left colon	214 (56.6%)
pT	pT1	7 (1.8%)
	pT2	64 (16.6%)
	pT3	247 (64.0%)
	pT4	68 (17.6 %)
pN	pN0	195 (50.5%)
	pN1	107 (28.2%)
	pN2	84 (27.7%)
pM	pM0	309 (80.1%)
	pM1	77 (19.9%)
stage	I	53 (13.7%)
	II	129 (33.4%)
	III	127 (32.9%)
	IV	77 (20.0%)
grading	G1	2 (0.5%))
	G2	290 (75.1%)
	G3	94 (24.4%)
follow-up (months)	mean (range)	37.7±3.4 (0-140)
	median	31.0

Discussion

Effects of pro-inflammatory and carcinogenic chemicals

For the present study, we used the mouse C57BL/6N strain, which shows a high incidence of colorectal tumors after DMH treatment (117, 118). Histological changes were identified early after DMH injection; however, definite cancers develop typically only after 24 weeks of treatment (118). Intrarectal infusion of MNU yielded a high incidence (up to 100%) of colonic cancer in previous studies with shrews (119). We detected initial inflammatory responses in both DMH and MNU treated animals, similar to the inflamed (DSS) colon. However at later stages, carcinogens caused significant changes in mucosal architecture and expression of Kv3.1, Kv1.3 and Kv1.5 and particularly Eag channels. This was not observed in the DSS model. Thus, expression oncogenic Eag channels appear to be a consequence of the carcinogen treatment and not simply a result from inflammation. This channel was also found in human colonic cancers, but not in normal tissues. It suggests that Eag has an oncogenic potential in the colonic epithelium. Interestingly, Eag was also detected in diverticulitis, which has the potential to change into colonic cancer. We hypothesize that expression of Eag in pre-neoplastic tissues supports malignancy and may drive the development towards colonic cancer.

Electrolyte transport changes during carcinogenesis and colitis

Several reports show altered electrolyte transport in early stages of tumor development. Using the present models, we confirm reduction of amiloride sensitive Na^+ absorption by

treatment with DMH, MNU and DSS. Inhibition of amiloride sensitive Na^+ absorption was not explained by changes in the expression profile of the three Na^+ channel subunits. A likely reason for reduced Na^+ absorption is an attenuation of the Na^+/K^+-ATPase in the distal colon (120). cAMP induced Cl^- secretion was reduced initially, but was up-regulated at later stages of DMH treatment. Stool irregularities, with changes from constipation to diarrhea are often observed in patients with intestinal tumors or inflammatory bowel disease and the present findings may therefore supply an explanation for these symptoms.

Expression of Kv channels during inflammation and carcinogenesis

Kv channels promote cell proliferation and support tumor development (103, 104). In multiplex RT-PCR, we found enhanced expression of the channels Kv1.3, Kv1.5 and Kv3.1 (Table 1). Kv1.3 (gene locus KCNA3) is essential for lymphocyte proliferation and supports development of cancer in prostate, colon and breast. Kv1.5 (gene locus KCNA5) supports proliferation of gastric cancer (102, 121). Moreover, expression of Kv1.5 correlates with the grade of malignancy of gliomas (122). The apparent dissociation constants (K_d) of 4-AP for Kv1.3, Kv1.5 and Kv3.1 channels are 195 µM, 270 µM and 29 µM respectively, which are in the range of the 4-AP concentration (100 µM) used in the present study (123). We suggest that Kv3.1 (gene locus KCNC1) is mainly responsible for the 4-AP dependent inhibition of ion transport in the malignant colon. Thus, this is the first study, which supplies evidence that Kv3.1 channels are involved in development of cancer. Expression of Kv3.1 is normally restricted to CNS and to a subpopulation of T lymphocytes (103). Kv3.4, another member of this subfamily of Kv channels, controls proliferation of oral and oesophageal squamous carcinoma cells (124).

An oncogenic role of Eag channels in the colon

According to previous reports, expression of Eag1 and Erg1 channels is strictly limited to excitable tissues. In contrast, malign epithelial tumors the cell cycle controlled Eag channel determines malignancy and metastasis of breast cancer (103, 105, 108, 125). Crypt cells of carcinogen treated mice demonstrated expression of Eag1, Erg1 and Elk1 in the present study. When normalized to the actin signal, expression of Eag1 was somewhat larger in the distal colon when compared to the proximal colon of DMH treated animals. However, the difference was not statistically different. Moreover, expression of Eag1 was found in human colorectal adenocarcinomas. FISH analysis showed amplification of the Eag1gene in 13 (3.4%) of the 386 tumor specimens. Eag1 amplification was significantly associated with adverse outcome. The low prevalence of Eag1 amplification does not question its importance, since mechanisms other than amplification may account for activation and over-expression in a larger fraction of tumors. For example another potassium channel, KCNK9 at

8q24.3, was previously found to be amplified in about 10%, but over expressed in 44% of breast cancers (126).

Taken together, carcinogenesis in the colon and colitis change expression of ion channels important for salt transport, which is likely to cause stool irregularities. Expression of the cell cycle regulated K^+ channel Eag1 is closely correlated with malignancy in the human and rodent colon and Eag1 gene amplification is associated with reduced surviving rate. These data suggested that Eag1 expression is important for tumor development in the human colon. Since Eag1 is already expressed at a pre-malignant stage, Eag1 transcripts detected in rectal biopsies or stool samples may serve as early diagnostic and prognostic markers, as demonstrated recently for cervical cancer (107). The present data may also be useful in developing new therapeutic strategies for the treatment of colonic cancer.

Chapter 5

Upregulation of colonic ion channels in APC-Min/+ mice

Abstract

The adenomatosis polyposis coli (*APC*) tumor suppressor gene is mutated in almost all human colonic cancers. Disturbances in Na^+ absorption have been observed in colonic cancer and ion channels such as ether a go-go (Eag) or Ca^{2+} sensitive BK channels have been recognized for their oncogenic potential. The APC-Min/+ mouse model is characterized by reduced APC expression and multiple intestinal neoplasia (Min). The activity of colonic ion channels was assessed by electrophysiological and molecular techniques. APC-Min/+ mice developed polyps in proximal and distal colon and experienced a significant weight loss during an observation period of 21 weeks. Rectal potential measurements *in vivo* indicated an increase in amiloride sensitive Na^+ absorption in APC-Min/+ mice. Quantitative Ussing chamber studies demonstrated enhanced Na^+ absorption via epithelial Na^+ channels (ENaC) and suggested enhanced activity of oncogenic BK and Eag1 channels. Patch clamp experiments on mid crypt cells showed similar results for APC-Min/+ and wt mice, suggesting that changes in channel activity take place in the surface epithelium. ENaC-mRNA and membrane protein expression was clearly enhanced in colonic surface epithelial cells. The data suggest that reduced expression of the *APC* gene with upregulation of the downstream proteins Akt and mTOR augments the activity of ENaC and oncogenic potassium channels. These changes reflect an imbalance due to reduced apoptosis and enhanced mitotic activity, and may have implications for the clinical outcome.

Introduction

Membrane ion channels have been demonstrated in previous studies to control cell proliferation. Changes in ion channel expression during development of cancer have been frequently observed (for review see (6)). Ion channel activity determines homeostatic parameters such as membrane voltage, intracellular ion concentration, and cell volume. Ion channels also control cytosolic pH and cell signaling by changes in the intracellular Ca^{2+} concentration (6, 44, 79). Some ion channels, like Eag1, fulfill specific tasks during the cell cycle (19, 41). Voltage gated K^+ channels are detected in breast and colonic cancer specimens and other malign tumors (16, 19, 41, 44, 60). Large conductance Ca^{2+} activated K^+ channels are found in tumors of prostate, breast and colorectum (88, 127). Previous in vitro studies demonstrate a contribution of K^+ channels to proliferation of colonic cancer cells, and experiments performed on animal models suggest an oncogenic role of these K^+ channels in vivo (60). To fully appreciate the changes in ion channel currents occurring during carcinogenesis in the colon, further in vivo studies are required, ideally on a genetically well defined mouse model (128).

Previous studies utilized chemical tumor models in order to assess potential changes in ion conductances during carcinogenesis in vivo. Treatment of the animals with carcinogens like dimethylhydrazine or N-methyl-N-nitrosourea induce colonic cancer, which is paralleled by changes in ion channel expression (60, 129). While these studies supply some insight into carcinogenesis in vivo, the drawbacks are individual drug susceptibility and inflammation (60). Here we studied a well defined genetic mouse model that is based on a mutation in the adenomatous polyposis coli (APC) gene. Heterozygote APC-Min/+ mice develop multiple intestinal neoplasia (Min) (128). Mutations in the human APC gene are responsible for familial adenomatous polyposis and are found in a large majority of colorectal cancers. We found that heterozygous APC-Min/+ animals demonstrate a change in expression of epithelial colonic Na^+ channels and show an increase in BK and Eag1 channel conductance, similar to human colonic carcinoma.

Results

Pathology of APC-Min/+ mice

APC-Min/+ mice demonstrated a normal postnatal development but started to loose weight from week 12 on. APC-Min/+ mice reached an age of 21.21 ± 0.81 weeks. By then they lost more than 20% weight (23.22 ± 0.8 g; n = 23) compared to wt animals (36.66 ± 1.51 g; n = 32). Wt animals were sacrificed at an age of 23.3 ± 0.77 weeks. Every APC-Min/+ animal had large visible polyps in proximal (0.47 ± 0.2) and distal (2.53 ± 1.0; n = 14) colon, but the number of polyps was much higher in small intestine and stomach (27.2 ± 7) (Fig. 5-1A). Large intestinal polyps consisted of hyperplastic adenomas, which did not yet show signs of malignancy (Fig. 5-1B).

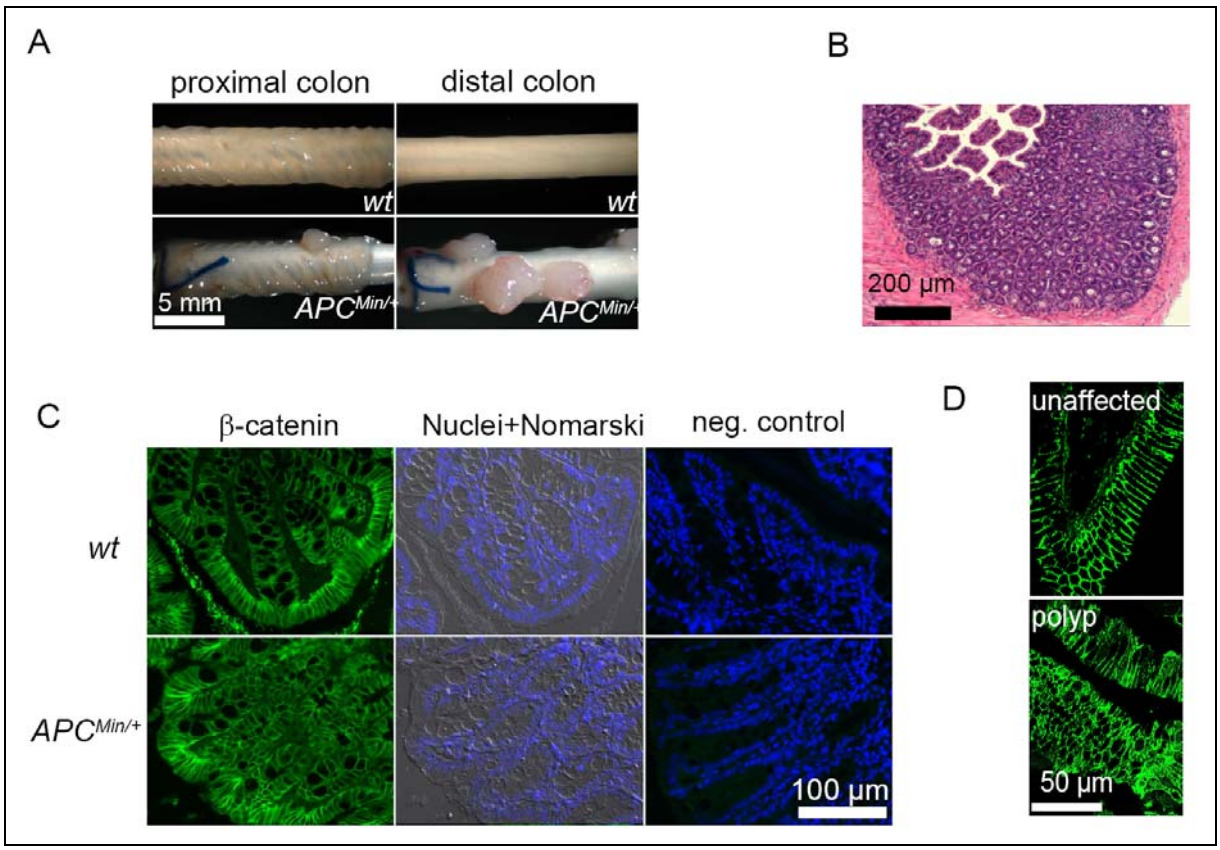

Fig. 5-1 Mucosal abnormalities in APC-Min/+ mice

A) Macroscopic aspect of inverted proximal and distal colonic mucosa of wild type (wt) and APC-Min/+ mice. Colonic mucosa of APC-Min/+ mice shows several large polyps. B) Hematoxylin/eosin staining of a distal colonic polyp from an APC-Min/+ animal. C) Staining of β-catenin in unaffected proximal colon of wt and APC-Min/+ mice. D) Confocal images of β-catenin in unaffected crypts and a polyp from proximal colon.

Although ß-catenin accumulation in crypts of APC-Min/+ animals had been described in previously (130), we found similar expression of ß-catenin in wt and APC-Min/+ animals in proximal and distal (Fig. 5-1C) colon. Confocal images of ß-catenin staining demonstrate regular membrane staining in unaffected small and large intestinal mucosa, while the staining was diffuse and cytosolic in the polyps (Fig. 5-1D).

Enhanced Na^+ absorption in APC-Min/+ mice

Rectal potentials were measured *in vivo* in anesthetized animals aged 9, 15 and 19 weeks, using a fine polyethylene catheter (c.f. Methods). From week 15 on, APC-Min/+ animals displayed increased lumen negative transrectal potential differences (RPD), when compared to wt animals (Fig. 5-2A,B). The RPD was mainly due to amiloride sensitive Na^+ absorption (RPD, since intrarectal application of amiloride via the catheter collapsed the lumen negative RPD. Thus, amiloride sensitive epithelial Na^+ absorption is significantly enhanced in APC-Min/+ animals (Fig. 5-2A,C and Table 5-1).

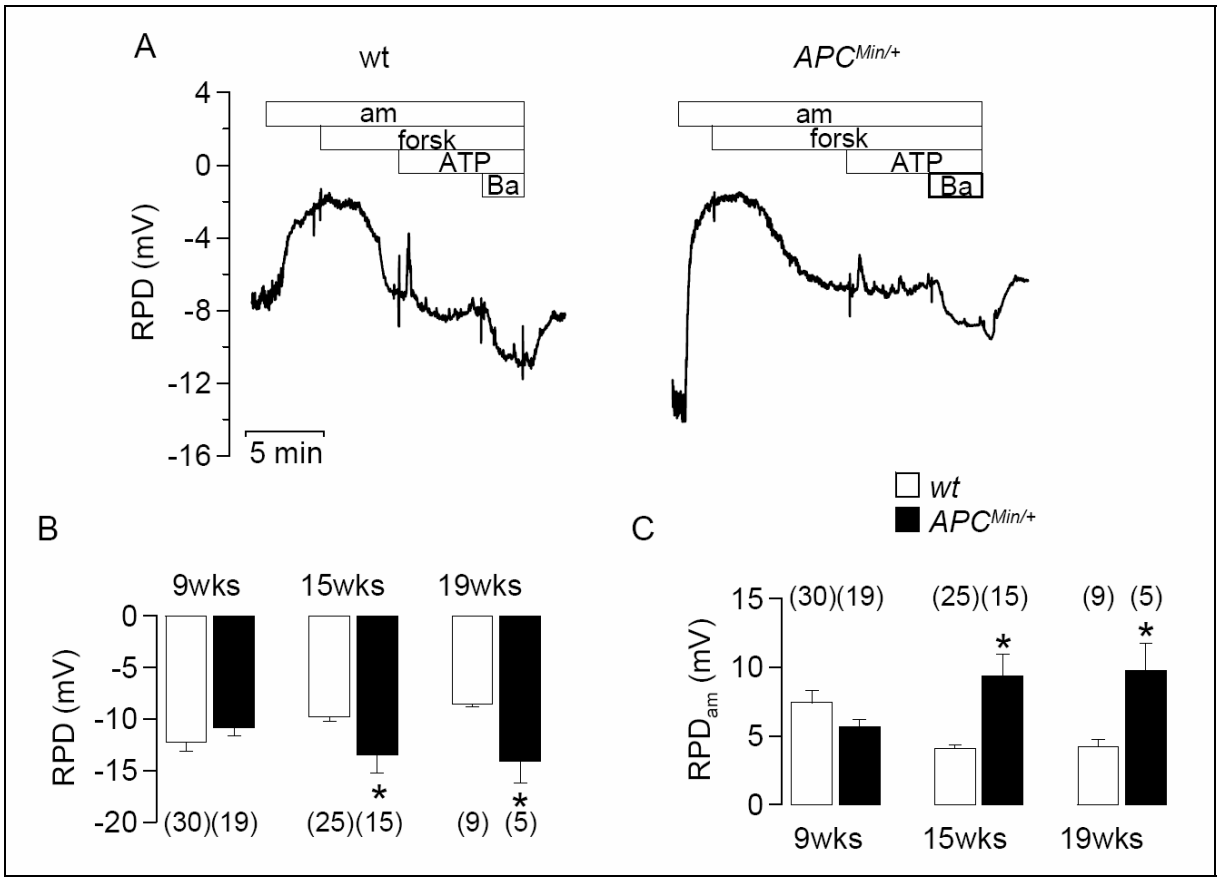

Fig. 5-2 Enhanced Na^+ absorption APC-Min/+ mice

A) Original recordings of the rectal potential difference (RPD) measured in wt and APC-Min/+ mice. Inhibition of ENaC by luminal application of amiloride (am, 20 µM) via the catheter reduced RPD, while forskolin (forsk, 2 µM) and barium (Ba, 5 mM) increase the

rectal potential difference. ATP (100 µM) induced a brief and transient decrease in RPD due to activation of BK K^+ channels. B) Summary of RPD measured in wild type (wt) and APC-Min/+ mice at 9, 15 and 19 weeks of age. C) Summary of the amount of RPD inhibited by amiloride in wild type (wt) and APC-Min/+ mice at 9, 15 and 19 weeks of age. Asterisks indicate significant differences compared to control (Student´s t-test). (Number of mice)

Table 5-1 Rectal potential difference in wt and APC-Min/+ mice

Under control conditions (RPD) and changes induced by rectal perfusion of amiloride (20 µM), forskolin 2 µM), ATP (100 µM), and Ba^{2+} (5 mM). Asterisks indicate significant difference when compared to wt animals. (Number of mice).

	rectal potential difference (mV)					
	9 weeks		15 weeks		20 weeks	
	wt (n=22-30)	APC-Min/+ (n=10-19)	wt (n=19-25)	APC-Min/+ (n=8-14)	wt (n=2-9)	APC-Min/+ (n=4-5)
RPD	-12.27 ± 0.9	-10.86 ± 0.8	-9.78 ± 0.4	**-13.52 ± 1.7***	-8.52 ± 0.2	**-14.11 ± 2.1***
RPD_{amil}	7.41 ± 0.9	5.65 ± 0.5	4.06 ± 0.3	**9.36 ± 1.6***	4.21 ± 0.6	**9.76 ± 2.0***
RPD_{forsk}	2.39 ± 0.3	2.06 ± 0.4	2.66 ± 0.4	2.16 ± 0.5	3.52 ± 0.5	3.24 ± 0.7
RPD_{ATP}	2.09 ± 0.2	2.04 ± 0.4	1.80 ± 0.3	1.82 ± 0.6	2.02 ± 1.4	1.31 ± 0.2
RPD_{Ba^+}	2.38 ± 0.2	2.58 ± 0.3	2.52 ± 0.2	**1.66 ± 0.2***	2.27 ± 0.3	2.44 ± 0.7

This was further quantified in continuous recordings of the transepithelial voltage, which is a measure for the epithelial transport (Fig. 5-3A). Electrogenic absorption of Na^+ by ENaC is normally limited to distal colon. However, in APC-Min/+ animals amiloride sensitive Na^+ transport (short circuit current, I_{sc}) was also detected in the proximal colon (Fig. 5-3B). In distal colon of APC-Min/+ animals, Na^+ absorption was largely upregulated (Fig. 5-3A,B). Other transport properties, like forskolin induced Cl^- secretion by the cystic fibrosis transmembrane conductance regulator (CFTR) Cl^- channel, and Ca^{2+} activated electrolyte transport in the distal colon were similar in APC-Min/+ and normal animals (data not shown).

Expression of oncogenic K^+ currents in APC-Min/+ mice

Expression of cell cycle regulated Eag1 and Ca^{2+} dependent BK channels has been reported for colonic cancer and other malignant tumors (60, 88, 127). Basolateral application of the Eag1 inhibitor astemizole (5 µM) inhibited I_{sc} in proximal and distal colon of both APC-Min/+ and normal mice, however, astemizole sensitive transport ($I_{sc\ aste}$) was augmented in proximal colon of APC-Min/+ mice (Fig. 5-3C). 4-aminopyridine (0.1 and 2 mM), which inhibits other types of voltage gated K^+ channels, had no effect on ion transport (data not shown). Luminal

paxillin (5 µM) inhibited K^+ secretion via BK channels to the same degree in wt (32.8 ± 12 µA/cm^2; n = 13) and APC-Min/+ (31.9 ± 19 µA/cm^2; n = 6) mice, suggesting similar baseline activity for BK channels. However, the activator of BK channels NS1619 (10 µM) stimulated more K^+ secretion in the distal colon of APC-Min/+, when compared to wt animals (Fig. 5-3D). Moreover, after activation of K^+ secretion by carbachol (100 µM), the BK channel inhibitor paxillin showed a stronger effect in APC-Min/+ mice (19.5 ± 9.7 µA/cm^2; n = 3), compared to wt (7.2 ± 3.4 µA/cm^2).

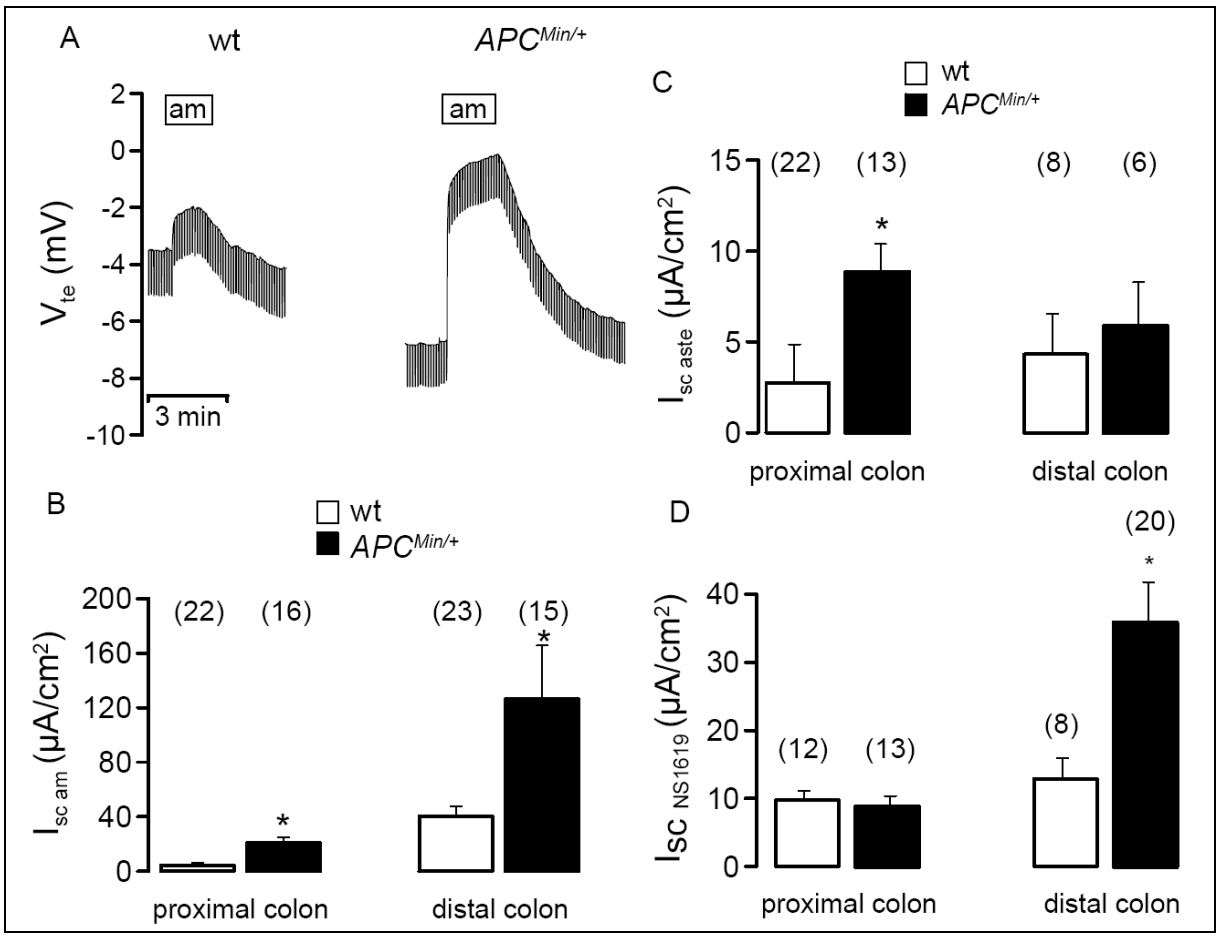

Fig. 5-3 Ion transport in the colon of APC-Min/+ mice.

A) Original recordings of the transepithelial voltage (V_{te}) measured in a perfused Ussing chamber. In APC-Min/+ mice the effect of amiloride (am, 20 µM) was enhanced compared to wt animals. B) Summary of the amiloride sensitive transport (Isc am) in proximal and distal colonic mucosa of wt and APC-Min/+ mice. C) Summary of the astemizole sensitive transport (Isc aste) in proximal and distal colonic mucosa of wt and APC-Min/+ mice. D) Summary of the K^+ secretion activated by the BK channel activator NS1619 (10 µM) in proximal and distal colonic mucosa of wt and APC-Min/+ mice. Asterisks indicate significant differences compared to control (Student´s t-test). (Number of mice).

Conductances properties were further examined in patch clamp experiments on mid and lower crypt cells (Table 5-2).

Table 5-2 Whole cell conductance (Gm) and membrane voltage (Vm) of epithelial cells from colonic crypts of wt mice and APC-Min/+ animals. (Number of mice).

	G_m (nS)		V_m (mV)	
	wt	APC-Min/+	wt	APC-Min/+
proximal colon	2.47 ± 0.41 (29)	2. 34 ± 0.3 (28)	-65.64 ± 2.74 (29)	-66.7 ± 3.26 (28)
distal colon	2.38 ± 0.24 (27)	3.01 ± 0.35 (37)	-68.71 ± 2.76 (27)	-62.87 ± 3.01 (37)

The baseline membrane voltage and conductance properties of epithelial cells from wt and APC-Min/+ mice were indistinguishable. We identified two populations of cells with either linear or outwardly rectifying whole cell currents (Fig. 5-4).

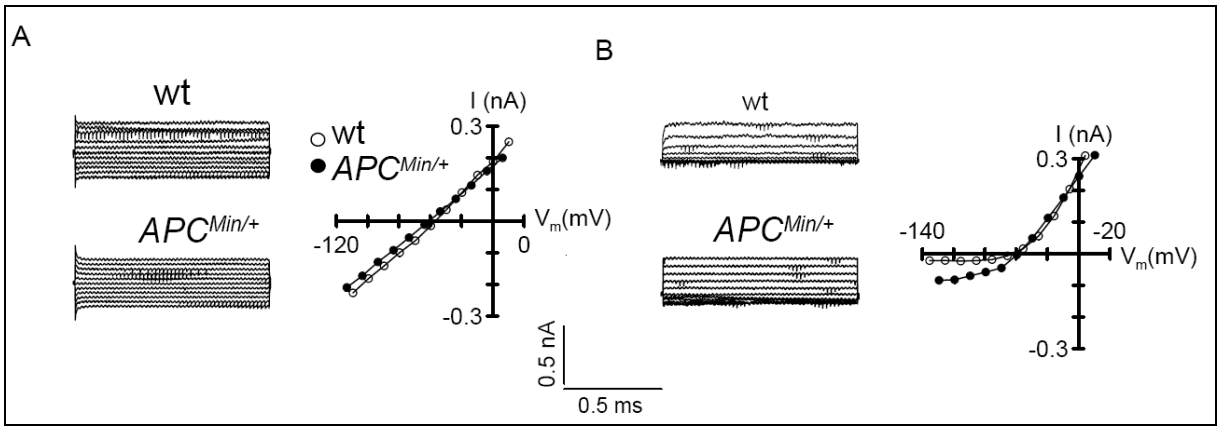

Fig. 5-4 Whole cell patch clamp experiments from colonic mid crypt and crypt base epithelial cells

Original current tracings (left panels) and current voltage relationships (right panels) suggest cells with linear (A) and outwardly rectifying (B) whole cell currents.

Moreover, cAMP- and Ca^{2+}- activated currents were similar in wt and APC-Min/+, and effects of paxillin, astemizole or 4-AP could not be detected (data not shown). Thus, Ca^{2+} activated BK channels and astemizole sensitive Eag1 channels must be expressed in the surface epithelium, which confirms previous results (55).

Enhanced expression of ENaC in APC-Min/+

The large increase in Na^+ absorption in the APC-Min/+ colon may be due to an increase in ENaC-activity or enhanced expression of the three α-, β-, γ-ENaC subunits. Immunostaining of all three ENaC-subunits was performed in proximal and distal colon (Fig. 5-5A,B).

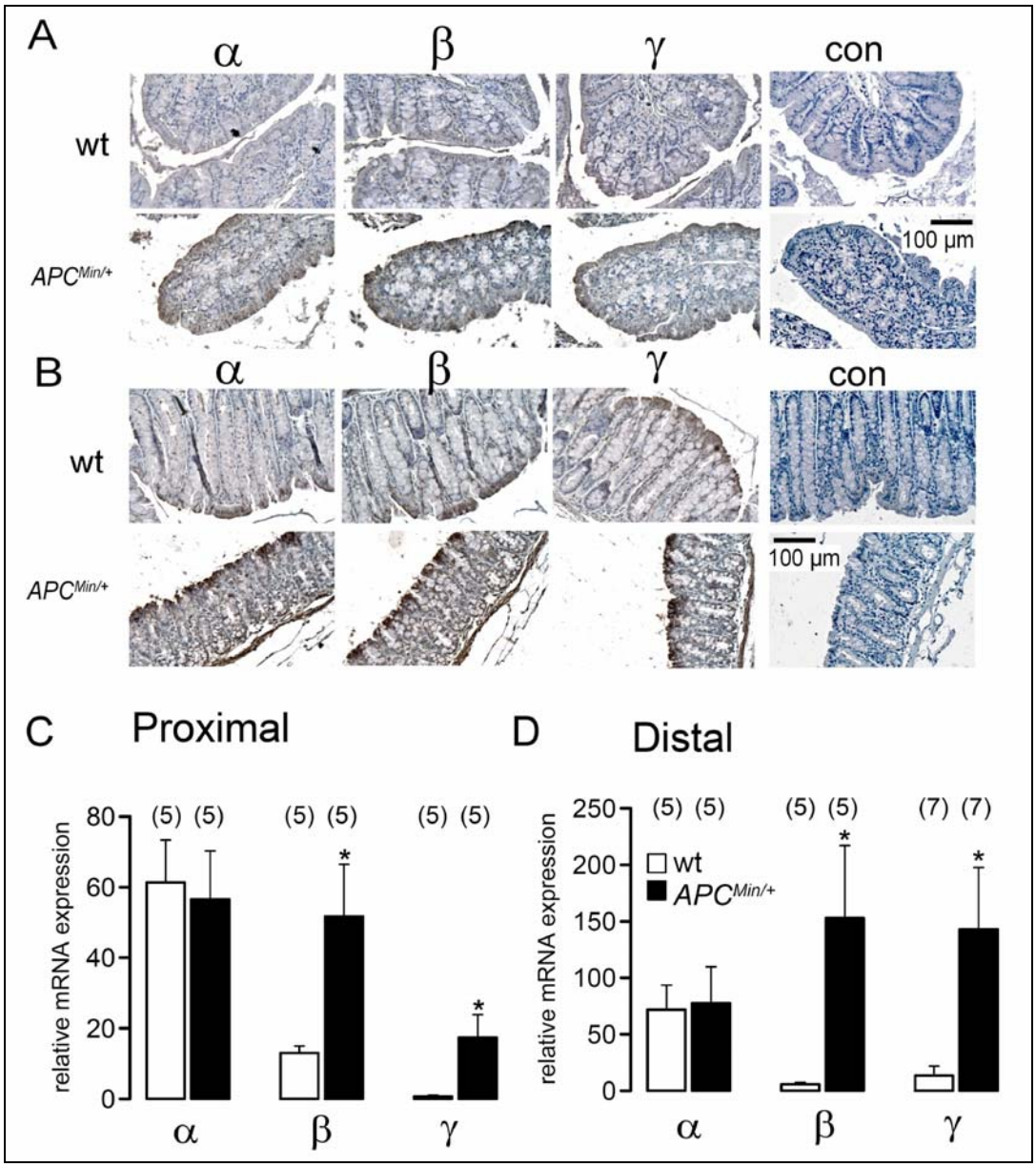

Fig. 5-5 Expression of ENaC in the colon of APC-Min/+ mice

Expression of α-, β-, and γ-subunits of the epithelial Na^+ channel ENaC in proximal (A) and distal colon (B) of wt and APC-Min/+ mice. No staining was obtained in the absence of primary antibodies (con). C,D) Summary of the results from real time PCR analysis indicates upregulation of mRNA expression for βENaC and γENaC in proximal and distal colon of APC-Min/+ and control mice. Asterisks indicate significant differences compared to control (Student´s t-test). (Number of mice).

In contrast to wt-animals α,β,γ-ENaC were clearly detectable in proximal colon of APC-Min/+ mice (Fig. 5-5A), and in the distal colon of APC-Min/+ mice expression of α,β,γ-ENaC was enhanced when compared to wt animals (Fig. 5-5B). Thus, enhanced Na^+ transport in the colon of APC-Min/+ mice is due to an increase in ENaC expression. Quantitative real time PCR analysis indicated enhanced expression of mRNA for β- and γ-ENaC in proximal and distal colon of APC-Min/+ mice (Fig. 5-5C,D). Quantification of total protein prepared from isolated colonic crypts, showed an increase in γ-ENaC protein expression in proximal and distal colon of APC-Min/+ mice (Fig. 5-6A,B,C).

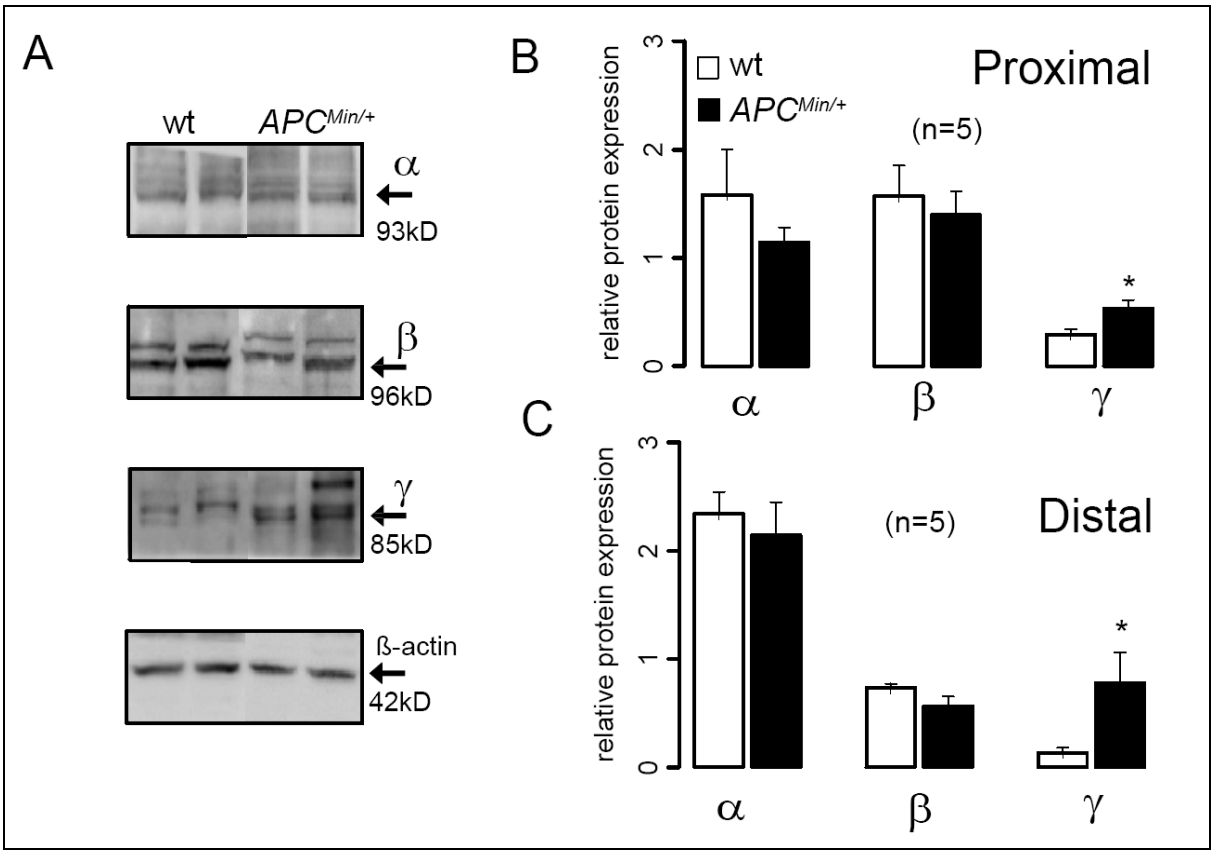

Fig. 5-6 Expression of ENaC in the colon of APC-Min/+ mice

A) Western blot analysis of the three α-, β-, and γ-subunits of the epithelial Na^+ channel ENaC in isolated distal colonic crypts. B,C) Summary of the expression of α-, β-, and γ-ENaC in proximal and distal colon of wt and APC-Min/+ mice. Asterisks indicate significant differences compared to control (Student´s t-test). (Number of mice).

Upregulation of the protein kinase B (Akt) in tumors of APC-Min/+ mice has been reported previously, and patients with colorectal carcinoma have elevated levels of Akt and cytoplasmic ß-catenin (131, 132). Because Akt could increase ENaC activity (133), ENaC could be upregulated in the colon of APC-Min/+ mice due to an increase in phospho-Akt.

Western blot analysis indicated upregulation of activated Akt-P-Thr308 (p-Akt) in APC-Min/+ mice in tumor tissues (polyp), but not in unaffected colonic mucosa (crypt) of APC-Min/+ and wt mice (Fig. 5-7A), suggesting that Akt may play a minor role in activating ENaC in APC-Min/+ mice.

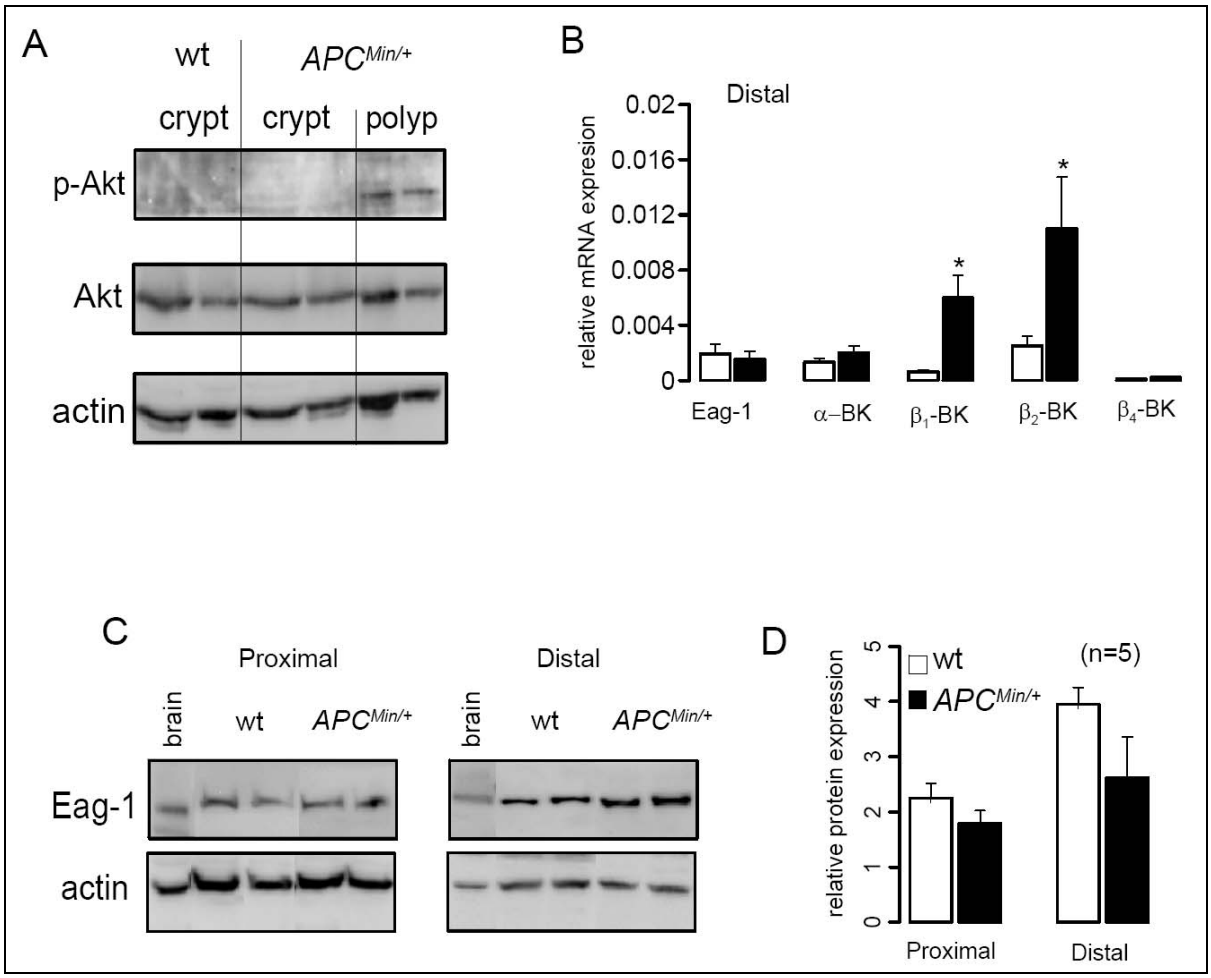

Fig. 5-7 Expression of Akt, Eag1 and BK in the colonic epithelium of APC-Min/+ mice

A) Western blot analysis of Akt and activated phospho-Akt (Akt-P-Thr308) in unaffected mucosa and polyps. B) Results from quantitative analysis of mRNA expression for Eag1 and α/β subunits of BK channels in isolated crypts from distal colon. C) Western blot analysis of expression of Eag1 protein in isolated crypts from proximal and distal colon and D) quantitative comparison between wild type and APC-Min/+ mice. Asterisks indicate significant differences compared to control (Student´s t-test). (Number of mice).

Enhanced K^+ channel activity in APC-Min/+ mice is not due to upregulation of BKα or Eag1

Currents through voltage gated Eag1 and large conductance Ca^{2+} activated BK channels are enhanced in the colon of APC-Min/+ mice (Fig. 5-3D). Using real time RT-PCR, we found no increase in mRNA expression of the channel forming BKα subunit or Eag1 in APC-Min/+ mice (Fig. 5-7B). Similarly, expression of Eag1 protein was unchanged in APC-Min/+ animals (Fig. 5-7C,D), and no obvious difference was found for BKα localized in the membrane of colonic crypt cells of wt and APC-Min/+ (supplement 4). However, for BK channels the regulatory β1- and β2-subunits were found to be upregulated in the distal colon of APC-Min/+ mice (Fig. 5-7B), which probably explains the enhanced Ca^{2+} activated K^+ currents in the distal colon of APC-Min/+ mice (Fig. 5-3D).

Discussion

Mutations in the APC gene reduce apoptosis and cause colonic cancer

According to the classical Knudson' two hit model both alleles of a tumor suppressor gene need to be mutated to trigger cancer. In contrast haploinsufficieny predicts a gene dosage effect along with additional oncogenic mutations, loss of tumor suppressors or epigenetic changes that are required for tumor formation (134). Heterozygous mutations in the gene encoding the adenomatosis polyposis coli (APC) protein are found at early stages of sporadic colorectal cancers, and are the cause for familial adenomatosis polyposis (135, 136). APC has a clear role in mediating phosphorylation and degradation of ß-catenin. Consequently loss of APC leads to accumulation of ß-catenin at adherens junctions and reduced ability of epithelial cells to traverse the crypts. APC mutations inhibit apoptosis by allowing constitutive survivin expression. Thus the cells remain in the crypts for an extended period of time, with the potential to receive additional toxic signals (137). Genetic instability of those crypt cells is reflected by a high anaphase bridge index with enhanced tolerance (136, 138).

APC-Min reduced apoptosis and enhanced Na^+ absorption

We analyzed changes in colonic ion transport occurring in heterozygous APC-Min/+ mice, since previous reports suggested a role of ion channels for cell proliferation and tumor formation (6). The remarkable upregulation of colonic Na^+ absorption in APC-Min/+ animals may be due to several reasons. i) Obviously the mammalian target of the rapamycin (mTOR) pathway is upregulated in APC-Min/+, which may lead to enhanced transcription of α,β,γ-ENaC subunits (139). Notably in preliminary experiments with APC-Min/+ animals, which received the mTOR inhibitor rapamycin Na^+ absorption and abnormal K^+ channel expression was abolished (unpublished from the authors laboratory). ii) Although cytosolic accumulation

of ß-catenin and Akt-p-Thr308 were only observed in adenomas (130, 131), low levels of Akt-p-Thr308 in normal crypts of APC-Min/+ mice may contribute to enhanced ENaC activity, due to a mechanism that involves phosphorylation of the ubiquitin ligase Nedd4-2 by Akt (133). iii) Expression of ENaC increases with differentiation and aging of the cells present in the surface epithelium. Reduced apoptosis in APC-Min/+ may expand the pool of ENaC expressing epithelial cells in the surface epithelium and the upper crypt.

Role of Na^+ absorption in colonic cancer

In the present study the animals received a chow enriched with highly saturated lipids, known to promote epithelial lesions and neoplasia (140). High fat/low fiber diet is often accompanied by constipation representing another cancer promoting factor (141), although the role of chronic constipation for cancer development is discussed controversially (142, 143). On the other hand, colonic polyposis and colorectal cancer is often accompanied by stool irregularities and constipation (144). The augmented Na^+ absorption in APC-Min/+ mice is likely to cause dehydration of the feces and constipation. Occasionally we observed symptoms of intestinal occlusion and rectal prolaps in APC-Min/+ animals. Another mouse model of colonic carcinogenesis that made use of chemical carcinogens, also produced enhanced Na^+ absorption (145). However reduced Na^+ absorption has been found during acute application of the carcinogens, probably due to induction of an inflammation (60, 129). Colonic inflammation like in ulcerative colitis has been shown to reduce electrogenic Na^+ transport and ENaC expression (146, 147).

Enhanced Eag1 and Ca^{2+} activated K^+ currents in APC-Min/+ mice

Apart from the change in Na^+ absorption, we present evidence for upregulation of potassium currents in the colonic epithelium of APC-Min/+ mice. These Eag1 and BK channels were shown to support proliferation of colonic cancer cells in vitro, and are expressed in samples of human colorectal cancer as well as colonic epithelium of carcinogen treated mice (6, 16, 41, 44, 60, 88). The present results provide further evidence for a contribution of K^+ currents to development of cancer (6). How are these channels activated by APC, since we did not detect a change in transcripts or total protein for Eag1. It is likely that Eag1 is regulated by ß-catenin or Akt, since a close member of the same family of voltage gated K^+ channels, Erg, has been shown to be activated by Akt (148). It is know that mutations in the APC gene alter cell cycle regulation, probably through upregulation of Erk-signaling (149). Since Eag1 is a cell cycle regulated K^+ channel, it is likely that these changes affect Eag1 activity.

Upregulation of Akt may also increase the activity of Ca^{2+} activated K^+ cannels, since membrane trafficking of BK channels was shown to be enhanced by Akt in a PI3-kinase

dependent manner in neurons (150). PI3-kinase dependent regulation of BK was also found in mouse distal colon (55). Apart from that BKβ1 and BKβ2 subunits were largely increased in the distal colon of APC-Min/+ animals (Fig. 5-7). Both channel subunits are known to increase apparent Ca^{2+} and estradiol sensitivity of BK channels (151). Taken together, enhanced activity of cell cycle regulated Eag1 channels and large conductance Ca^{2+} activated K^+ channels are closely correlated with malignancy, and are associated with adverse outcome and reduced overall survival of patients (60). Thus the present results may provide a basis for new therapeutic strategies for the treatment of colonic cancer.

References

1. Burt, R. W., Lipkin, M. (1992) Gastrointestinal cancer. In the genetic basis of common diseases. *Oxford: Oxford University Press.* 650-680

2. Parker, S. L., Tong, T., Bolden, S., Wingo, P. A. (1997) Cancer statistics 1997. *CA Cancer J.Clin.* **47,** 5-27

3. Kinzler, K. W., Vogelstein, B. (1996) Lessons from hereditary colorectal cancer. *Cell.* **87,** 159-170

4. Wasan, H. S., Novelli, M., Bee, J., Bodmer, W. F. (1997) Dietary fat influences on polyp phenotype in multiple intestinal neoplasia mice. *Proc. Natl. Acad. Sci. U.S.A.* **94,** 3308-3313

5. Lehmann-Horn, F., Jurkat-Rott, K. (1999) Voltage-gated ion channels and hereditary disease. *Physiol. Rev.* **79,** 1317-1372

6. Kunzelmann, K. (2005) Ion channels and cancer. *J. Membr. Biol.* **205,** 159-173

7. Kunzelmann, K., Mall, M. (2002) Electrolyte transport in the colon: Mechanisms and implications for disease. *Physiological Reviews.* **82,** 245-289

8. Nathke, I. (2006) Cytoskeleton out of the cupboard: colon cancer and cytoskeletal changes induced by loss of APC. *Nat. Rev. Cancer.* **6,** 967-974

9. Debongnie, J. C., Phillips, S. F. (1978) Capacity of the human colon to absorb fluid. *Gastroenterology.* **74,** 698-703

10. Ho, S. B. (1992) Cytoskeleton and other differentiation markers in the colon. *J Cell Biochem. Suppl.* **16G,** 119-128

11. Köckerling, A., Sorgenfrei, D., Fromm, M. (1993) Electrogenic Na^+ absorption of rat distal colon is confined to surface epithelium: a voltage-scanning study. *Am. J. Physiol.* **264,** C1285-C1293

12. Senda, T., Iizuka-Kogo, A., Onouchi, T., Shimomura, A. (2007) Adenomatous polyposis coli (APC) plays multiple roles in the intestinal and colorectal epithelia. *Med. Mol. Morphol.* **40,** 68-81

13. Chandy, K. G., Gutman, G. A. (1993) Nomenclature for mammalian potassium channel genes. *Trends Pharmacol. Sci.* **14,** 434

14. Wang, Z. (2004) Roles of K^+ channels in regulating tumour cell proliferation and apoptosis. *Pflugers Arch.* **448,** 274-286

15. Wonderlin, W. F., Strobl, J. S. (1996) Potassium channels, proliferation and G1 progression. *J. Membr. Biol.* **154,** 91-107

16. Lastraioli, E., Guasti, L., Crociani, O., Polvani, S., Hofmann, G., Witchel, H., Bencini, L., Calistri, M., Messerini, L., Scatizzi, M., Moretti, R., Wanke, E., Olivotto, M., Mugnai, G., Arcangeli, A. (2004) herg1 gene and HERG1 protein are overexpressed in colorectal cancers and regulate cell invasion of tumor cells. *Cancer Res.* **64,** 606-611

17. Ghiani, C. A., Yuan, X., Eisen, A. M., Knutson, P. L., DePinho, R. A., McBain, C. J., Gallo, V. (1999) Voltage-activated K^+ channels and membrane depolarization regulate accumulation of the cyclin-dependent kinase inhibitors p27(Kip1) and p21(CIP1) in glial progenitor cells. *J. Neurosci.* **19,** 5380-5392

18. Bauer, C. K., Schwarz, J. R. (2001) Physiology of eag K^+ channels. *J. Membr. Biol.* **182,** 1-15

19. Pardo, L. A., del Camino, D., Sanchez, A., Alves, F., Brüggemann, A., Beckh, S., Stühmer, W. (1999) Oncogenic potential of EAG K^+ channels. *EMBO J.* **18,** 5540-5547

20. Hofmann, G., Bernabei, P. A., Crociani, O., Cherubini, A., Guasti, L., Pillozzi, S., Lastraioli, E., Polvani, S., Bartolozzi, B., Solazzo, V., Gragnani, L., Defilippi, P., Rosati, B., Wanke, E., Olivotto, M., Arcangeli, A. (2001) HERG K^+ channels activation during beta(1) integrin-mediated adhesion to fibronectin induces an up-regulation of alpha(v)beta(3) integrin in the preosteoclastic leukemia cell line FLG 29.1. *J. Biol. Chem.* **276,** 4923-4931

21. Bianchi, L., Wible, B., Arcangeli, A., Taglialatela, M., Morra, F., Castaldo, P., Crociani, O., Rosati, B., Faravelli, L., Olivotto, M., Wanke, E. (1998) herg encodes a K^+ current highly conserved in tumors of different histogenesis: a selective advantage for cancer cells? *Cancer Res.* **58,** 815-822

22. Cherubini, A., Taddei, G. L., Crociani, O., Paglierani, M., Buccoliero, A. M., Fontana, L., Noci, I., Borri, P., Borrani, E., Giachi, M., Becchetti, A., Rosati, B., Wanke, E., Olivotto, M., Arcangeli, A. (2000) HERG potassium channels are more frequently expressed in human endometrial cancer as compared to non-cancerous endometrium. *Br. J. Cancer.* **83,** 1722-1729

23. Pillozzi, S., Brizzi, M. F., Balzi, M., Crociani, O., Cherubini, A., Guasti, L., Bartolozzi, B., Becchetti, A., Wanke, E., Bernabei, P. A., Olivotto, M., Pegoraro, L., Arcangeli, A. (2002) HERG potassium channels are constitutively expressed in primary human acute myeloid leukemias and regulate cell proliferation of normal and leukemic hemopoietic progenitors. *Leukemia.* **16,** 1791-1798

24. Smith, G. A., Tsui, H. W., Newell, E., Jiang, X., Zhu, X. P., Tsui, F. W., Schlichter, L. C. (2002) Functional up-regulation of HERG K^+ channels in neoplastic hematopoietic cells. *J. Biol. Chem.* **277,** 18528-18534

25. Zou, A., Lin, Z., Humble, M., Creech, C. D., Wagoner, P. K., Krafte, D., Jegla, T. J., Wickenden, A. D. (2003) Distribution and functional properties of human KCNH8 (Elk1) potassium channels. *Am. J. Physiol. Cell Physiol.* **285,** C1356-C1366

26. Takayama, T., Miyanishi, K., Hayashi, T., Sato, Y., Niitsu, Y. (2006) Colorectal cancer: genetics of development and metastasis. *J. Gastroenterol.* **41,** 185-192

27. Ionov, Y., Peinado, M. A., Malkhosyan, S., Shibata, D., Perucho, M. (1993) Ubiquitous somatic mutations in simple repeated sequences reveal a new mechanism for colonic carcinogenesis. *Nature.* **363,** 558-561

28. Thibodeau, S. N., Bren, G., Schaid, D. (1993) Microsatellite instability in cancer of the proximal colon. *Science.* **260,** 816-819

29. Aaltonen, L. A., Peltomaki, P., Leach, F. S., Sistonen, P., Pylkkanen, L., Mecklin, J. P., Jarvinen, H., Powell, S. M., Jen, J., Hamilton, S. R., . (1993) Clues to the pathogenesis of familial colorectal cancer. *Science.* **260,** 812-816

30. Lindblom, A., Tannergard, P., Werelius, B., Nordenskjold, M. (1993) Genetic mapping of a second locus predisposing to hereditary non-polyposis colon cancer. *Nat. Genet.* **5,** 279-282

31. Fearon, E. R., Vogelstein, B. (1990) A genetic model for colorectal tumorigenesis. *Cell.* **61,** 759-767

32. Yeo, C. J. (1999) Tumor suppressor genes: a short review. *Surgery.* **125,** 363-366

33. van Es, J. H., Giles, R. H., Clevers, H. C. (2001) The many faces of the tumor suppressor gene APC. *Exp. Cell Res.* **264,** 126-134

34. Midgley, C. A., White, S., Howitt, R., Save, V., Dunlop, M. G., Hall, P. A., Lane, D. P., Wyllie, A. H., Bubb, V. J. (1997) APC expression in normal human tissues. *J. Pathol.* **181,** 426-433

35. Polakis, P. (1997) The adenomatous polyposis coli (APC) tumor suppressor. *Biochim. Biophys. Acta.* **1332,** F127-F147

36. Clarke, A. R. (2005) Studying the consequences of immediate loss of gene function in the intestine: APC. *Biochem. Soc. Trans.* **33,** 665-666

37. Fiala, E. S. (1977) Investigations into the metabolism and mode of action of the colon carcinogens 1,2-dimethylhydrazine and azoxymethane. *Cancer.* **40,** 2436-2445

38. Moser, A. R., Pitot, H. C., Dove, W. F. (1990) A dominant mutation that predisposes to multiple intestinal neoplasia in the mouse. *Science.* **247,** 322-324

39. Fodde, R., Smits, R. (2001) Disease model: familial adenomatous polyposis. *Trends Mol. Med.* **7,** 369-373

40. Dietrich, W. F., Lander, E. S., Smith, J. S., Moser, A. R., Gould, K. A., Luongo, C., Borenstein, N., Dove, W. (1993) Genetic identification of Mom-1, a major modifier locus affecting Min-induced intestinal neoplasia in the mouse. *Cell.* **75,** 631-639

41. Pardo, L. A. (2004) Voltage-gated potassium channels in cell proliferation. *Physiology (Bethesda.)* **19,** 285-292

42. Stuhmer, W., Alves, F., Hartung, F., Zientkowska, M., Pardo, L. A. (2006) Potassium channels as tumour markers. *FEBS Lett.* **580,** 2850-2852

43. Schonherr, R. (2005) Clinical relevance of ion channels for diagnosis and therapy of cancer. *J. Membr. Biol.* **205,** 175-184

44. Spitzner, M., Ousingsawat, J., Scheidt, K., Kunzelmann, K., Schreiber, R. (2007) Role of voltage gated K^+ channels for proliferation of colonic cancer cells. *FASEB J.* **21,** 35-44

45. Kunzelmann, K., Milenkovic, V. M., Spitzner, M., Barro Soria, R., Schreiber, R. (2007) Calcium dependent chloride conductance in epithelia: Is there a contribution by Bestrophin? *Pflügers Arch. (in press)*

46. Pauli, B. U., Abdel-Ghany, M., Cheng, H. C., Gruber, A. D., Archibald, H. A., Elble, R. C. (2000) Molecular characteristics and functional diversity of CLCA family members. *Clin. Exp. Pharmacol. Physiol.* **27,** 901-905

47. Jentsch, T. J., Stein, V., Weinreich, F., Zdebik, A. A. (2001) Molecular structure and physiological function of chloride channels. *Physiol. Rev.* **82,** 503-568

48. Sun, H., Tsunenari, T., Yau, K. W., Nathans, J. (2001) The vitelliform macular dystrophy protein defines a new family of chloride channels. *Proc. Natl. Acad. Sci. U.S.A.* **99,** 4008-4013

49. Qu, Z., Fischmeister, R., Hartzell, H. C. (2004) Mouse bestrophin-2 is a bona fide Cl^- channel: identification of a residue important in anion binding and conduction. *J. Gen. Physiol.* **123,** 327-340

50. Tsunenari, T., Sun, H., Williams, J., Cahill, H., Smallwood, P., Yau, K. W., Nathans, J. (2003) Structure-function analysis of the bestrophin family of anion channels. *J. Biol. Chem.* **278,** 41114-41125

51. Rosenthal, R., Bakall, B., Kinnick, T., Peachey, N., Wimmers, S., Wadelius, C., Marmorstein, A. D., Strauss, O. (2005) Expression of bestrophin-1, the product of the VMD2 gene, modulates voltage-dependent Ca^{2+} channels in retinal pigment epithelial cells. *FASEB J.* **20,** 178-180

52. Barro Soria, R., Spitzner, M., Schreiber, R., Kunzelmann, K. (2006) Bestrophin 1 enables Ca^{2+} activated Cl^- conductance in epithelia. *J. Biol. Chem. (in press)*

53. Pardo, L. A., Contreras-Jurado, C., Zientkowska, M., Alves, F., Stuhmer, W. (2005) Role of voltage-gated potassium channels in cancer. *J. Membr. Biol.* **205,** 115-124

54. Dharmsathaphorn, K., McRoberts, J. A., Mandel, K. G., Tisdale, L. D., Masui, H. (1984) A human colonic tumor cell line that maintains vectorial electrolyte transport. *Am. J. Physiol.* **246,** G204-G208

55. Puntheeranurak, S., Schreiber, R., Kunzelmann, K., Krishnamra, N. (2007) Control of ion transport in mouse proximal and distal colon by prolactin. *Cell Physiol. Biochem.* **19,** 77-88

56. Schwab, A., Wojnowski, L., Gabriel, K., Oberleithner, H. (1994) Oscillating activity of a Ca^{2+}-sensitive K^+ channel. A prerequisite for migration of transformed Madin-Darby canine kidney focus cells. *J. Clin. Invest.* **93,** 1631-1636

57. Alessandro, R., Flugy, A. M., Russo, D., Stassi, G., De Leo, A., Corrado, C., Alaimo, G., De Leo, G. (2005) Identification and phenotypic characterization of a subpopulation of T84 human colon cancer cells, after selection on activated endothelial cells. *J. Cell Physiol.* **203,** 261-272

58. Boyd, D. D., Wang, H., Avila, H., Parikh, N. U., Kessler, H., Magdolen, V., Gallick, G. E. (2004) Combination of an SRC kinase inhibitor with a novel pharmacological antagonist of the urokinase receptor diminishes in vitro colon cancer invasiveness. *Clin. Cancer Res.* **10,** 1545-1555

59. Szabo, I., Gulbins, E., Apfel, H., Zhang, X., Barth, P., Busch, A. E., Schlottmann, K., Pongs, O., Lang, F. (1996) Tyrosine phosphorylation-dependent suppression of a voltage-gated K^+ channel in T lymphocytes upon Fas stimulation. *J. Biol. Chem.* **271,** 20465-20469

60. Ousingsawat, J., Spitzner, M., Puntheeranurak, S., Terracciano, L., Tornillo, L., Bubendorf, L., Kunzelmann, K., Schreiber, R. (2007) Expression of voltage gated potassium channels in human and mouse colonic carcinoma. *Clinical Cancer Research.* **13,** 824-831

61. Schwab, A. (2001) Ion channels and transporters on the move. *News Physiol. Sci.* **16,** 29-33

62. Rao, J. N., Platoshyn, O., Li, L., Guo, X., Golovina, V. A., Yuan, J. X., Wang, J. Y. (2002) Activation of K^+ channels and increased migration of differentiated intestinal epithelial cells after wounding. *Am. J. Physiol. Cell Physiol.* **282,** C885-C898

63. Fischmeister, R., Hartzell, H. C. (2005) Volume sensitivity of the bestrophin family of chloride channels. *J. Physiol.* **562,** 477-491

64. O'Grady, S. M., Lee, S. Y. (2005) Molecular diversity and function of voltage-gated (Kv) potassium channels in epithelial cells. *Int. J. Biochem. Cell Biol.* **37,** 1578-1594

65. Abdul, M., Hoosein, N. (2002) Voltage-gated potassium ion channels in colon cancer. *Oncol. Rep.* **9,** 961-964

66. Schonherr, R. (2005) Clinical relevance of ion channels for diagnosis and therapy of cancer. *J. Membr. Biol.* **205,** 175-184

67. Conti, M. (2004) Targeting K^+ channels for cancer therapy. *J. Exp. Ther. Oncol.* **4,** 161-166

68. Ahn, S., Nelson, C. D., Garrison, T. R., Miller, W. E., Lefkowitz, R. J. (2003) Desensitization, internalization, and signaling functions of beta-arrestins demonstrated by RNA interference. *Proc. Natl. Acad. Sci. U.S.A.* **100,** 1740-1744

69. Baxter, D. F., Kirk, M., Garcia, A. F., Raimondi, A., Holmqvist, M. H., Flint, K. K., Bojanic, D., Distefano, P. S., Curtis, R., Xie, Y. (2002) A novel membrane potential-sensitive fluorescent dye improves cell-based assays for ion channels. *J. Biomol. Screen.* **7,** 79-85

70. Lal, A., Lash, A. E., Altschul, S. F., Velculescu, V., Zhang, L., McLendon, R. E., Marra, M. A., Prange, C., Morin, P. J., Polyak, K., Papadopoulos, N., Vogelstein, B., Kinzler, K. W., Strausberg, R. L., Riggins, G. J. (1999) A public database for gene expression in human cancers. *Cancer Res.* **59,** 5403-5407

71. Patel, A. J., Maingret, F., Magnone, V., Fosset, M., Lazdunski, M., Honore, E. (2000) TWIK-2, an inactivating 2P domain K^+ channel. *J. Biol. Chem.* **275,** 28722-28730

72. Grace, A. A., Camm, A. J. (1998) Quinidine. *N. Engl. J. Med.* **338,** 35-45

73. Diochot, S., Schweitz, H., Beress, L., Lazdunski, M. (1998) Sea anemone peptides with a specific blocking activity against the fast inactivating potassium channel Kv3.4. *J. Biol. Chem.* **273,** 6744-6749

74. Garcia-Ferreiro, R. E., Kerschensteiner, D., Major, F., Monje, F., Stühmer, W., Pardo, L. A. (2004) Mechanism of Block of hEag1 K^+ Channels by Imipramine and Astemizole. *J. Gen. Physiol.* **124,** 301-317

75. Cao, Y. J., Dreixler, J. C., Couey, J. J., Houamed, K. M. (2002) Modulation of recombinant and native neuronal SK channels by the neuroprotective drug riluzole. *Eur. J. Pharmacol.* **449,** 47-54

76. Ousingsawat, J., Spitzner, M., Puntheeranurak, S., Terracciano, L., Tornillo, L., Bubendorf, L., Kunzelmann, K., Schreiber, R. (2006) Expression of voltage gated potassium channels in human and mouse colonic carcinoma. *Clinical Cancer Research. (submitted)*

77. Wakabayashi, S., Shigekawa, M., Pouyssegur, J. (1997) Molecular physiology of vertebrate Na^+/H^+ exchangers. *Physiological Reviews.* **77,** 51-74

78. Kahl, C. R., Means, A. R. (2003) Regulation of cell cycle progression by calcium/calmodulin-dependent pathways. *Endocr. Rev.* **24,** 719-736

79. Schreiber, R. (2005) Ca^{2+} signaling, intracellular pH and cell volume in cell proliferation. *J. Membr. Biol.* **205,** 129-137

80. Kazerounian, S., Pitari, G. M., Shah, F. J., Frick, G. S., Madesh, M., Ruiz-Stewart, I., Schulz, S., Hajnoczky, G., Waldman, S. A. (2005) Proliferative signaling by store-operated calcium channels opposes colon cancer cell cytostasis induced by bacterial enterotoxins. *J. Pharmacol. Exp. Ther.* **314,** 1013-1022

81. Fischer, K. G., Leipziger, J., Rubini-Illes, P., Nitschke, R., Greger, R. (1996) Attenuation of stimulated Ca^{2+} influx in colonic epithelial (HT29) cells by cAMP. *Pflugers Arch.* **432,** 735-740

82. Wang, X. T., Nagaba, Y., Cross, H. S., Wrba, F., Zhang, L., Guggino, S. E. (2000) The mRNA of L-type calcium channel elevated in colon cancer: protein distribution in normal and cancerous colon. *Am. J. Pathol.* **157,** 1549-1562

83. Abdul, M., Hoosein, N. (2002) Expression and activity of potassium ion channels in human prostate cancer. *Cancer Lett.* **186,** 99-105

84. Suzuki, T., Takimoto, K. (2004) Selective expression of HERG and Kv2 channels influences proliferation of uterine cancer cells. *Int. J. Oncol.* **25,** 153-159

85. Patt, S., Preussat, K., Beetz, C., Kraft, R., Schrey, M., Kalff, R., Schonherr, K., Heinemann, S. H. (2004) Expression of ether a go-go potassium channels in human gliomas. *Neurosci. Lett.* **368,** 249-253

86. Elso, C. M., Lu, X., Culiat, C. T., Rutledge, J. C., Cacheiro, N. L., Generoso, W. M., Stubbs, L. J. (2004) Heightened susceptibility to chronic gastritis, hyperplasia and metaplasia in Kcnq1 mutant mice. *Hum. Mol. Genet.* **13,** 2813-2821

87. Czarnecki, A., Dufy-Barbe, L., Huet, S., Odessa, M. F., Bresson-Bepoldin, L. (2003) Potassium channel expression level is dependent on the proliferation state in the GH3 pituitary cell line. *Am. J. Physiol. Cell Physiol.* **284,** C1054-C1064

88. Yao, X., Kwan, H. Y. (1999) Activity of voltage-gated K^+ channels is associated with cell proliferation and Ca^{2+} influx in carcinoma cells of colon cancer. *Life Sci.* **65,** 55-62

89. Patel, A. J., Lazdunski, M. (2004) The 2P-domain K^+ channels: role in apoptosis and tumorigenesis. *Pflugers Arch.* **448,** 261-273

90. Mu, D., Chen, L., Zhang, X., See, L. H., Koch, C. M., Yen, C., Tong, J. J., Spiegel, L., Nguyen, K. C., Servoss, A., Peng, Y., Pei, L., Marks, J. R., Lowe, S., Hoey, T., Jan, L. Y., McCombie, W. R., Wigler, M. H., Powers, S. (2003) Genomic amplification and oncogenic properties of the KCNK9 potassium channel gene. *Cancer Cell.* **3,** 297-302

91. Klimatcheva, E., Wonderlin, W. F. (1999) An ATP-sensitive K^+ current that regulates progression through early G1 phase of the cell cycle in MCF-7 human breast cancer cells. *J. Membr. Biol.* **171,** 35-46

92. Abdul, M., Hoosein, N. (2002) Voltage-gated sodium ion channels in prostate cancer: expression and activity. *Anticancer Res.* **22,** 1727-1730

93. Chang, K. W., Yuan, T. C., Fang, K. P., Yang, F. S., Liu, C. J., Chang, C. S., Lin, S. C. (2003) The increase of voltage-gated potassium channel Kv3.4 mRNA expression in oral squamous cell carcinoma. *J. Oral Pathol. Med.* **32,** 606-611

94. Farias, L. M., Ocana, D. B., Diaz, L., Larrea, F., Avila-Chavez, E., Cadena, A., Hinojosa, L. M., Lara, G., Villanueva, L. A., Vargas, C., Hernandez-Gallegos, E., Camacho-Arroyo, I., Duenas-Gonzalez, A., Perez-Cardenas, E., Pardo, L. A., Morales, A., Taja-Chayeb, L., Escamilla, J., Sanchez-Pena, C., Camacho, J. (2004) Ether a go-go potassium channels as human cervical cancer markers. *Cancer Res.* **64,** 6996-7001

95. Arcangeli, A., Bianchi, L., Becchetti, A., Faravelli, L., Coronnello, M., Mini, E., Olivotto, M., Wanke, E. (1995) A novel inward-rectifying K^+ current with a cell-cycle dependence governs the resting potential of mammalian neuroblastoma cells. *J. Physiol.* **489,** 455-471

96. Peres, A., Zippel, R., Sturani, E. (1988) Serum induces the immediate opening of Ca^{2+}-activated channels in quiescent human fibroblasts. *FEBS Lett.* **241,** 164-168

97. Rutili, G., Arfors, K. E. (1977) Protein concentration in interstitial and lymphatic fluids from the subcutaneous tissue. *Acta Physiol. Scand.* **99,** 1-8

98. Lang, F., Gulbins, E., Szabo, I., Lepple-Wienhues, A., Huber, S. M., Duranton, C., Lang, K. S., Lang, P. A., Wieder, T. (2004) Cell volume and the regulation of apoptotic cell death. *J. Mol. Recognit.* **17,** 473-480

99. Elbashir, S. M., Harborth, J., Lendeckel, W., Yalcin, A., Weber, K., Tuschl, T. (2001) Duplexes of 21-nucleotide RNAs mediate RNA interference in cultured mammalian cells. *Nature.* **411,** 494-498

100. Pei, L., Wiser, O., Slavin, A., Mu, D., Powers, S., Jan, L. Y., Hoey, T. (2003) Oncogenic potential of TASK3 (Kcnk9) depends on K^+ channel function. *Proc. Natl. Acad. Sci. U.S.A.* **100,** 7803-7807

101. Nitschke, R., Riedel, A., Ricken, S., Leipziger, J., Benning, N., Fischer, K., Greger, R. (1996) The effect of intracellular pH on cytosolic Ca^{2+} in HT_{29} cells. *Pflügers Arch.* **433,** 98-108

102. Kunzelmann, K. (2005) Ion channels and cancer. *J.Membr.Biol.* **205,** 159-173

103. Pardo, L. A. (2004) Voltage-gated potassium channels in cell proliferation. *Physiology (Bethesda)***, 19,** 285-292

104. Pardo, L. A., Contreras-Jurado, C., Zientkowska, M., Alves, F., Stuhmer, W. (2006) Role of voltage-gated potassium channels in cancer. *J. Membr. Biol.* **205,** 115-124

105. Camacho, J. (2006) Ether a go-go potassium channels and cancer. *Cancer Lett.* **233,** 1-9

106. Wonderlin, W. F. and Strobl, J. S. (1996) Potassium channels, proliferation and G1 progression. *J. Membr. Biol.* **154,** 91-107

107. Farias, L. M., Ocana, D. B., Diaz, L., Larrea, F., Avila-Chavez, E., Cadena, A., Hinojosa, L. M., Lara, G., Villanueva, L. A., Vargas, C., Hernandez-Gallegos, E., Camacho-Arroyo, I., Duenas-Gonzalez, A., Perez-Cardenas, E., Pardo, L. A., Morales, A., Taja-Chayeb, L., Escamilla, J., Sanchez-Pena, C., and Camacho, J.

(2004) Ether a go-go potassium channels as human cervical cancer markers. *Cancer Res.* **64,** 6996-7001

108. Pardo, L. A., del Camino, D., Sanchez, A., Alves, F., Bruggemann, A., Beckh, S., and Stuhmer, W. (1999) Oncogenic potential of EAG K^+ channels. *EMBO J.* **18,** 5540-5547

109. Schreiber, R. (2005) Ca^{2+} signaling, intracellular pH and cell volume in cell proliferation. *J. Membr. Biol.* **205,** 129-137

110. Fiala, E. S. (1977) Investigations into the metabolism and mode of action of the colon carcinogens 1,2-dimethylhydrazine and azoxymethane. *Cancer.* **40,** 2436-2445

111. Frei, J. V., Swenson, D. H., Warren, W., and Lawley, P. D. (1978) Alkylation of deoxyribonucleic acid in vivo in various organs of C57BL mice by the carcinogens N-methyl-N-nitrosourea, N-ethyl-N-nitrosourea and ethyl methanesulphonate in relation to induction of thymic lymphoma. Some applications of high-pressure liquid chromatography. *Biochem. J.* **174,** 1031-1044

112. Narisawa, T., Wong, C. Q., Maronpot, R. R., and Weisburger, J. H. (1976) Large bowel carcinogenesis in mice and rats by several intrarectal doses of methylnitrosourea and negative effect of nitrite plus methylurea. *Cancer Res.* **36,** 505-510

113. Davies, R. J., Weidema, W. F., Sandle, G. I., Palmer, L., Deschner, E. E., and DeCosse, J. J. (1987) Sodium transport in a mouse model of colonic carcinogenesis. *Cancer Res.* **47,** 4646-4650

114. Bleich, M., Ecke, D., Schwartz, B., Fraser, G., and Greger, R. (1997) Effects of the carcinogen dimethylhydrazine (DMH) on the function of rat colonic crypts. *Pflügers Arch.* **433,** 254-259

115. Kononen, J., Bubendorf, L., Kallioniemi, A., Barlund, M., Schraml, P., Leighton, S., Torhorst, J., Mihatsch, M. J., Sauter, G., and Kallioniemi, O. P. (1998) Tissue microarrays for high-throughput molecular profiling of tumor specimens. *Nat. Med.* **4,** 844-847

116. Sobin, L. W. C. (2002) UICC, TNM Classification of malignant tumors. *New York, Wiley*.

117. Diwan, B. A. and Blackman, K. E. (1980) Differential susceptibility of 3 sublines of C57BL/6 mice to the induction of colorectal tumors by 1,2-dimethylhydrazine. *Cancer Lett.* **9,** 111-115

118. Greene, F. L., Lamb, L. S., and Barwick, M. (1987) Colorectal cancer in animal models - a review. *J. Surg. Res.* **43,** 476-487

119. Yang, J., Shikata, N., Mizuoka, H., and Tsubura, A. (1996) Colon carcinogenesis in shrews by intrarectal infusion of N-methyl-N-nitrosourea. *Cancer Lett.* **110,** 105-112

120. Davies, R. J., Sandle, G. I., and Thompson, S. M. (1991) Inhibition of the Na^+, K^+-ATPase pump during induction of experimental colon cancer. *Cancer Biochem. Biophys.* **12,** 81-94

121. Abdul, M. and Hoosein, N. (2002) Voltage-gated potassium ion channels in colon cancer. *Oncol. Rep.* **9,** 961-964

122. Preussat, K., Beetz, C., Schrey, M., Kraft, R., Wolfl, S., Kalff, R., and Patt, S. (2003) Expression of voltage-gated potassium channels Kv1.3 and Kv1.5 in human gliomas. *Neurosci. Lett.* **346,** 33-36

123. Grissmer, S., Nguyen, A. N., Aiyar, J., Hanson, D. C., Mather, R. J., Gutman, G. A., Karmilowicz, M. J., Auperin, D. D., and Chandy, K. G. (1994) Pharmacological characterization of five cloned voltage-gated K^+ channels, types Kv1.1, 1.2, 1.3, 1.5, and 3.1, stably expressed in mammalian cell lines. *Mol. Pharmacol.* **45,** 1227-1234

124. Chang, K. W., Yuan, T. C., Fang, K. P., Yang, F. S., Liu, C. J., Chang, C. S., and Lin, S. C. (2003) The increase of voltage-gated potassium channel Kv3.4 mRNA expression in oral squamous cell carcinoma. *J. Oral Pathol. Med.* **32,** 606-611

125. Stuhmer, W., Alves, F., Hartung, F., Zientkowska, M., Pardo, L. A. (2006) Potassium channels as tumour markers. *FEBS Lett.* **580,** 2850-2852

126. Mu, D., Chen, L., Zhang, X., See, L. H., Koch, C. M., Yen, C., Tong, J. J., Spiegel, L., Nguyen, K. C., Servoss, A., Peng, Y., Pei, L., Marks, J. R, Lowe, S., Hoey, T., Jan, L. Y., McCombie, W. R., Wigler, M. H., and Powers, S. (2003) Genomic amplification and oncogenic properties of the KCNK9 potassium channel gene. *Cancer Lett.* **3,** 297-302

127. Bloch, M., Ousingsawat, J., Simon, R., Gasser, T. C., Mihatsch, M. J., Kunzelmann, K., Bubendorf, L. (2005) KCNMA1 gene amplification promotes tumor cell proliferation in prostate cancer. *Oncogen.* **26,** 2525-2534

128. Fodde, R., Edelmann, W., Yang, K., van Leeuwen, C., Carlson, C., Renault, B., Breukel, C., Alt, E., Lipkin, M., Khan, P. M., . (1994) A targeted chain-termination mutation in the mouse Apc gene results in multiple intestinal tumors. *Proc. Natl. Acad. Sci. U.S.A.* **91,** 8969-8973

129. Bleich, M., Ecke, D., Schwartz, B., Fraser, G., Greger, R. (1997) Effects of the carcinogen dimethylhydrazine (DMH) on the function of rat colonic crypts. *Pflügers Arch.* **433,** 254-259

130. Kongkanuntn, R., Bubb, V. J., Sansom, O. J., Wyllie, A. H., Harrison, D. J., Clarke, A. R. (1999) Dysregulated expression of beta-catenin marks early neoplastic change in Apc mutant mice, but not all lesions arising in Msh2 deficient mice. *Oncogene.* **18,** 7219-7225

131. Moran, A. E., Hunt, D. H., Javid, S. H., Redston, M., Carothers, A. M., Bertagnolli, M. M. (2004) Apc deficiency is associated with increased Egfr activity in the intestinal enterocytes and adenomas of C57BL/6J-Min/+ mice. *J. Biol. Chem.* **279,** 43261-43272

132. Dihlmann, S., Kloor, M., Fallsehr, C., von Knebel, D. M. (2005) Regulation of AKT1 expression by beta-catenin/Tcf/Lef signaling in colorectal cancer cells. *Carcinogenesis.* **26,** 1503-1512

133. Lee, I. A., Dinudom, A., Kumar, S., Cook, D. I. (2007) Akt mediates the effect of insulin on epithelial sodium channels by inhibiting Nedd4-2. *(submitted)*

134. Fodde, R., Smits, R. (2002) Cancer biology. A matter of dosage. *Science.* **298,** 761-763

135. Su, L. K., Kinzler, K. W., Vogelstein, B., Preisinger, A. C., Moser, A. R., Luongo, C., Gould, K. A., Dove, W. F. (1992) Multiple intestinal neoplasia caused by a mutation in the murine homolog of the APC gene. *Science.* **256,** 668-670

136. Nathke, I. (2006) Cytoskeleton out of the cupboard: colon cancer and cytoskeletal changes induced by loss of APC. *Nat. Rev. Cancer.* **6,** 967-974

137. Zhang, T., Otevrel, T., Gao, Z., Gao, Z., Ehrlich, S. M., Fields, J. Z., Boman, B. M. (2001) Evidence that APC regulates survivin expression: a possible mechanism contributing to the stem cell origin of colon cancer. *Cancer Res.* **61,** 8664-8667

138. Aoki, K., Tamai, Y., Horiike, S., Oshima, M., Taketo, M. M. (2003) Colonic polyposis caused by mTOR-mediated chromosomal instability in Apc+/Delta716 Cdx2+/- compound mutant mice. *Nat. Genet.* **35,** 323-330

139. Land, S. C., McTavish, N., and Wilson, S. M. (2007) Modulation of dexamethasone-evoked alpha-ENaC expression by the mammalian target of rapamycin (mTOR). *Acta Physiologica.* **189-S653,** P08-L6-14

140. Rao, C. V., Hirose, Y., Indranie, C., Reddy, B. S. (2001) Modulation of experimental colon tumorigenesis by types and amounts of dietary fatty acids. *Cancer Res.* **61,** 1927-1933

141. Sonnenberg, A., Muller, A. D. (1993) Constipation and cathartics as risk factors of colorectal cancer: a meta-analysis. *Pharmacology.* **47 Suppl 1,** 224-233

142. Kune, G. A., Kune, S., Field, B., Watson, L. F. (1988) The role of chronic constipation, diarrhea, and laxative use in the etiology of large-bowel cancer. Data from the Melbourne Colorectal Cancer Study. *Dis. Colon Rectum.* **31,** 507-512

143. Chan, A. O., Hui, W. M., Leung, G., Tong, T., Hung, I. F., Chan, P., Hsu, A., But, D., Wong, B. C., Lam, S. K., Lam, K. F. (2007) Patients with functional constipation do not have increased prevalence of colorectal cancer precursors. *Gut.* **56,** 451-452

144. Weitz, J., Koch, M., Debus, J., Hohler, T., Galle, P. R., Buchler, M. W. (2005) Colorectal cancer. *Lancet.* **365,** 153-165

145. Davies, R. J., Weidema, W. F., Sandle, G. I., Palmer, L., Deschner, E. E., DeCosse, J. J. (1987) Sodium transport in a mouse model of colonic carcinogenesis. *Cancer Res.* **47,** 4646-4650

146. Barmeyer, C., Harren, M., Schmitz, H., Heinzel-Pleines, U., Mankertz, J., Seidler, U., Horak, I., Wiedenmann, B., Fromm, M., Schulzke, J. D. (2004) Mechanisms of diarrhea in the interleukin-2-deficient mouse model of colonic inflammation. *Am. J. Physiol. Gastrointest. Liver Physiol.* **286,** G244-G252

147. Amasheh, S., Barmeyer, C., Koch, C. S., Tavalali, S., Mankertz, J., Epple, H. J., Gehring, M. M., Florian, P., Kroesen, A. J., Zeitz, M., Fromm, M., Schulzke, J. D. (2004) Cytokine-dependent transcriptional down-regulation of epithelial sodium channel in ulcerative colitis. *Gastroenterology.* **126,** 1711-1720

148. Zhang, Y., Wang, H., Wang, J., Han, H., Nattel, S., Wang, Z. (2003) Normal function of HERG K^+ channels expressed in HEK293 cells requires basal protein kinase B activity. *FEBS Lett.* **534,** 125-132

149. Dikovskaya, D., Schiffmann, D., Newton, I. P., Oakley, A., Kroboth, K., Sansom, O., Jamieson, T. J., Meniel, V., Clarke, A., Nathke, I. S. (2007) Loss of APC induces

polyploidy as a result of a combination of defects in mitosis and apoptosis. *J. Cell Biol.* **176,** 183-195

150. Chae, K. S., Martin-Caraballo, M., Anderson, M., Dryer, S. E. (2005) Akt activation is necessary for growth factor-induced trafficking of functional K_{Ca} channels in developing parasympathetic neurons. *J. Neurophysiol.* **93,** 1174-1182

151. Valverde, M. A., Rojas, P., Amigo, J., Cosmelli, D., Orio, P., Bahamonde, M. I., Mann, G. E., Vergara, C., Latorre, R. (1999) Acute activation of Maxi-K channels (hSlo) by estradiol binding to the beta subunit. *Science.* **285,** 1929-1931

Danksagung

Mein Dank gebührt allen Personen, die zum Gelingen dieser Arbeit beigetragen haben.

Ich möchte mich an dieser Stelle zuerst recht herzlich bei Herrn Prof. Dr. Karl Kunzelmann für die Betreuung während der vorangegangenen Promotionseignungsprüfung und dieser Arbeit bedanken. Ohne ihn wäre es für mich nicht möglich gewesen zu promovieren.

Mein weiterer Dank gilt auch in besonderem Maße Herrn PD Dr. Rainer Schreiber, der mich in jeder erdenklichen Art und Weise während meiner gesamten Arbeit unterstützt hat. Diskussionen mit ihm waren jederzeit sehr fruchtbar und halfen mir in vielen wissenschaftlichen Belangen immer weiter.

Für die Korrektur der Arbeit danke ich Dr. Gudrun Köhl aus dem Klinikum der Universität Regensburg.

Ernestine Tartler und Agnes Paech gebührt mein vielfacher Dank, sowohl für die Durchführung von Experimenten als auch für ihre große und stets vorhandene Hilfsbereitschaft, mit der mir beide das Arbeiten im Labor sehr erleichterten.

Bei meinen Kollegen, gefundenen Freunden in unserer Arbeitsgruppe und den befreundeten Nachbararbeitsgruppen möchte ich mich für die große Unterstützung während der gesamten Promotionszeit bedanken. Vielen Dank an Euch: Tanja, René, Vladimir, Higgl, Gabi, Rosi, Kerstin, Joana, Raquel, Fadi, Supaporn, Ji und die gesamte Arbeitsgruppe Warth.

Weiterer Dank auch an Euch liebe Simone, Steffi, Robert, Regine, Friedel und Rosi. Es war immer sehr schön mit Euch Western Blots und andere Sachen zu diskutieren und die Mittagspause mit leckerem Essen und Kuchen verbringen zu können.

Diese Arbeit wurde durchgeführt mit der finanziellen Unterstützung von:
DFG SCHR 752/2-1, DFG SCHR 752/2-2, Wilhelm Sander Stiftung und DFG SFB699 A7.

Besonderer Dank geht an meine Familie, speziell an meine Mutter und Tante Gabi, meinen Freund Sebastian und an meine ganzen anderen lieben Freunde, ohne die vieles nur schwer und manches unmöglich gewesen wäre.

Abbreviations

%	percent
2P	two pore
4-AP	4-aminopyridine
A	ampere
aa	amino acid
ACF	aberrant crypt foci
Ag	silver
amil	amiloride
AMP	adenosinemonophosphate
ANOVA	analysis of variance
APC	adenomatous polyposis coli
Arm	armadillo
as	antisense
Asef	APC-stimulated guanine nucleotide exchange factor
aste	astemizole
ATCC	american type culture collection
ATP	Adenosinetriphosphate
Ba^{2+}	Barium
BAC	bacterial artificial chromosome
BCECF	acetomethyl ester (2´,7´)-bis(carboxyethyl)-5(6)-carboxyfluorescein
Best1	bestrophin 1
BK	big conductance
BL6	C57BL/6J mouse strain
bp	base pairs
BrdU	5-bromo-2´-deoxyuridine
BSA	bovine serum albumine
C	celsius
c	centi, cyclic
Ca^{2+}	calcium
CaCC	Ca^{2+} activated chloride channels
CCH	carbachol
cDNA	complementary deoxyribonucleic acid
CF	cystic fibrosis
CFTR	cystic fibrosis transmembrane conductance regulator
CHO	chinese hamster ovary cells
CIN	chromosomal instability
Cl^-	chloride
CO_2	carbon dioxide
CRC	colorectal cancer
D, Da	dalton
DLG	drosophila tumor suppressor discs large
DMEM	Dulbecco’s modified eagle medium
DMH	dimethylhydrazine
DMSO	dimethylsulfoxide
DNA	deoxyribonucleic acid
dNTP	deoxynucleosidtriphosphate
DRA	downregulated in adenoma
DSS	dextran sodium sulfate
Eag	ether-á-go-go
EB1	end-binding protein 1
ECL	enhanced chemiluminescence

EGF	epithelial growth factor
EGTA	ethylenglycol-bis(β-aminoethylether)-N,N,N',N'-tetra acetic acid
EIPA	5-(N-Ethyl-N-Isopropyl) amiloride
ELISA	enzyme-linked immunosorbent assay
Elk	eag-like
ENaC	epithelial sodium channel
ENU	ethylnitrosourea
ER	endoplasmatic reticulum
Erg	eag-related
f	female, femto
FACS	fluorescence activated cell sorting
FAP	familial adenomatous polyposis
FBS	fetal bovine serum
Fig	figure
FISH	fluorescence *in situ* hybridization
FMP	FLIPR Membrane Potenial
g	gram
G1	gap phase 1
G2	gap phase 2
GFP	green fluorescent protein
GI	gastrointestinal
Glut1	glucose tranporter type 1
G_m	membrane conductance
GSK3β	glycogen synthase kinase 3β
h	hour
H^+	proton
HBE	human bronchial epithelial cells
HNPCC	hereditary nonpoliposis colorectal cancer
HRP	horseradish peroxidase
HT_{29}	human colonic cancer cells
I	current
i	intracellular
IBMX	3-isobutyl-1-methylxanthine
IC_{50}	half maximal inhibition
IgG	immune globulin G
I_{SC}	short circuit currents
k	kilo
K^+	potassium
K_2HPO_4	dipotassium hydrogen phosphate
K_{2P}	two-pore potassium channel
KAP3	kinesin superfamily-associated protein 3
K_{Ca}	calcium-activated potassium channel
K_d	dissociation constant
KH_2PO_4	potassium dihydrogen phosphate
K_{ir}	inward rectifier potassium channel
ko	knock out
Kv	voltage gated
l	liter
LEF	lymphoid enhancer factor
Lmo2	LIM domain only 2 T-cell oncogene
m	milli, meter
M	male, mega, molar
M	mitosis
max	maximal
MDCK	Madin-Darby canine kidney cells
MDR-1	multi drug resistance protein 1

Mg^{2+}	magnesium
min	minute
min	minimal
Min	multiple intestinal neoplasia
M-MLV	moloney murine leukemia virus
MMR	missmatch repair
MNU	N-methyl-N-nitrosourea
mol	molar
Mom-1	modifier of Min
mRNA	messenger ribonucleic acid
MSI	microsatellite instability
mTOR	mammalian target of the rapamycin
n	nano, number
Na^+	sodium
Na_2HPO_4	Disodium hydrogen phosphate
NaH_2PO_4	Monosodium dihydrogen phosphate
NES	nuclear export signal
nf-1	neurofibromatosis type 1
NFA	niflumic acid
NH_4	ammonium
NHE	sodium/proton exchanger
NKCC1	Na^+- $2Cl^-$- K^+ cotransporter type 1
NLS	nuclear localization signal
°	degree
p	pico
PAGE	polyacrylamid gel electrophoresis
PBS	phosphate buffered saline
PCR	polymerase chain reaction
PE	polyethylene
Pen	penicillin
PP2A	protein phosphatase 2A
PTEN	phosphatase and tensin homolog deleted on chromosome 10
PTP	protein tyrosine phosphatase
R	observed fluorescence ratio
rb1	retinoblastoma
RNA	ribonucleic acid
RPD	rectal potential difference
RT	reverse transcriptase, room temperature
R_{te}	Transepithelial resistance
RVD	regulatory volume decrease
s	seconds, sense
S	DNA synthesis phase
S/TXV	serine/treonin any valine
SAMP	serine arginine methionine proline
S_{b2}	fluorescence of calcium-bound fura-2 at 380 nm
SCID	severe combined immune-deficient
SDS	sodiumdodecylsulfate
S_{f2}	fluorescence of free fura-2 at 380 nm
si	short interference
SK	short conductance
SOC	store operated calcium channel
Strep	streptomycin
TASK	TWIK-related acid sensitive potassium channel
TBS	tris buffered saline
TCF	T-cell factor
terf	terfenadine

TGF- β	transforming growth factor-β
TPeA	tetrapentylammonium
TT	thymidine thymidine
TWIK	two pore weakly inwardly rectifying potassium channel
V	volt
V_m	membrane voltages
VOCC	voltage gated calcium channel
V_{te}	transepithelial voltage
wt	wild type
wt-1	Wilms' tumor

Erklärung

Hiermit versichere ich, dass ich die vorliegende Arbeit selbstständig verfasst und keine anderen als die angegebenen Hilfsmittel benutzt habe.

(Melanie Spitzner)

Regensburg, den 31.01.2008

Publications used in this thesis

Spitzner M, Martins JR, Ousingsawat J, Barro Soria R, Scheidt K Schreiber R, and Kunzelmann K

Ca^{2+} activated Cl^- channels and cell cycle regulated Eag K^+ channels in fast growing T_{84} colonic carcinoma cells. under revision. *JBC*

Spitzner M, Ousingsawat J, Scheidt K, Kunzelmann K and Schreiber R

Voltage-gated K^+ channels support proliferation of colonic carcinoma cells. *The FASEB Journal.* 21:35-44

Ousingsawat J, **Spitzner M**, Puntheeranurak S, Terracciano L, Tornillo L, Bubendorf L, Kunzelmann K and Schreiber R

Expression of voltage-gated potassium channels in human and mouse colonic carcinoma. *Clin. Cancer Research.* 13:824-831

Ousingsawat J, **Spitzner M**, Schreiber R and Kunzelmann K

Upregulation of colonic ion channels in $APC^{Min/+}$ mice. under revision. *Pflügers Archiv*

Publication list

Spitzner M, Martins JR, Ousingsawat J, Barro Soria R, Scheidt K Schreiber R, and Kunzelmann K

Ca^{2+} activated Cl^- channels and cell cycle regulated Eag K^+ channels in fast growing T_{84} colonic carcinoma cells. *JBC.* 2008 Jan 25

Ousingsawat J, **Spitzner M**, Schreiber R and Kunzelmann K

Upregulation of colonic ion channels in $APC^{Min/+}$ mice. Submitted to: *Pflügers Archiv*

Spitzner M, Ousingsawat J, Scheidt K, Kunzelmann K and Schreiber R

Voltage-gated K^+ channels support proliferation of colonic carcinoma cells. *The FASEB Journal.* 21:35-44

Ousingsawat J, **Spitzner M**, Puntheeranurak S, Terracciano L, Tornillo L, Bubendorf L, Kunzelmann K and Schreiber R

Expression of voltage-gated potassium channels in human and mouse colonic carcinoma. *Clin. Cancer Research.* 13:824-831

Kunzelmann K, Milenkovic VM, **Spitzner M**, Barro Soria R and Schreiber R

Calcium-dependent chloride conductance in epithelia: is there a contribution by Bestrophin? *Pflügers Archiv.* 2007 Mar 15

Puntheeranurak S, Schreiber R, **Spitzner M**, Ousingsawat J, Krishnamra N, and Kunzelmann K

Control of ion transport in mouse proximal and distal colonic by prolactin. *Cellular Physiology and Biochemistry.* 19:77-88

Kunzelmann K, **Spitzner M**, Ousingsawat J, Delgardo JR und Schreiber R

Neue diagnostische und therapeutische Möglichkeiten? *Onkologie heute.* 02/2006:18-21

Barro Soria R, **Spitzner M**, Schreiber R, and Kunzelmann K

Bestrophin 1 enables Ca^{2+} activated conductance in epithelia. *J. Biol. Chem.* 2006 Sep 26